National Library of Canada

Acquisitions and Bibliographic Services Branch

395 Wellington Street
Ottawa, Ontario
K1A 0N4

Bibliothèque nationale du Canada

Direction des acquisitions et des services bibliographiques

395, rue Wellington
Ottawa (Ontario)
K1A 0N4

Your file Votre référence

Our file Notre référence

NOTICE

The quality of this microform is heavily dependent upon the quality of the original thesis submitted for microfilming. Every effort has been made to ensure the highest quality of reproduction possible.

If pages are missing, contact the university which granted the degree.

Some pages may have indistinct print especially if the original pages were typed with a poor typewriter ribbon or if the university sent us an inferior photocopy.

AVIS

La qualité de cette microforme dépend grandement de la qualité de la thèse soumise au microfilmage. Nous avons tout fait pour assurer une qualité supérieure de reproduction.

S'il manque des pages, veuillez communiquer avec l'université qui a conféré le grade.

La qualité d'impression de certaines pages peut laisser à désirer, surtout si les pages originales ont été dactylographiées à l'aide d'un ruban usé ou si l'université nous a fait parvenir une photocopie de qualité inférieure.

Canada

SURFACE MODIFYING MACROMOLECULES FOR BIOMATERIALS

by

Yi-wen Tang

A thesis submitted to the School of Graduate Studies and Research in partial fulfilment of the

requirements for the degree of

MASTER OF APPLIED SCIENCE

in the Department of Chemical Engineering

University of Ottawa

January, 1995

ISBN 0-612-04905-1

Canada

UNIVERSITÉ D'OTTAWA
UNIVERSITY OF OTTAWA

ABSTRACT

Polyurethanes have been the materials of choice for the manufacturing of many conventional blood-contacting devices such as vascular grafts, cardiac assist devices and total artificial hearts. Some of these applications have been successful in their short-term use; however, their long-term function still remains a problem. The deficiency of these devices originates from the foreign nature of the implant materials with respect to the body. Most implant materials initiate a natural physiological response that defends the body by attacking the foreign surface. The response is a series of events which leads to the eventual degradation of the material by enzymes released from cells of the body. The degradation products from the material may produce further feedback to the foreign body response. In addition, when the materials contact blood, the formation of a thrombus commonly occurs. The thrombus may also trigger the biodegradation process by a series of complex events. Therefore, there is still a need to develop polyurethanes of improved biocompatibility and biostability.

In this thesis, new biomaterials were developed by incorporating surface modifying macromolecules (SMMs) that enriched the surface with a fluoro-chemistry. The new surface chemistry was intended to interact in a positive manner with the biological media. The surfaces were specifically designed to resist enzymatic degradation by cholesterol esterase. The SMMs contained a linear polyurethane as the prepolymer component and the prepolymer was end-capped by a fluorinated alcohol. A series of different SMMs were synthesized with various prepolymer chain chemistries and a range of reactant stoichiometries. The SMMs were blended with a base polymer (polyester-urea-urethane) with the aim of reducing the latter material's degradation by enzyme.

Following a screening process, several SMMs were selected for further study. The SMM materials and the blend of these SMMs with the polyester-urea-urethane base polymer were characterized with respect to their bulk and the surface properties, response to their biodegradation in the presence of enzyme and their fibrinogen adsorption characteristics. The SMMs were found to have selectively migrated to the

surface of the polymer mixtures as expected. The bulk thermal properties (e.g. glass transition temperature) were found to be unaltered for polyurethane samples containing up to 5% SMM.

The "fluorine tail" of the SMMs allowed the substrate surfaces to achieve very low surface wettability. Contact angle values (water/air) for the new materials were as high as 116°, which is higher than that of Teflon^R. Furthermore, X-ray photoelectron spectroscopy (XPS) surface analysis data showed that there was a fluorine enrichment from the surface to the outermost 100 Å.

The biodegradation tests of the materials containing SMMs and the polyester-urea-urethane were carried out using a radiolabel method. The cumulative radiolabelled product release was a measurement of the biodegradation. The enzyme used in this work was the hydrolytic enzyme, cholesterol esterase - an enzyme released by monocyte derived macrophages associated with the foreign body response. The results indicated that the SMMs served as barriers to inhibit the biodegradation of the base polymer. The biostability test of SMM materials themselves were carried out in a similar system and the results showed that the SMMs were enzymatically stable relative to the base polymer.

Measurements of fibrinogen adsorption, an indication of the tendency of surfaces to stimulate thrombosis, showed that the SMM blended materials significantly reduced fibrinogen adsorption.

A biodegradation test of a polyether-urea-urethane containing one of the SMMs optimized for the polyester-urea-urethane showed that the SMM was unable to inhibit degradation of the polyether-urea-urethane. This suggested that the SMM was not universally effective and that the microstructure of, and the interaction between, SMMs and the base polymer were also important factors to be considered during the investigations of the stability of polyurethanes.

The work of this thesis has made the following scientific contributions: i) a general method for the synthesis of surface modifying macromolecules (SMMs) and the general procedure for blending the additives into the base polyurethanes were developed; ii) improved biostability and biocompatibility of a polyester-urea-urethane by the surface protection of SMMs was demonstrated; iii) an understanding of the interactions between

polymeric additives and base polyurethanes was developed; and iv) an improved understanding of the relationship of biostability/biocompatibility for polyurethane materials with their surface properties and microdomain structure was presented.

ACKNOWLEDGMENTS

When I said goodbye to my parents and motherland two years ago, I never thought I was going to complete a research project within these two years and enjoy a happy life in this North American country. There would not have been a successful completion of this research without the contributions of the following people. I have to thank my supervisor, Dr. D. G. Taylor who introduced me to Dr. J. P. Santerre and Dr. R. S. Labow, my research advisors. Dr. Taylor gave me his support, understanding and kindness throughout these two years. In particular, he showed great interest in this research, a new area for him as well, and rapidly gained an understanding and made recommendations for my work. This was not easy for him and I learned a lot from his attitude as a scientist which will benefit me throughout my life. I would like to thank Dr. J. P. Santerre for accepting me as a student, despite my difficulties with the English language. His guidance served greatly from the initial planning stages to the completion of this thesis. From his constructive recommendations, I have learned how to be a more efficient researcher. I would further like to thank him for his encouragement throughout these two years and the opportunities he has given me to present my work in several conferences. I am indebted to Dr. R. S. Labow, who assisted in the supervision of my biodegradation tests as well as assisting me with my English. She treats her students as her own children and this made the research group feel like my new family.

I am also grateful to Mr. D. Duguay and Mr. D. Erfle for their continuing help in the lab. Their insight and good organizational skills provided me with good models of a graduate student. I also have to thank Dr. D. Cooney of the National Research Council of Canada, Institute for Environmental Chemistry, Ottawa, who contributed to my DSC studies. I thank Dr. R. Sodhi, who performed XPS measurements at the Centre for Biomaterials, University of Toronto. I am grateful to Mrs. G. Waghray, the technician in Dr. Labow's lab, and Miss A. Seshadri, a student of McGill University now, who assisted me with some of my biodegradation tests. I also have to thank Mr. Glen McClung, the technician in Dr. J. Brash's lab, who performed the fibrinogen

adsorption tests on my research materials.

Finally, I am indebted to Ms. Kim Lee for her continued support during this project. She took care of me as her younger sister and let me enjoy the life in this country which was, in a sense, also part of my studies. Also, I would like to take this opportunity to thank my family for their understanding, support and patience during my academic career.

NOMENCLATURE

BA-L	Zonyl^{R} fluorotelomer intermediate
BA-L (Low)	the first distillation fraction of BA-L
BA-L (Int)	the second distillation fraction of BA-L
BA-L (High)	the third distillation fraction of BA-L
CE	cholesterol esterase
^{14}C-HDI	carbon 14 radiolabelled 1,6,-diisocyanato-hexane
^{14}C-TDI	carbon 14 radiolabelled toluene-2,4,-diisocyanate
DMAC	N, N,-dimethylacetamide
DMF	N, N,-dimethylformamide
DMSO	dimethyl sulphoxide
DSC	differential scanning calorimetry
ED	ethylenediamine
GPC	gel permeation chromatography
HDI	1,6,-diisocyanato-hexane
PCL	polycaprolactone diol 1250
PPO	polypropylene oxide 1000
PTMO	polytetramethylene oxide 1000
SMM	surface modifying macromolecule
TCTFE	1,1,2,-trichlorotrifluoroethane
Tg	glass transition temperature
Tm	melting temperature
XPS	X-ray photoelectron spectroscopy
PPO-212L	polymer synthesized with HDI, PPO, and BA-L (Low) stoichiometry of HDI:PPO:BA-L (Low) is 2:1:2
PPO-322I	polymer synthesized with HDI, PPO, and BA-L (Int)

	stoichiometry of HDI:PPO:BA-L (Int) is 3:2:2
PPO-322H	polymer synthesized with HDI, PPO, and BA-L (High) stoichiometry of HDI:PPO:BA-L (High) is 3:2:2
PTMO-212L	polymer synthesized with HDI, PTMO, and BA-L (Low) stoichiometry of HDI:PTMO:BA-L (Low) is 2:1:2
PTMO-212I	polymer synthesized with HDI, PTMO, and BA-L (Int) stoichiometry of HDI:PTMO:BA-L (Int) is 2:1:2
PTMO-212H	polymer synthesized with HDI, PTMO, and BA-L (High) stoichiometry of HDI:PTMO:BA-L (High) is 2:1:2
PTMO-322L	polymer synthesized with HDI, PTMO, and BA-L (Low) stoichiometry of HDI:PTMO:BA-L (Low) is 3:2:2
PTMO-322I	polymer synthesized with HDI, PTMO, and BA-L (Int) stoichiometry of HDI:PTMO:BA-L (Int) is 3:2:2
PTMO-322H	polymer synthesized with HDI, PTMO, and BA-L (High) stoichiometry of HDI:PTMO:BA-L (High) is 3:2:2
PTMO-432L	polymer synthesized with HDI, PTMO, and BA-L (Low) stoichiometry of HDI:PTMO:BA-L (Low) is 4:3:2
PTMO-432I	polymer synthesized with HDI, PTMO, and BA-L (Int) stoichiometry of HDI:PTMO:BA-L (Int) is 4:3:2
PTMO-432H	polymer synthesized with HDI, PTMO, and BA-L (High) stoichiometry of HDI:PTMO:BA-L (High) is 4:3:2
TDI/PCL/ED	base polyester-urea-urethane synthesized with TDI, PCL, and ED
TDI/PTMO/ED	base polyether-urea-urethane synthesized with TDI, PTMO, and ED
^{14}C-TDI/PCL/ED	radiolabelled base polyester-urea-urethane synthesized with ^{14}C-TDI, PCL, and ED
^{14}C-TDI/PTMO/ED	radiolabel base polyether-urea-urethane synthesized with ^{14}C-TDI, PTMO, and ED

CONTENTS

LIST OF FIGURES

LIST OF TABLES

1. INTRODUCTION

Over the past few decades, significant improvements in material science and surgical techniques have made it possible to replace some parts of the human body with synthetic medical implants. The materials used to fabricate these implants belong to the family of "biomaterials". There has been significant time and money invested into research to improve the material quality, engineering design and manufacturing procedures associated with these devices (1,2). Polyurethanes constitute a family of biomaterials which has been successful in a variety of applications. Their excellent mechanical properties and moderate biological properties have led to their use in medical devices such as pacemaker leads, vascular grafts and artificial hearts (3). However, the search for an appropriate material to be used in long-term implantation remains a challenge because of the difficulty in finding materials that satisfy all mechanical, biocompatibility and biostability requirements simultaneously (4).

With regards to long-term implantation, which may range from one month to several years to a lifetime, these materials must be able to resist both the harsh environment created during the acute inflammatory response immediately following implantation and the long-term presence of other blood components during the chronic inflammatory phase of inflammation. Hence, the biostability and biocompatibility of these materials is of major concern. Poor biostability and/or biocompatibility character may result in erosion of the device, the release of toxic products following breakdown of a device, and the loss of structural integrity leading to the eventual failure of the device (5). In most cases, device related infection, blood coagulation or a highly activated immune responses may result in the removal of the device.

The role of blood components in the degradation of biomaterials has been a subject of several studies during the past decade, but has not yet been fully characterized (5). It is suspected that the interaction between white blood cells such as leucocytes and the medical device is the starting point for the degradation process. This is followed by the release of oxidative species and lysosomal enzymes (6). These two classes of

components have been identified as the two primary candidates related to the destruction of implanted material (6).

There is good experimental evidence that blood-material interactions occur at the inner few atomic layers from the material surface (7). This implies that, as long as the material does not contain any leachable components, its bulk chemistry, which is distant from the biological interface, does not effect its *in vivo* performance. Accordingly, all biomaterial applications have requirements that can be divided into bulk property and surface property categories. An elastomer for an artificial heart, for example, must have good bulk mechanical properties such as flex life, toughness, flexibility, and processability (8). This same material must also have a surface which does not cause blood to clot or the adjacent tissue to become inflamed (9). However, in many classes of polymers, the relationship between the surface variables and the bulk properties is not well understood. Likewise, the relationship between the surface chemistry and the *in vivo* response of the material is difficult to delineate because of the limitations of existing surface analysis instruments (10). The study of polymer biocompatibility through surface chemistry is also complicated by the fact that many commercially available polymers contain additives or impurities that are surface-active. In addition, the chances are remote that an optimum in both surface and bulk properties could be found with a single material.

Based on this dilemma, scientists started to use surface treatments or coatings to improve the surface-blood compatibility of materials with desired mechanical properties (11). Another method that has been used is to blend surface-active molecules into base polymers for the purpose of improving biostability and biocompatibility. Since air is a low free surface energy fluid (12), the interface between air and the polymer will have the lowest possible energy when the polymer surface also has a low energy component. The migration of the blood compatible additives through a polymer has successfully been used to lower the polymer surface energy and, therefore, overall interfacial energy (13). This effect is thought to minimize the activation of blood constituents for coagulation, cell adhesion, and other adverse biological processes (14).

It should be noted that in many block polymer systems, such as polyurethanes,

another mechanism for interfacial energy minimization exists. By reorienting of the surface molecular layer, one of the blocks can preferentially populate the surface (15). This means that when a polymer is placed into the blood stream and exposed to a polar aqueous environment, the polymer may attempt to reorient its polar blocks toward the surface in order to minimize the energy differential at the blood-polymer interface. Thus, the design and the manufacture of new biomedical polymers must take into account both the possible migration of surface active species and the reorientation of the surface layer that will occur in different environments.

Based on the above discussion, it can be seen that long-term biostability and biocompatibility are principal concerns in the use of common biomaterials such as polyurethanes. This study will concentrate on the design and synthesis of a new class of polymeric additives, called surface modifying macromolecules (SMMs), which, when added to polyurethanes, will lead to a new surface chemistry composed primarily fluorine elements. The driving force behind the generation of this new surface chemistry exists due to the low surface energy component of the macromolecules (i.e. the "fluorine tails") and also due to the incompatibility of specific SMM components with the base polymer. As a result, SMMs are expected to migrate to the polyurethane surface in high concentrations, even when only a small amount of SMMs are blended with the base polymer.

Because the SMMs have relatively high molecular weights (between 1.5×10^4 to 5.5×10^4) and have similar chemical structures to that of the base polymer, they remain partially anchored to the base polymer. The purpose of this amphiphilic design is to specifically provide a surface protection for polyurethanes against hydrophilic enzyme by virtue of the higher hydrophobicity and stability of the fluorine tails within the SMM. Hence, the design of SMMs that migrate to the surface and remain stable in a biological environment is the primary focus of this study. Considering that reorientation of polyurethanes due to changes in environment occurs, the ability of SMMs to remain anchored to the base polymer turns out to be an important concern as well. By the simultaneous study of the SMMs' ability to inhibit enzyme induced degradation, SMM-base polymer interactions, and their surface properties, more information regarding the

relationship between surface chemistry, biostability and biocompatibility for polyurethanes are anticipated.

2. BACKGROUND

2.1. Biomaterials: Applications and Biocompatibility

Artificial materials have been used in conjunction with biological substances for a long time. In fact, the first clinical application of a "biomaterial" dates back to 1759, when Hallowell united the edges of a lacerated brachial artery using a wooden peg and twisted thread (16). Although there is no universally accepted definition for a biomaterial, it has been defined by D. F. Williams (17) as "a material that is used in the treatment of patients and which, at some stage, interfaces with tissue for a significant length of time so that the interaction between the tissue and the material is an important factor in the treatment". This definition excludes those materials used only transiently by a surgeon or physician, such as the steel used for a scalpel blade, or the tungsten carbide used in a dental burr, where there is little time for interactions to have any significance.

Biomaterials can be synthetic products made from metals, plastics,or ceramics. However, they can also be biological in origin, such as collagenous tissues that have been treated to make them suitable for implantation (18).

Biomaterial science and its applied field - medical devices - have exploded during the past forty years (16). It has been reported that, in 1991, the estimated use of biomaterials in therapeutic medicine exceeded two billion dollars, with a steep increase in use expected for the future (20). Table 2.1. lists many of the biomaterials used in widespread clinical use. Table 2.2 provides estimates of the numbers of biomaterial containing devices used in clinical settings. Materials for totally implanted devices constitute the most obvious category of biomaterials. In addition, there are those materials used in the mouth for dental treatment as well as several types of devices that penetrate the skin and reside both inside and outside the body. Some materials are used totally extracorporeally and include assist devices such as membrane blood oxygenators and haemodialysis equipment.

Table 2.1. Commonly used biomaterials (19).

Material	Applications
Silicon rubber	Catheters, tubing
Dacron	Vascular grafts
Teflon	Catheters, vascular grafts
Cellulose	Dialysis membranes
Poly(methyl methacrylate)	Intraocular lenses, bone cement
Polyurethanes	Catheters, pacemakers
Hydrogels	Ophthalmologic devices
Carbon	Heart valves
Stainless steel	Orthopaedic devices
Titanium	Orthopaedic and dental devices
Alumina	Orthopaedic and dental devices
Hydroxyapaptite	Orthopaedic and dental devices
Collagen (reprocessed)	Ophthalmologic and burns

Once a biomaterial is implanted into the human body, biocompatibility becomes the most important issue to determine whether this material is suitable for use. Biocompatibility is "a term to describe the state of affairs when a biomaterial exists within a physical environment, without either the material adversely and significantly affecting the body, or the environment of the body adversely and significantly affecting the material" (17). These adverse effects include, in part, thrombogenesis (i.e. formation of a blood clot) on artificial surfaces induced by the blood components such as proteins (fibrinogen, γ-globulin, albumin), platelets, white blood cells and red blood cells; inflammatory response by the immune system to the foreign bodies; and the release of toxic products from degraded materials or leachable monomers or additives.

The first event that occurs after blood contacts a surface is the deposition of a protein layer at the blood-material interface (21). Fibrinogen is the major protein adsorbed at the blood interface, but many other plasma proteins, including albumin and γ-globulin, may also be deposited (6). Platelet deposition follows protein adsorption on artificial surfaces. A critical stage is reached (usually when the protein layer is 100 to 200 Å thick) about 1 minute after blood contact, when platelets make their first adhesive

Table 2.2. Selected biomedical implant applications: magnitude of use[a] (19).

Applications	Number Used per Year
Ophthalmologic	
Intraocular lenses	1,400,000
Contact lenses	250,000,000[b]
Retinal surgery implants	50,000
Cardiovascular	
Vascular grafts	350,000
Arteriovenous shunts	150,000
Heart Valves	75,000
Pacemakers	130,000
Blood bags	30,000,000
Reconstructive	
Knees	65,000
Breast prostheses	100,000
Hips	90,000
Penile	40,000
Other devices	
Wound drains	3,000,000
Catheters	200,000,000
Oxygenator	500,000
Renal dialysers	16,000,000
Sutures	20,000,000

a. Approximate annual usage in United States
b. Worldwide

contact (22). After deposition, platelets undergo morphological changes and release adenosine diphosphate (ADP). ADP causes more platelets to stick to those already attached to the surface, leading to platelet aggregation (23). Meanwhile, the adsorbed fibrinogen is polymerized to fibrin which forms a network structure with the platelets and other cellular constituents. The resulting thrombus poses a serious threat to the device recipient due to the potential for thrombo-emboli. Therefore blood-surface interactions represent an important issue in biomaterial development.

When a foreign material enters, or is placed within, the body, it is likely to arouse host defensive mechanisms that have evolved to specifically reject foreign bodies.

These mechanisms are called the inflammatory response (24). The occurrence of macrophages and lymphocytes in histological sections of tissues is a direct indication of inflammation. Studies have shown that inflammation is achieved by the release of various biologically active substances which are mediators of the inflammatory response (25).

The implantation of the material can introduce not only a local irritancy, but also a systemic biological response at a distant site once an absorbed agent enters the circulatory system. If degradation of the implanted material occurs, a toxic agent may possibly be produced with an associated risk (26). The toxicological aspects of materials can be divided into several categories: i) local tissue response; ii) systemic toxic effect; iii) allergic response; iv) carcinogenic, teratogenic, and mutagenic effects; and v) cellular-material interactions (26).

Although the leachable and biologically active constituents of a biomaterial are important components affecting biocompatibility, the surgeon's skill in inserting the device is also an important factor which will influence the ultimate biocompatibility as well as the biostability of the device (26). It is therefore impossible to determine with absolute certainty whether a specific material will or will not be biocompatible. In each case, the benefit-to-risk ratio becomes the central issue for the use of a device (26).

2.2. Biomedical Polyurethanes

Since their introduction in the 1930's, polyurethanes have been used in various biomedical applications including endotracheal tubes, aortic grafts and vascular tubing, cardiac assist devices and heart by-pass devices, artificial heart valves, pacemaker leads, roller pump tubing in artificial hearts and blood pumps, mammary prostheses and dialysis membranes (27). The first implant studies with polyurethanes were carried out in the late 1950's using polyester-urethanes, but the materials were shown to be rapidly hydrolysed at the ester groups (28). Later, polyether-urethanes were introduced that contained hard-segments of urea and soft-segments of polyether linked by a urethane group. A high modulus of elasticity, some degree of biocompatibility, resistance to flex

fatigue and excellent mechanical stability over long implant periods were observed in some applications (29). Other researchers studying segmented polyether-urethanes observed excellent thromboresistance (30). Unfortunately, some applications of polyurethanes have indicated a cause for concern, particularly with respect to the biodegradation of materials used in implants such as vascular grafts and pacemaker leads (31).

2.2.1. Polyurethane Chemistry

Polyurethanes consist of a repeating unit containing a urethane link. Although many variations of polyurethanes exist due to the possible combination of different structural groups in the chain, the segmented polyurethane (SPU), of particular interest to the present work, contains three major components: (a) a diisocyanate, (b) a long chain diol (usually a polyester or polyether), and (c) a chain extender in the form of a short chain diol or diamine.

Figure 2.1 depicts the chemical structure of a typical polyurethane. A long flexible soft-segment is attached by way of a urethane link to a rather stiff block referred to as the hard-segment. Soft-segments are normally derived from hydroxyl-terminated oligomers composed of aliphatic polyesters or polyethers ranging in molecular weight from 500 to 5000. The hard-segment is formed by the reaction of a low molecular weight diisocyanate with a low molecular weight diol or diamine chain extender (32).

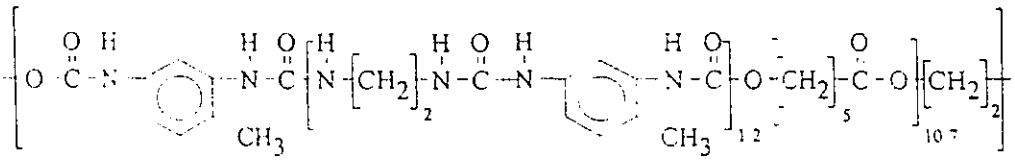

HARD SEGMENT SOFT SEGMENT

Figure 2.1. Chemical structure of a typical polyurethane.

Diisocyanates

Common diisocyanates used in polyurethane synthesis include toluene diisocyanate (TDI), diphenylmethane-4,4'-diisocyanate (MDI) and 1,6-hexamethylene diisocyanate (HDI). The structures of these compounds are shown in Figure 2.2.

Both TDI and MDI are aromatic diisocyanates yielding polymers which tend to yellow after prolonged exposure to sunlight. The methylene group in MDI is also susceptible to oxidation via a proton abstraction mechanism, involving auto-oxidation of the aromatic urethane groups to form a quinoneimide (33) (see Figure 2.3).

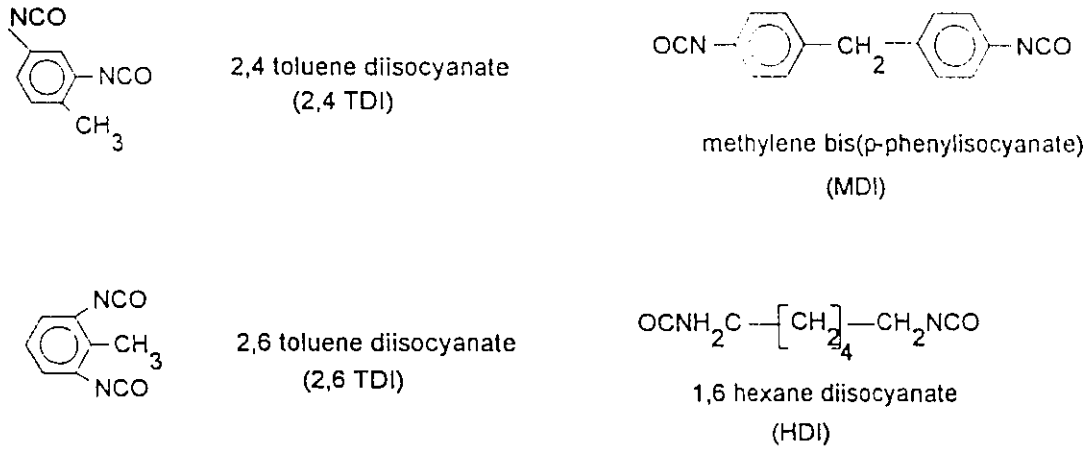

Figure 2.2. Typical diisocyanates used for polyurethane synthesis.

HDI is an aliphatic diisocyanate which has better light stability as well as better resistance to hydrolysis and thermal degradation than its aromatic counterparts (34). However, it is less reactive than the aromatic diisocyanates. Catalysts such as dibutyltin dilaurate or dibutyltin dicaprylate are usually employed in polyurethane synthesis with HDI (35).

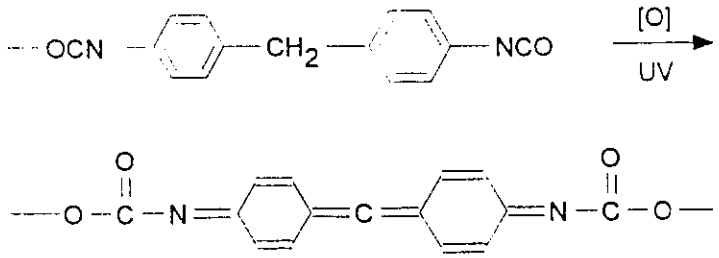

diquinone-imide (chromophoric)

Figure 2.3. Auto-oxidation of the aromatic urethane group (33).

Oligomeric Diols

Diols used in the synthesis of SPU include hydroxyl-terminated low molecular weight polyesters, polyethers, hydrocarbon polymers and polydimethyl siloxanes (36). Some examples are shown in Figure 2.4. Polyester-based polyurethanes possess relatively good material properties; however, they are susceptible to hydrolytic cleavage of the ester linkage (33). In contrast, the polyether-based polyurethanes have been reported to exhibit a relatively high resistance to hydrolytic cleavage (33).

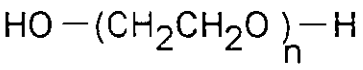

polyethylene oxide (PEO)

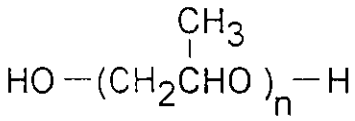

polypropylene oxide (PPO)

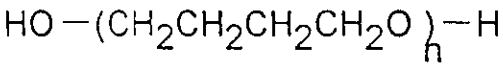

polytetramethylene oxide (PTMO)

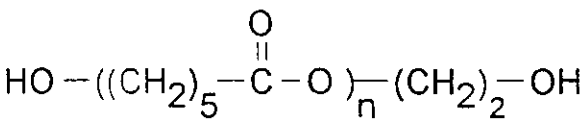

polycaprolactone diol (PCL)

Figure 2.4. Chemical structures of typical oligomerical soft segments.

Chain Extenders

Aliphatic and aromatic diols and diamines can be used as chain extenders. In general, polyurethanes prepared with diamines as chain extenders have better physical properties than polyurethanes chain-extended with diols (37). Further, the use of aliphatic chain extenders with an even number of backbone carbon atoms leads to polyurethanes with superior mechanical properties than those produced from chain extenders having an odd number of backbone carbon atoms. This may be due to an enhanced crystalline order within the hard segment domains (36). Figure 2.5 shows some commonly used chain extenders.

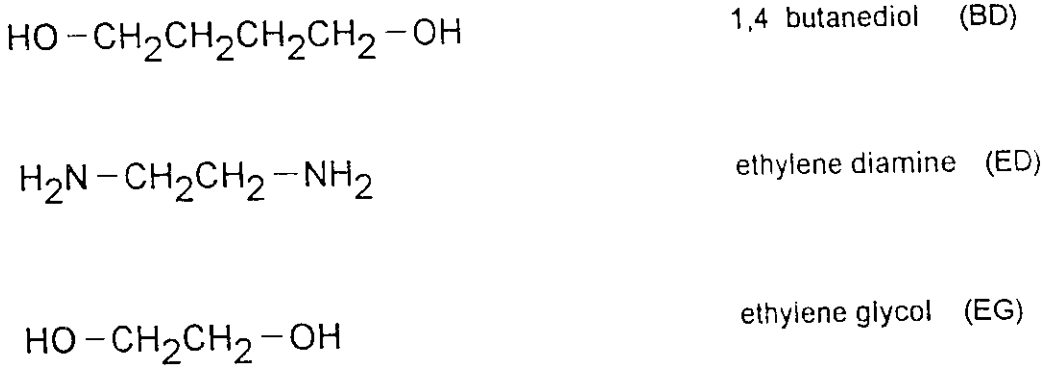

Figure 2.5 Typical chain extenders.

Synthesis and Control

Quite often, the synthesis of polyurethanes is performed in solution, and the choice of solvent may affect the rate of the uncatalyzed reaction or, in the case of a catalytic reaction, the effectiveness of the catalysts. In general, solvents that readily complex with an active hydrogen compound or catalyst (for example, by hydrogen bonding or dipole moment interactions) will result in slower reactions than will solvents that cannot readily associate with either reactants or catalysts (38). Common solvents

used in solution synthesis include N,N-dimethylacetamide (DMAC), dimethylsulfoxide (DMSO), dimethylformamide (DMF), and tetrahydrofuran (THF). These are all polar solvents that can provide a nonreactive medium in which the diisocyanate, the oligomeric diols, the diol or diamine, and the synthesized polymers are all soluble.

Although polyurethane formation is an exothermic process, additional thermal energy is required to produce high molecular weight polymers. However, temperatures above 80°C should be avoided because, in this range, isocyanates will react with urethanes to yield allophanates, or react with ureas to yield biurets. (In these cases, the -NCO- reacts not with the targeted -OH or $-NH_2$, but with urethane linkages -NHCOO- or urea linkages -NHCONH-.) Both allophanates and biurets are synthesis by-products of linear polyurethanes and will result in a crosslinked product if not controlled (38).

One of the more common techniques used for producing a polyurethane elastomer is the prepolymer method, in which an excess of diisocyanate reacts with a polyol to form an "extender diisocyanate", i.e. a prepolymer. The prepolymer is then converted to a long chain polymer by means of a chain extender. The advantage of this two-step method is that the diol-diisocyanate reaction is completed prior to the reaction with the chain-extender and thus leads to more uniform polymers.

The use of high purity reactants is absolutely essential to the successful synthesis of high molecular weight linear polyurethanes. Trace metals and salts will cause diisocyanates to react with urethane and/or urea groups, forming crosslinks and/or branches (36). Water is another contaminant which is to be avoided because of its reactivity with isocyanates (35). Water can be eliminated by solvent distillation, by diol degassing and by conducting reactions under dry, inert gases.

2.2.2. Polyurethane Structure, Properties, and Characterization

Polyurethane Structure and Properties

Polyurethane elastomers are segmented block copolymers, composed of alternating soft and hard blocks. The soft-segments, usually polyesters or polyethers, have glass

transition temperatures, Tg, (i. e. their softening or melting temperatures) below the temperature of use, and are therefore rubbery materials. The hard-segments can be diisocyanates, extended with diols or diamines. As their Tg is above the normal utilization temperature, the hard-segments are rigid, and/or crystalline. Thermodynamic incompatibility between the segments induces their segregation into hard- and soft-segment domains, respectively (see Figure 2.6). The hard-segment domains act as fillers or physical crosslinks for the rubbery soft segment matrix (38).

The factors which affect phase segregation in polyurethanes include segment polarity, chain length and crystallization, tendency for hard-segment/soft-segment interactions (e.g. via hydrogen bonding), overall sample composition, molecular weight, and synthesis temperature (39).

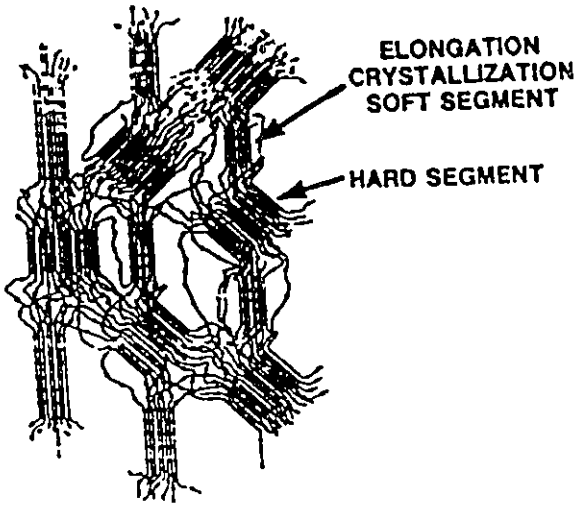

Figure 2.6. Morphological structure of a segmented polyurethane (40).

Several models for describing polyurethane morphology have been proposed and illustrate the domain structure. One of these models assumes that, in most instances, the soft and hard blocks are joined at the domain interfaces. However, phase segregation may be incomplete, so that some of the urethane blocks are also dispersed in the rubbery matrix. A typical domain size in the direction of the chain axis is approximately 50 Å (38).

The microphase separation discussed above provides polyurethanes with excellent elastomeric behaviour; hence, the physical properties of the polyurethane elastomers are directly related to the extent of hard- and soft-segment domain segregation. In general, increasing the soft-segment molecular weight with fixed hard-segment length yields polyurethanes with the following characteristics: a lower tensile strength and modulus and higher elongation at break, due to the decrease in the hard-segment content; lower Tg (i.e. enhanced chain mobility in the presence of a small number of relatively immobile hard-segments); an increased tendency of the soft-segments to crystallize; and an increased tendency for the hard-segment domains to be mixed in the soft-segment matrix (continuous phase) (41). On the other hand, increasing the hard-segment content at constant soft-segment molecular weight results in increased crystallinity, increased hard-segment melting temperature, increased interfacial area, increased tensile strength and modulus and decreased ultimate elongation (36).

Characterization

There are several methods available for characterizing polymer structure (see Table 2.3). These include chemical and spectroscopic methods, gel permeation chromatography, light scattering methods, and the thermal analysis methods (42). To characterize the state of intermolecular bonding, to identify thermal properties of polyurethanes, and to analyze the microphase separation, differential scanning calorimetry (DSC) is usually applied (see Figure 2.7). DSC is a quantitative study of thermal transitions in polymers. A polymer sample and an inert reference are heated, usually in a nitrogen atmosphere, and thermal transitions in the sample are detected and measured. Sample sizes vary from about 0.5 mg to about 10 mg, and the sample holder consists of a very small aluminum cup. The reference is either an empty cup or a cup containing an inert material in the temperature range of interest. The sample and reference are provided with individual heaters, and energy is supplied to keep the sample and reference temperatures constant. The electrical power difference between sample and reference ($d\Delta Q/dt$) is then recorded.

Table 2.3. Spectroscopic, scattering and thermal methods commonly used for studying polymers (excluding the surface) (42).

Vibrational
Infrared (IR)
Raman
Spin resonance
Nuclear magnetic resonance (NMR) (proton and carbon-13)
Electron spin resonance (ESR)
Electronic
Ultraviolet (UV)-visible
Fluorescence
Scattering
X-ray
Electron
Neutron
Thermal
Differential scanning calorimetry (DSC)
Differential thermal analysis (DTA)
Thermomechanical analysis (TMA)
Pyrolysis-gas chromatography (PGC)

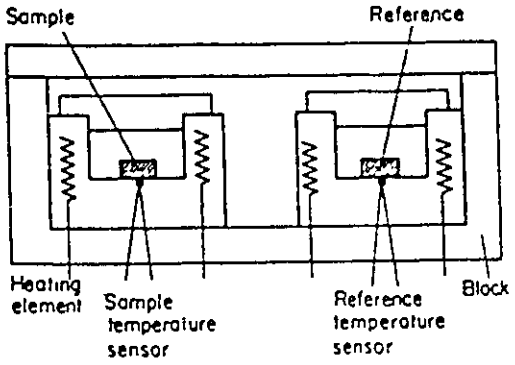

Figure 2.7. Schematic representation of differential scanning calorimetry (DSC) measuring cells (42).

An idealized DSC thermogram for a hypothetical crystallizable polymer is depicted in Figure 2.8, illustrating the types of transitions of interest to the polymer chemist. The glass transition (A in Figure 2.8) is indicated by an endothermic shift in the initial baseline because of the sample's increased heat capacity. (Note: endothermic transitions lie below the baseline in these thermograms, while exothermic transitions lie above, although this can vary with different devices.)

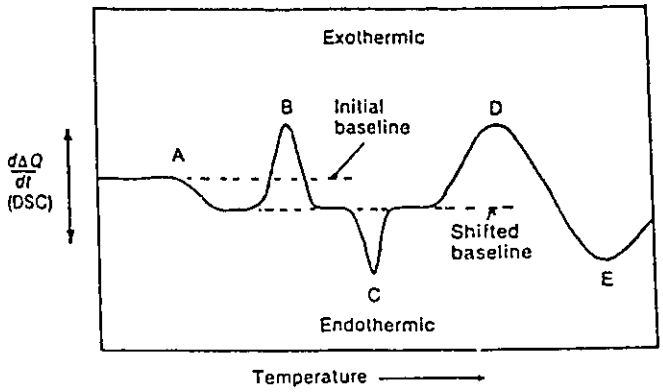

Figure 2.8. Idealized differential scanning calorimetry (DSC) thermogram: (A) temperature of glass transition, Tg; (B) crystalline melting point, Tm; (C) crystallization; (D) crosslinking; and (E) vaporization (42).

2.2.3. Polyurethane Surface Analysis and Characterization

Surface analysis has played an increasingly important role in characterizing polyurethanes, particularly for biomedical applications. A fundamental knowledge of the surface structure and chemistry is essential for understanding the interactions between these materials and living systems. Table 2.4 summarizes and compares the advantages and limitations of a number of methods available for characterizing surfaces.

Electron spectroscopy for chemical analysis (ESCA), also called x-ray photoelectron spectroscopy or XPS, is based upon the emission of electrons from matter in response to irradiation by photons of sufficient energy to cause ionization of core-level

Table 2.4. Capabilities and concerns with common methods to characterize biomaterial surfaces (43).

Method	*Principle*	*Depth analyzed*	*Concerns*	*Spatial resolution*	*Analytical sense*
Contact angle	Liquid wetting of surfaces is used to estimate the energy of surface	3-20Å	Liquid swells, penetrates or extracts sample	Low or high, depending upon the chemistry	1 mm
XPS	X-rays cause the emission of electrons of characteristic energy	10-250Å	X-ray damage; interpretation can be complex	0.1%	10-150μm
Auger electron spectroscopy	A focused electron beam cause the emission of auger electrons	50-100Å	Severe sample damage; quantitation	0.1%	100Å
SIMS	Ion bombardment leads to the emission of surface secondary ions	10Å-1μm	Sample damage; quantitation	very high	500Å
SEM	Secondary electron emission caused by a focused electron beam is measured and spatially imaged	5Å	Sample damage; preparation artifacts	High, but not quantitative	40Å typically

electrons. These electrons are emitted with an energy characteristic of the atoms from which they emerged. Since photo-emitted electrons have little ability to penetrate matter, only those electrons released near the surface (in the outermost 80 Å) can escape to be counted. The XPS technique is illustrated in Figure 2.9. Given a well developed theory which assists interpretation and the fact that the sample preparation is easy and there is minimal damage to the sample, XPS is one of the most commonly used methods in surface characterization of polyurethanes (43).

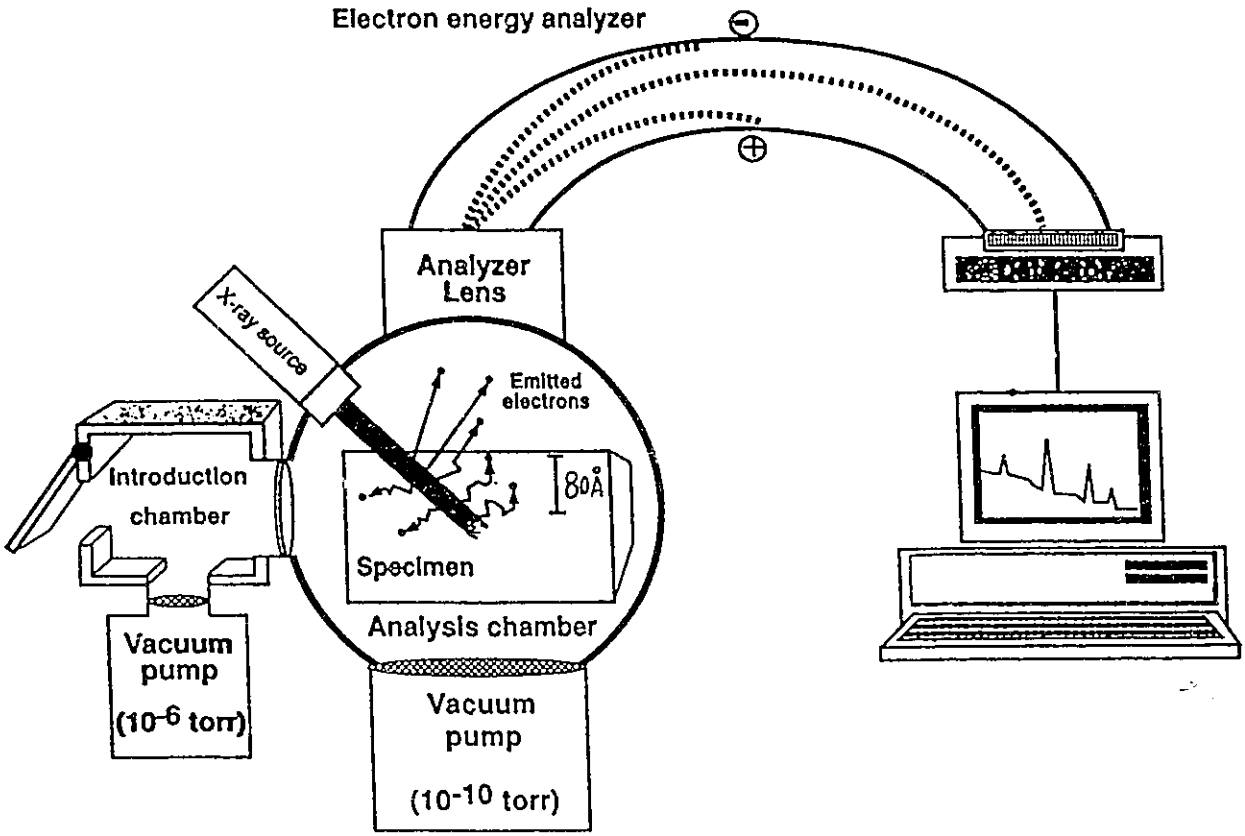

Figure 2.9. Schematic diagram showing the components of a typical XPS instrument (44).

The contact-angle method involves the measurement of the angle with which a drop of liquid contacts a surface. This represents one of the earliest methods used to investigate surface composition, but one that is still popular because of its simplicity and the low cost of the apparatus. Contact angle measurement theory is based on the thermodynamics of wetting, whereby the minimization of the free energy of the system will yield a unique contact angle. However, in real systems, it has been observed

experimentally that a liquid drop on a solid surface could yield several different stable contact angles. These fall between two well reproducible values, the maximum being called the advancing angle and the minimum being referred to as the receding angle. The difference between these two observed values is known as the "contact angle hysteresis" (45).

The establishment of reproducible measurement techniques helped in the further development of contact angle theory, and, as a result, measurement of contact angle hysteresis has become a valuable analytical tool, providing information about surface energies, roughness and heterogeneity. For example, Holly and Refojo (46) proposed a structural change in the gel-air phase boundary when they measured the advancing and receding angles of water in air and of air in water on poly(2-hydroxyethyl methacrylate). In particular, they proposed that the hydrophilic group, buried in the aqueous phase within the gel when the surface was exposed to air, was able to quickly reorient in a water environment. They went on to suggest that the hydrogel surface was capable of changing its free energy through reorientation of the polymer side chains and chain segments, depending on the nature of the adjacent phase (i.e. air or water).

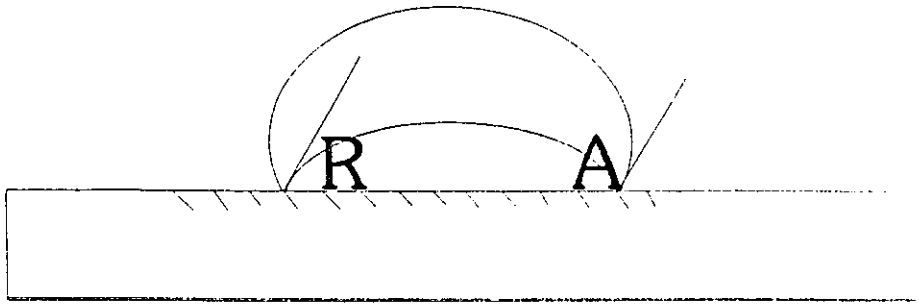

Figure 2.10. Schematic diagram showing the advancing angle (A) and receding angle (R) (45).

The most commonly used method to measure contact angles is the drop (or bubble) method which is carried out by increasing or decreasing the volume (drop or bubble) until the three-phase boundary moves over the surface (see Figure 2.10).

however, inaccuracies in the measurements can be induced by vibration (which is almost impossible to be removed from the system), by contamination of the measurement liquid (by the surface under study or from the environment), by substrate surface roughness, by penetration of the measurement liquid into the solid and/or related swelling, or by relative humidity effects during the measurement. However, contact angle measurement is still widely used for the surface characterization of polyurethanes (45).

2.3. Challenge of Biomedical Polyurethanes

2.3.1. Medical Applications and Associated Problems

Due to their excellent physical and mechanical properties and relatively good blood compatibility, polyurethanes have found widespread use in the biomedical industry. Different types of polyurethanes have been synthesized and are commercially available for biomedical applications. For example, Biomer® was used in artificial hearts (47), Pellethane® was used as pacemaker lead insulation (48), Cardiothane® has been used in left-heart-assistant blood conduits, and Adriprene® has been applied in a left-heart-assist blood pump (49). However, several problems have arisen since their introduction in the biomedical industry. Darby at Travenol Laboratories alerted the scientific community that a medical grade polyurethane, Pellethane-2383-80A, after several hours of sterilization, contained an aromatic diisocyanate-related component, methylene bis(p-phenyldiamine) (MDA) (50). MDA has been reported to be carcinogenic (38). In addition, a relatively short-term cardiac implant was discovered with insulation failure due to a previously undiscovered cracking mechanism (51). Controversy also has arisen about the use of Pellethane 2363-80A polyurethane because of biodegradation in the form of shallow surface fissures (52). In November, 1983, a French physician reported the failure of 10 Medtronic 6991-U leads (made with Pellethane 2363-80A), and in January, 1984, the Lancaster General Hospital (Maryland, U.S.A.) noted a 20% failure rate with Medtronic 6972 pacemaker leads (52). As a result, 27,000 model 6972 bipolar leads,

manufactured between December, 1975, and February, 1982, were involved in an FDA class II recall (33).

Laboratory tests have also suggested that Biomer is degraded *in vitro*. For example, Tyler et al. (53) exposed two lots of Biomer (BSUA001 and BSP067) to papain, leucine aminopeptidase (hydrolytic enzymes) and hydrogen peroxide (an oxidizing agent) for 24 hours. BSP067 had statistically significant changes in the molecular weight distribution for all three treatments, while BSUA001 only showed changes after exposure to hydrogen peroxide. In addition, biodegradation problems have been complicated by other problems such as calcification (54) and thrombosis (55).

2.3.2. Degradation of Polyurethanes

Chemical Degradation (i.e.Unrelated to Enzymes)

There are many pathways by which polyurethanes are chemically degraded. Some of them include

i. hydrolysis (reaction with water);
ii. thermolysis (reaction due to heat);
iii. oxidation (reaction with oxygen, initiated either with heat (thermooxidation) or by light (photooxidation)); and
vi. solvolysis (degradation related to solvents, such as alcohols).

The most common forms of degradation are hydrolysis and oxidation, which are discussed further below.

(I) Hydrolysis

The three bonds most susceptible to hydrolytic degradation in polyurethanes are those of the ester, urea and urethane groups (Figure 2.11). In various polyurethane systems, the polyester-based polyurethane hydrolyzes quite rapidly, typically two to four times faster than polyether-based polyurethane (33).

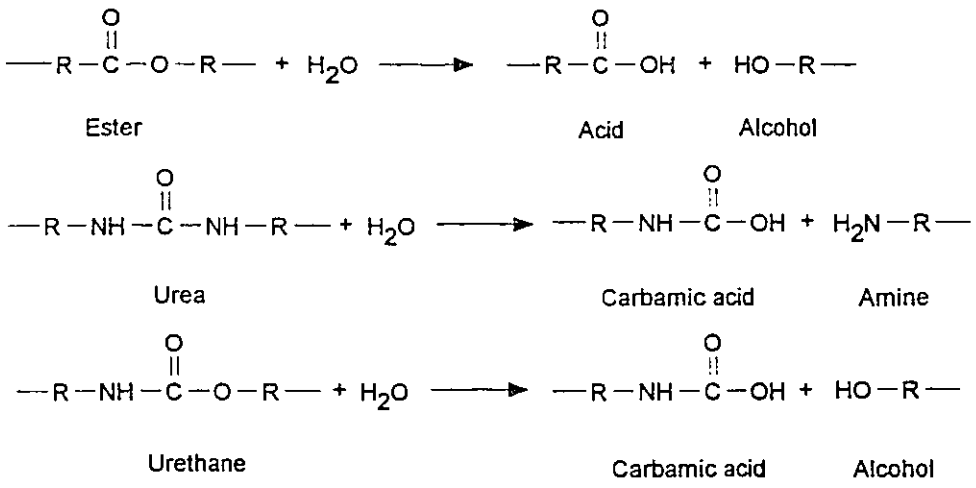

Figure 2.11. Hydrolysis reactions.

(II) Oxidation

Although polyether-based polyurethanes display more hydrolytic stability, they are particularly susceptible to oxidation (35,36). The reaction can proceed via a mechanism involving a peroxide radical. Meijs performed experiments in which Pellethane 2368-80A was treated with 25% (w/w) hydrogen peroxide at 100°C for times ranging from 24 hours to 336 hours. Significant decreases in ultimate tensile properties and molecular weights were observed. IR spectral changes were similar to those found after *in vivo* degradation (56). DSC analysis showed that hydrogen peroxide-induced degradation resulted in greater mobility in the soft domain. Studies conducted with low molecular-weight model compounds for the hard- and soft-segments confirmed that the methylene group adjacent to oxygen in these materials was susceptible to oxidation. A series of polyurethanes containing various polyol soft-segments that were aged in $AgNO_3$ solution suffered from surface cracking (56). However, the oxidative resistance in those polyurethanes containing aliphatic hydrocarbon soft-segments (e.g. hydrogenated poly(butadiene) HPBD) was significantly improved over the PTMO based-polyurethane (57).

In vivo Degradation of Polyurethanes

For implanted polyurethanes, degradation occurs in part due to poor biostability. Thus, biodegradation is defined as "the structural or chemical changes in a biomaterial that are initiated or accelerated by vital activity of the biological environment" (33). Hence, biodegradation can not be directly equated with the *in vitro* degradation of a biomaterial, since the latter does not involve the complete vital activity of the host organ (33).

Following implantation of a biomaterial, wound healing, as well as responses to foreign bodies, will occur. The sequence of these events is illustrated in Figure 2.12. Immediately following injury, fluid, proteins and blood cells escape from the vascular system into the injured tissue in a process called exudation. The effect of the injury and/or the biomaterial *in situ* on plasma or cells can produce chemical factors that mediate many of the vascular and cellular responses of inflammation (58,59). The predominant cell type present in the inflammatory response varies with the age of the injury. In general, neutrophils predominate during the first several days following injury - this period is called acute inflammation. The major role of the neutrophils in acute inflammation is to phagocytose microorganisms and foreign materials.

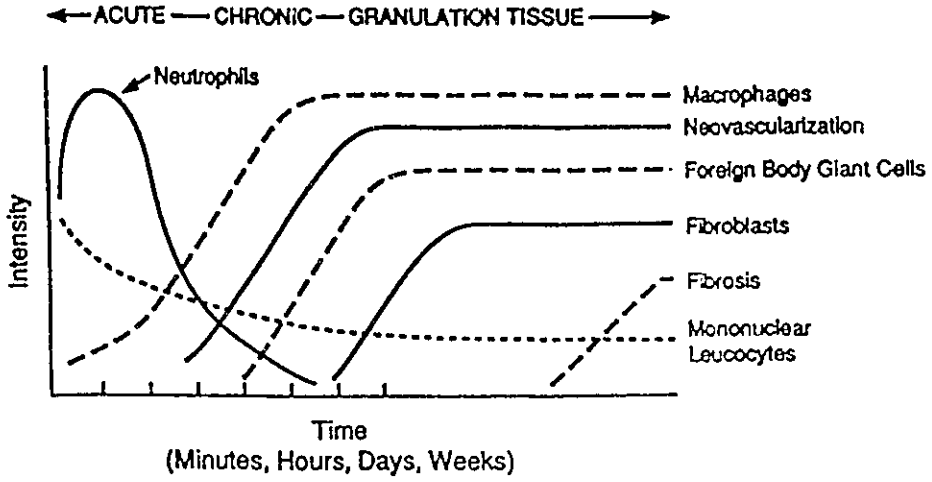

Figure 2.12. The sequence of events following implantation of a biomaterial (60).

The neutrophils are then replaced by monocytes as the major cell type for several reasons: (i) neutrophils are short-lived, disintegrating after 24 to 48 hours; (ii) following emigration from the vasculature, monocytes differentiate into macrophages, and these cells are very long-lived (up to months); and (iii) monocyte emigration may continue for days to weeks, depending on the injury and implanted biomaterial. This period of monocyte activity is referred to as chronic inflammation.

Although biomaterials are not generally phagocytosed by neutrophils or macrophages because of their size and disparity (i.e. the surface of the biomaterial is greater than the size of the cell), "frustrated phagocytosis" may occur (60,61). This process does not involve engulfment of the biomaterial but does cause the extracelluar release of leukocyte products in an attempt to degrade the biomaterial (62,63). Chronic inflammation is characterized by the presence of macrophages, monocytes and lymphocytes, with the proliferation of blood vessels and connective tissue (64-66). The macrophage is probably the most important cell in chronic inflammation. Its attachment to polymeric implants is well known, and cellular enzyme activity at the polymer-tissue interface associated with this cell has been reviewed (59). In fact, macrophages possess a formidable array of chemical weapons designed to digest foreign objects in the body. They contain a number of enzymes that can break down all manner of chemical structures; for example esterase-cleaving enzymes are released, such as cholesterol esterase, which can attack the urethane, urea, and ester bonds in polyurethanes (67). The release of superoxide and hydrogen peroxide from macrophages has also been documented (68). It is suspected that these oxidative agents do not necessarily cleave polymer chains, but assist the hydrolytic enzymes to degrade polyurethanes. It is therefore difficult to design polyurethanes that are inert to all the reactive species that macrophages can direct against the implant.

The number of enzymes and chemicals involved, and their potential interactions, also make it difficult to design model systems to mimic macrophage attack. However, quantitative *in vivo* evaluation of the components of the inflammatory response has been carried out using a subcutaneous wound cage system in order to assess the biocompatibility of specific biomaterial polymers (69,70). Polymers such as Biomer®,

Pellethane®, polydimethylsiloxane (PDMS) and low-density polyethylene (PE) have been evaluated using this system (71-73). These data support the notion that implantation stimulates acute and chronic inflammatory responses which lead to the formation of foreign-body giant cells on the polymer surface (provided that these macrophages are able to adhere to it), followed by the release of enzymes and/or other factors that may degrade the polymer. Hence, a strategy to prevent degradation might be to provide the polyurethane with a surface that is more biocompatible, allowing good cell growth so that the implant can be quickly covered with scar tissue and integrated into the surrounding tissues.

Enzyme Induced Degradation

Enzymes are often considered to be the main contributors to biodegradation since the consequence of cell-polymer interactions is the release of oxidative and hydrolytic enzymes. Although it is not normally thought that enzymes are able to catalyze the degradation of synthetic polymers which form a solid substrate, the characteristic ability of enzymes to reduce the activation energy of chemical reactions permits a degradation process within the aqueous enzyme-containing environment.

Ratner et al. (74) evaluated three polyether-urethanes and one polyester-urethane treated with papain, chymotrypsin or leucine aminopeptidase. They observed variations in molecular weight and polydispersity and found that the polyester-urethane underwent the least amount of degradation, which was unexpected given their reported susceptibility to hydrolytic degradation in comparison to polyether-urethanes. Further, Bouvier et al. (75) demonstrated the degradation of a polyether-urethane after incubation for 5 months in a concentrated trypsin solution. They observed changes in polymer chemistry using Fourier transform infra-red spectroscopy (FTIR) and attributed this to the degradation of the polyether soft-segment. Both Marchant et al. (76) and Zhao et al. (77) found degradation of a polyether-urea-urethane by a papain over a period of two weeks to one month after incubation occurred, primarily at the surface of the polymer. Phua et al. (78) observed enzyme-mediated degradation of Biomer® by papain and urease. In that

case the onset of degradation was assessed over periods of one to six months.

Based on the knowledge that biodegradation occurs *in vivo* by hydrolysis or oxidation, Smith et al. (79) studied the enzymatic degradation of a polyether-urea-urethane, which resembles Biomer®, by hydrolytic enzymes such as trypsin, chymotrypsin, esterase, papain, bromelin, ficin, cathepsin C and collagenase, as well as oxidative enzymes such as xanthine oxidase and cytochrome oxidase. Using a series of ^{14}C-labelled polyurethanes, degradation was measured up to 15 days after incubation in the various enzyme solutions. This new method yielded rate data by assuming that the extent of degradation could be represented by the release of the radiolabelled compounds into the incubation solution. From the daily measured d.p.m. (disintegration per minute), they observed that the polyether-urethane was affected by esterase and cathepsin. However, no effect was observed with either of the oxidative enzymes or with collagenase. Oddly enough, the d.p.m. values for papain, bromelin, ficin, chymotrypsin, trypsin were repeatedly lower than the values associated with the controls. This reversed behaviour was thought to be due to the enzymatic degradation of polyurethanes by a mechanism resulting in products that were not retained in the incubation solution, and hence not detected during subsequent measurement of radioactivity. In a further study (80), these same researchers synthesized a similar polyether-urea-urethane which contained more hard-segments than the previous one, and they found that this polymer was sensitive only to esterase. They also tested the effect of liver homogenate on the Biomer®-like polyurethane. The results showed that liver homogenate could degrade this polymer. But, polyether-urethanes prepared from polyethers of molecular weights of 650 or 2000 were unaffected by any of the enzymes.

Santerre et al. (67) reported the effects of cholesterol esterase, collagenase, cathepsin B and xanthine oxidase on polyester-urea-urethanes and polyether-urea-urethanes. Using the radiolabel technique discussed above, the extent of degradation was determined for both materials at incubation times of up to 30 days. They observed that the polyester-urea-urethane was susceptible to enzymatic degradation by cholesterol esterase but not by the other enzyme systems. Recently, they found that polyether-urea-urethanes were also prone to degradation by cholesterol esterase but required five-fold

more cholesterol esterase to yield significant amounts of radiolabel release (81). Furthermore, they observed that polyester-urea-urethanes could be degraded by elastase (82) and carboxyl esterase (83).

Different enzymes are likely to degrade polyurethanes by different mechanisms (69). Most of the work has made use of hydrolytic enzymes *in vitro* and it has been proposed that papain hydrolyses urethane and urea linkages while urease attacks urea linkages only (70). Hence studies suggest that hydrolytic enzymatic attack may preferentially occur at the urea and urethane linkages located in the interphase between soft and hard regions, as those linkages are more accessible (67). Little is understood about the detailed mechanism of enzymatic biodegradation. Duguay et al. (84) recently presented a mechanistic model for the degradation process which highlights the importance of enzyme adsorption and surface chemistry. This model simulated various interactions of the polymer and enzyme, leading to a better understanding of the enzymatic degradation process.

The oxidative enzymatic attack *in vitro* also remains poorly understood because of the short life of the oxidative species produced by oxidative enzymes. Santerre et al. (85) incubated radiolabelled polyether-urethane and polyester-urethane with horseradish peroxidase and found no liberation of radiolabelled segments from either the polyether or polyester polyurethanes. However, Anderson et al. (86) proposed an oxidative degradation mechanism for the *in vivo* degradation of polyether-urethanes. According to their observation, the process starts with macrophage adhesion, activation and foreign-body giant cell (FBGC) formation onto the implanted polyether-urethane. Activated macrophages and FBGC release superoxide anion radicals and enzymes, and acidify the local interfacial environment. The superoxide anion radicals rapidly combine with protons to form hydroperoxide radicals. It is proposed that this oxidative species, the hydroperoxide radical, then attacks the α-carbon of the polyether-urethane soft-segment and subsequently oxidizes it to an ester linkage. Since the ester group is not stable in the presence of esterase or acid, it is hydrolysed to a carboxylic acid and alcohol.

2.4. Inhibition of Polymer Biodegradation

Although biodegradation of medical polyurethanes used in long-term implants remains a problem, the desirable mechanical properties (fatigue life, tensile strength, and elongation) of polyurethanes for use in a large number of applications have provided the incentive to resolve this issue. This has led to many studies on the mechanism of biodegradation and the development of new polyurethanes which are less susceptible to degradation.

For example, VASOR, Inc. has developed a non-ether polyurethane (87) in order to avoid the susceptibility of polyether macroglycols to oxidation. Three monomers were used to form the experimental polyurethane: an aliphatic diisocyanate, an ether-free macroglycol, and 1,4-butanediol (BD). The specimens of the experimental polyurethane, a positive control elastomer, and a negative control elastomer were exposed for six months to an *in vivo* (rabbit) environment which was conducive to the formation of microcracks. No indication of degradation was observed in the experimental polymer. However, the mechanical properties of this new material have not been reported.

Due to their resistance to hydrolytic degradation, polyether macroglycol-prepared polyurethanes are still used in medical applications. Gunatillake et al. (88) tried to change the chain length of polyethers and prepared polyether macrodiols that contained 6, 8, or 10 carbon atoms between the ether oxygen. The resulting macrodiols were more hydrophobic than PTMO. New polyurethanes were then synthesized with MDI (4,4'-diphenylmethanediisocyanate) and BD. Hydrogen peroxide and sodium hypochlorite were chosen as representative oxidative reagents for *in vitro* testing. The hydrolytic stability was assayed under neutral, acidic (2 M hydrochloric acid) and basic conditions (5 M sodium hydroxide). Results indicated that the new polyurethanes were more resistant to hydrolysis and to hydrogen peroxide-induced oxidation than were the PTMO-based materials. The polyoctamethylene oxide-based polyurethane displayed good resistance to sodium hypochlorite. However, these new polyurethanes were bulk synthesized and their chemical, physical and mechanical properties were highly dependent on the reaction conditions as well as stoichiometry, leading to variable biodegradation properties.

Some other approaches to enhance polyurethane stability, such as incorporating polydimethylsiloxane, hydrogenated polybutadiene or polyethylene oxide soft segments into polyurethane hard segments have been investigated by Cooper et al. (89-91). This group has also considered sulfonate grafted polyurethanes. Polydimethyl siloxane containing polyurethanes showed severe degradation when exposed to oxidative conditions in the presence of organic carboxylic salt, though this same polymer did not degrade in pure oxidative environments. Polyethylene oxide, meanwhile, was susceptible to hydrolysis and oxidation. In contrast, hydrogenated polybutadiene seemed to perform relatively well in these specific studies. Sulfonated polyurethanes with antioxidants performed well in short-term tests; however, without these stabilizers they demonstrated cracking after one month of exposure (92). On the other hand, in 2,4, and 6 month implant studies Han et al. (93) demonstrated favourable results for a sulfonated polyether urethane in regards to both biostability and calcification resistance.

Recently, Ward et al. (94) coupled surface-active (oligomeric) end-groups, which had a range of chemical structures and/or optional functional groups, to the polymer chain during synthesis via a terminal isocyanate group. The oligomeric end-groups were shown to have a higher tendency to migrate to the surface and thus yield a new surface chemistry. In this manner, the original polymer backbone was left intact so that the polymer retained its strength and processability. Using hydrophobic and hydrophilic end-groups, amphipathic structures resulted in which the hydrophobic/hydrophilic balance could be easily varied. However, no *in vitro* or *in vivo* biostability tests have been performed to date.

Given that the ether and ester bonds in the previous polyurethanes were the weak links with respect to biodegradation (95-98), Corvita Corporation (Miami, FL) developed a new "biostable" material, Corethane™ , a polycarbonate urethane, which consisted of a poly(1,6-hexyl 1,2-ethyl carbonate) diol as the polycarbonate macroglycol. The diisocyanate and the chain extender were MDI and BD respectively. Using the Stokes' 400% stain method (6) in rabbits for period of up to 6 months, all Pellethane® 2363-80A control samples demonstrated breakthrough and severe surface cracking, whereas no breakthrough of Corthane™ samples occurred. Further, the surfaces of the latter

samples, as examined by SEM, were smooth and free of cracks (99, 100). In addition, it was shown that Corethane™ samples appeared resistant to strong oxidizing acid (0.5 M nitric acid) as were Pellethane® samples (101). Corethane™ was also found to demonstrate better resistance to hydrogen peroxide attack than the polyether urethanes (103). Coremer™ polycarbonate urea urethane, the polyurea version of Corethane™ , has been used for high flex fatigue applications, such as left ventricular assist device pump diaphragms and the membranes on the artificial heart. However, biostability data on Coremer™ is not available at this time (102).

In summary, because of the lack of knowledge regarding the biological mechanism of the biodegradation process, the overall stability in demanding applications, such as long-term medical implants (e.g. pacemaker leads), remains an area in which there is much need for improvement.

2.5. Surface Modification of Polyurethanes

Polyurethane elastomers provide a number of distinct advantages over other elastomers. These include their higher tensile strength that allows the size of components to be reduced, as well as a wider durometer range permitting the polymer's stiffness and rigidity to be custom-tailored to the application. Such properties are usually attributed to the aggregated semicrystalline structure of the hard segment, combined with the amorphous nature of the soft-segment (76). It is therefore important to maintain the bulk properties of polyurethanes when considering modifications to enhance their stability. In addition, there is good experimental evidence to show that the blood-material interactions which occur at smooth surfaces are only affected by the composition of the upper few molecular layers of the polymer (103). Given this, many investigators have concentrated on the surface region, rather than the bulk polymer, in order to improve biocompatibility. This has led to the development of several surface modifying agents that have been introduced into polyurethanes to change their surface chemistry while retaining the bulk polymers' properties.

2.5.1. Biological Modification of Polyurethanes

The surface modification techniques of polyurethanes have been developed in two ways. The first one incorporates a biological component using a variety of bio-active species such as heparin and heparin fragments, heparinase, urokinase, streptokinase, albumin and endothelial cells (104) . Heparin, for example, is commonly employed as an anticoagulant. In work by Park and colleagues (105), heparin was immobilized onto a polyurethane and the surface shown to adsorb fewer platelets and inhibit the release of platelet-derived agents. However, heparin can also sometimes cause undesirable acute effects (e.g. haemorrhage, anaphylaxis and thrombocytopenia) and chronic complications (e.g. osteoporosis, hyperlipidaemia and alopecia) (105).

Endothelial cells have been used in an attempt to cover synthetic vascular grafts with cells that elicit antithrombotic activity. However, this work has not been successful to date. Other biological entities (e.g. enzymes, amino acids, antibodies, and other proteins, antigens, peptide sequences, nucleic acids, DNA and RNA sequences, microbial and mammalian cells) have likewise been incorporated onto polyurethanes in order to prepare compatible composites (106). Because these components are not covalently attached to the polymer surface, the major drawback of these methods is that the lifetime of the incorporated component, in constant contact with biological media, is reduced due to leaching or diffusion from the surface.

2.5.2. Chemical Modification of Polyurethanes

A second approach to surface modification is related to chemically altering the surface. This method is based on the knowledge that a material having a low surface free energy will display good blood compatibility (107), and on the notion that an interfacial energy tending towards zero at the blood-polymer interface may be considered to be antithrombogenic. Hari et al. (108) grafted HEMA (a polymerizable monomer), acrylamide and polyethylene glycol (PEG) onto a dualistic polyurethane (Angioflex) using a preswelling technique preceded by exposure to γ-irradiation. They optimised the surface free energy of the materials to about 35.0 ergs/cm^2 (this value was obtained from

contact angle data which were related to surface tension). They then measured the protein adsorption as well as platelet and lymphocyte adhesion on these surfaces. It was observed that both platelet and lymphocyte adhesion onto the modified surfaces were significantly reduced compared to the untreated surface. Further, the mole ratio of fibrinogen to albumin adsorbed was lower on the modified surfaces, suggesting that the modified surfaces had better antithrombogenicity in accordance with Brash's observation (109) that a lower fibrinogen/albumin mole ratio indicates better antithrombotic properties.

Ionic groups such as sulphonate have also been incorporated onto polyurethanes. Hergenrother et al. (110) formulated sulphonated polyurethane blends made from highly sulphonated polyurethanes mixed with the unsubstituted base polyurethane (Pellethane 2363-80A). XPS data revealed some enrichment of the sulphonate component at the polymer's surface when compared to its bulk composition. Deposition profiles indicated that the blended polymer experienced less platelet adhesion while no difference in fibrinogen adsorption was observed between the two materials. It was concluded that further studies were needed to determine the proper ratio of sulphonated to non-sulphonated materials in order to achieve changes in both platelet adhesion and fibrinogen adsorption.

A polymer surface can also be modified by plasma reaction of a gas which does not deposit on the material but rather chemically modifies the surface. Several kinds of gases, such as argon, hydrogen, oxygen, nitrogen, water, ammonia, and carbon monoxide, can be used. The irradiation effect of the plasma causes the modification of the polymer surface by creating chemically reactive species. Thus the modification is limited to a very thin layer at the surface and consequently the bulk characteristics of the polymer are preserved (111). The biocompatibility of such films can be altered by changing the composition of the gas. Yasuda et al. (112) developed a plasma film prepared by deposition of volatile carbon-oxygen organic compounds onto solid supports, and the materials showed promising results for culturing cells.

The unique chemical and thermal stability of fluorinated polymers led to early and sustained interest in their potential applications. Auman (113) developed rigid fluorinated

dianhydrides, which have been shown to reduce not only the moisture absorption and dielectric constant, but also the thermal expansion coefficient. Such materials have also been found to be largely insensitive to standard solvents. Some perfluorocarbon polymers (that is, polymers containing only carbon, fluorine and oxygen) have also been developed and include homopolymers of polytetrafluoroethylene (PTFE), copolymers of tetrafluoroethylene (TTE), and fluorinated ethylene propylene (FEP). These polymers display high crystalline melting points (greater than 250°C), high melt viscosities, and high thermal stability (114). The reason for their stability rests with the inert nature and strength of the covalent bonds between the elements in the polymer chain. There are various uses of PTFE and FEP for prosthetic implantation (115, 116). However, the material was seen to stiffen as early as 6 months post-implantation.

Han et al. (117) grafted perfluorodecanoic acid (PFDA) onto the surface of a polyurethane (Pellethane 2362-80A, called PU later). The surface structure and the chemical nature of the highly hydrophobic PFDA-grafted PU were examined using a series of surface analysis techniques. XPS data demonstrated C-F enrichment at the outermost layer. SIMS (static secondary ion mass spectroscopy) experimental data also supported this result. Meanwhile, the critical surface tension, γ_c, of the PU-PEDA surface revealed the extremely low value of 6.9 dyn/cm due to the optimal orientation of $-CF_3$ groups to the uppermost surface. Furthermore, they compared the contact angle value of the PU-PFDA surface with the untreated PU and found that the modified surface had a significantly higher advancing contact angle than that of untreated surface. It is known that fluoropolymers having a γ_c of 5-10 dyn/cm exhibit a water/oil repellence because of their inert character and low surface free energy (118). Accordingly, it was thought that the PFDA-grafted PU surface may contribute to improved blood compatibility, since blood's main component is water. In later experiments, these researchers compared platelet adhesion and deformation on the surface of PU-PFDA, PU and hydrophilic PEO (polyethylene oxide) grafted PUs, and found that the hydrophobic surface was significantly more blood compatible than that of the untreated PU surface. It was also interesting to note that the enhanced blood compatibility of the very hydrophobic PU-PFDA was equivalent to that of the hydrophilic PU-PEO surface (119).

This highlights the need for careful interpretation of surface analysis data with respect to predicting the outcome of biocompatibility testing.

The method of incorporating additives into polyurethanes for improving blood compatibility was originally proposed by Ward et al. (120) as early as 1984. They showed this method was efficient because only a small weight percentage of additive was required to modify the surface properties, while the bulk properties remained unchanged. Their surface modifying amphiphilic polymer additive showed very promising results for implanted polyether-urea-urethane catheters (120). It has also been noted that the commercial polyurethanes such as Biomer® contained a standard antioxidant, a polymeric additive. To test whether this additive contributed to the biocompatibility of Biomer®, Branstedt (121) mixed an antifoam agent, Methacrol 2138F, (poly(diisopropylaminoethyl methacrylate-co-decyl methacrylate)), which was similar to the additive in Biomer®, into a base polyether-urea-urethane which had the same composition as Biomer®. The results indicated that, with loading of this additive, the degree of protein adsorption was significantly reduced.

Ratner et al. (122) blended Advawax (Morton Thikol), a stearamide used as an extrusion lubricant for processing polyurethanes, into commercial Pellethane®. A C_{1s} spectrum showed that the surface of the polymer mixture looked almost identical to that of the Advawax alone. Hence, adding Advawax transformed the surface into a highly hydrocarbon-rich environment which was believed to reduce platelet adhesion. However, their experiments also showed that the chemistry at the surface of the polymer mixture returned to that of the commercial Pellethane® after exposure to water. The effectiveness of surface-active additives to enhance biocompatibility has been debated, since the additives may leach out of the polymer matrix because they are not covalently bonded with the base polymer. This, in turn, could lead to a toxic response or further biostability problems (33).

2.6. Research Objective

From this overview, it is apparent that polyurethanes remain very promising biomaterials. However, the materials now available need to be improved with respect to their biocompatibility and biostability. The findings in the above studies provide the impetus for the following work, which seeks to develop a fluorinated polymeric additive, a surface modifying macromolecule (SMM), which not only remains at the surface of a polymer substrate to protect polyurethanes from hydrolytic enzyme degradation, but also interacts with the base polymer to reduce its chance of being leached out. The biodegradation of the new materials will be studied with a hydrolytic enzyme in order to test their ability to stabilize the polyurethane base polymer.

3. EXPERIMENTAL PROCEDURES

3.1. Materials

Materials used for the synthesis of the base polyurethane, a polyester-urea-urethane, are listed in Table 3.1, and those used for the surface modifying macromolecules (SMMs) are indicated in Table 3.2.

Table 3.1. Materials used in base polyurethane synthesis.

Material	Supplier	Abbreviation
Toluene-2,4-diisocyanate	Eastman Kodak, Rochester, NY., U.S.A.	TDI
Polycaprolactone Diol 1250	Aldrich Chemical Company, Milwaukee, WI., U.S.A.	PCL
Ethylenediamine	Aldrich Chemical Company, Milwaukee, WI., U.S.A.	ED
Prepurified Nitrogen	Canox, Toronto, ON., Canada	Nitrogen
^{14}C-Toluene-2,4-diisocyanate	NEN Dupont, Mississauga, ON., Canada	^{14}C-TDI
Dimethyl Sulphoxide	BDH, Toronto, ON., Canada	DMSO

3.2. Material Preparation and Polymer Synthesis

This section outlines the experimental procedures for the synthesis of the base polyurethane and SMM materials. Material preparation for both base polymer and SMM synthesis will be introduced first and the detailed synthesis procedures for these materials

will be described separately. All polymers were prepared using the same general procedure. However, some specific reaction conditions had to be determined for both the base polyurethane synthesis and SMM synthesis in order to obtain polymers having suitable mechanical properties and optimal molecular weight.

Table 3.2. Materials used in SMM synthesis.

Material	Supplier	Abbreviation
1,6-Diisocyanato-hexane	Aldrich Chemical Company, Milwaukee, WI., U.S.A.	HDI
Polypropylene Oxide 1000	Aldrich Chemical Company, Milwaukee, WI., U.S.A.	PPO
Polytetramethylene Oxide 1000	Dupont, Mississauga, ON., Canada	PTMO
Zonyl® BA-L Fluorotelomer Intermediate	Van Waters & Rogers Montreal, QC., Canada	BA-L
N,N-Dimethylaceta-mide	Aldrich Chemical Company, Milwaukee, WI., U.S.A.	DMAC
Dibutyltin Dilaurate	Aldrich Chemical Company, Milwaukee, WI., U.S.A.	Catalyst
1,1,2,-Trichlorotri-fluoroethane (99.9%)	BDH, Toronto, ON., Canada	TCTFE
Acetone	BDH, Toronto, ON., Canada	
^{14}C-1,6-Diisocyanato-hexane	Aldrich Chemical Company, Milwaukee, WI., U.S.A.	^{14}C-HDI

3.2.1. Solvent Distillation

Due to the reactivity of diisocyanates with water, solvents were distilled within 24 hours of their use in the polymer synthesis. Approximately 400 mL of dimethyl sulphoxide (DMSO) was distilled for each base polyurethane reaction, while 200 mL of N,N,- dimethylacetamide (DMAC) was distilled for each SMM reaction. DMSO was distilled at about 45°C and approximately 8 mPa (as indicated by gauge pressure), while DMAC was distilled at about 30°C and approximately 8 mPa. The distillate was collected in a dry flask, which was then capped, sealed with teflon tape and stored in a refrigerator until needed. A schematic diagram of the distillation apparatus is shown in Appendix 1.

3.2.2. Oligomeric Diol Degassing

Prior to their use in the synthesis, polycaprolactone diol (PCL) was degassed at 60°C, polytetramethylene oxide (PTMO) was degassed at 55°C, and polypropylene oxide (PPO) was degassed at 50°C. In each case the degassing was carried out for 24 hours at a pressure of approximately 8 mPa. This treatment removed trace amounts of water and other undesirable low molecular weight impurities.

3.2.3. Diisocyanate Distillation

Toluene-2,4,-diisocyanate (TDI) and 1,6-diisocyanato-hexane (HDI) were distilled at approximately 70°C and 0.8 mPa in order to purify the material and remove any dimerized diisocyanate from the commercial materials. In each case, glass wool was used to insulate the condenser to maintain the temperature for distillation. The first 25 mL of these two diisocyanates collected was discarded. The distilled diisocyanates were then stored in sealed bottles at 4°C until required for the synthesis.

3.2.4. BA-L Distillation

BA-L was separated into three fractions through a combination of atmospheric and vacuum distillations. The first fraction, called BA-L (Low), was distilled at 102°C at atmospheric pressure as a clear liquid. The second fraction, BA-L (Int), was distilled between 70 and 80°C at 4 mPa pressure as a white semisolid material. The last fraction, referred to as BA-L (High), was distilled between 80 and 100°C at 4 mPa as a light yellow solid (for details of the complete separation procedure, see Appendix 2).

3.2.5. Base Polyurethane Synthesis

A positive control polyurethane (i.e. a polyurethane that could be enzymatically degraded) was synthesized in order to validate the protective character of the SMM materials. Previous work in our lab had shown that the poly-ester-urea-urethane, TDI/PCL/ED, could be degraded by cholesterol esterase and other enzymes (67, 81-83).

The base polyurethane synthesis was performed using a two step procedure: (i) the prepolymer formation and (ii) the chain extension. A reaction scheme is shown in Figure 3.1. For the prepolymer preparation, a 2.2:1 mole ratio of TDI:PCL was used. A 15% w/v solution of TDI dissolved in freshly distilled DMSO was added dropwise to a batch reaction vessel containing a 40% w/v solution of PCL dissolved in DMSO and held at approximately 60°C under a dry nitrogen atmosphere, in a glove box. After reacting the heated mixture for 2 hours with stirring, the prepolymer was cooled to room temperature. Note that reaction temperatures in excess of 80°C would favour undesirable side reactions such as allophanate and biuret formation (36); hence the reactor temperature was maintained within a range of 60 to 70°C.

The second step of the polyurethane synthesis shown in Figure 3.1 is the chain extension of the prepolymer. The chain extender was added to the prepolymer according to a molar ratio of 1.2:1, which assumed that the NCO function left in the prepolymer which would react with the NH_2 function in chain extender, provided complete conversion of reactants in the first step took place. ED-DMSO solution (2.5% w/v ED) was added dropwise to the cooled reaction mixture (i.e., at 25°C) from the prepolymer

STEP 1

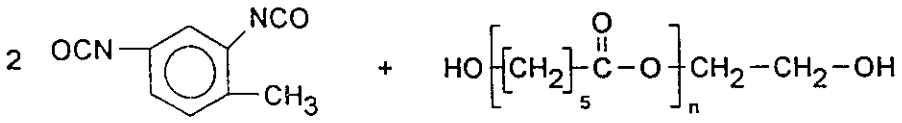

TDI PCL

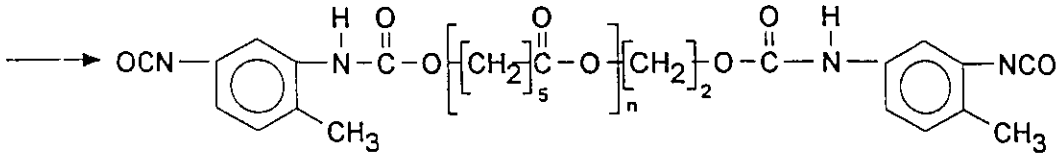

prepolymer

STEP 2

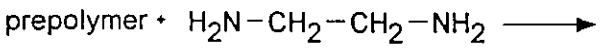

ED

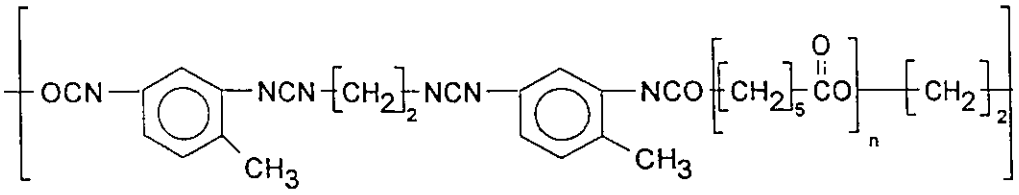

hard segment soft segment

Base Polyester -urea-urethane

Figure 3.1. Synthesis procedure of base polymer TDI/PCL/ED.

synthesis while stirring. As the reaction progressed the mixture became very viscous. This reaction was usually completed within 15-20 minutes, yielding a gel. The gel was then left overnight to dissolve back into solution. The viscous polymer solution was subsequently precipitated in distilled water and the washed polymer was chopped into small pieces. The pieces were washed in distilled water several times to remove residual DMSO and dried in an oven at 50°C for 48 hours. Once the polymer was dry, it was redissolved in DMSO at 15% w/w and centrifuged at 3000 rpm for 30 minutes at room temperature. Centrifugation was done to purify the solution by removing any insoluble substances such as gels of undissolved polymer. Upon purification, the polymer solution was reprecipitated while stirring in distilled water. Again, the polymer was cut into small pieces and washed several times in distilled water and finally put onto a Teflon® sheet and dried in an oven at 50°C for 48 hours.

The ^{14}C-radiolabelled analog of the base polymer ^{14}C-TDI/PCL/ED was synthesized for biodegradation testing. The ^{14}C-TDI was custom synthesized by Dupont Canada (product# CUS030C). For the polymer synthesis, ^{14}C-TDI was added to the non-radiolabelled TDI in order to yield a total TDI aliquot for the polymerization that contained 0.2 mCi (milli curie). This amount of radiolabel would yield a detectable count of released product from the polymer when incubated with cholesterol esterase (67).

3.2.6. Polymer Nomenclature

Before discussing the SMM synthesis, it is appropriate to introduce the nomenclature of abbreviations that identify the various polymers.

Because there was only one base polyurethane used in this work, it is simply referred to as TDI/PCL/ED or base polymer. The nomenclature used to identify the various SMMs was based on a sequence of alternating letters and numbers which identify the polyether type, stoichiometry and BA-L fraction associated with the specific polymer.

All SMMs investigated were synthesized using HDI. The molecular weight of the two polyethers (PPO and PTMO) used in the synthesis was approximately 1000. The

abbreviations for the polyethers used in the synthesis are defined in Table 3.2. An example of an SMM abbreviation is shown in Table 3.3.

Table 3.3. Sample SMM abbreviation.

e.g. PPO-322I	
PPO	Polypropylene oxide 1000 is the polyether used in this SMM synthesis.
322	The mole ratio of HDI:PPO:BA-L (Int.) is 3:2:2 respectively.
I	The intermediate fraction of BA-L is used here. Other fractions were defined in section 3.2.4.

3.2.7. Synthesis of Fluorinated Surface Modifying Macromolecules (SMMs)

There were twelve different fluorinated SMMs synthesized in the first stage of this work. HDI was used to replace the more classical aromatic diisocyanates (i.e. TDI and MDI) which have been reported to degrade to carcinogenic materials (50, 123). For example, toluenediamine (TDA), a product from degraded TDI, has tested "positive" for carcinogenicity in every carcinogenesis bioassay according to the material safety data sheet (MSDS) provided by the material supplier. However, hexanediamine (HDA), a product from degraded HDI, has not been tested in this type of assay according to the MSDS as well as the Merck Index hand book (124).

At the first stage of this work, twelve SMMs were synthesized without systematic formulation. The reactant mass and solvent (DMAC) volume used for the prepolymer synthesis of the twelve SMMs are given in Table 3.4. Based on biodegradation test results described in section 3.5, only five of these twelve SMMs proceeded to the second stage of material development. A typical SMM is shown in Figure 3.2.

STEP 1

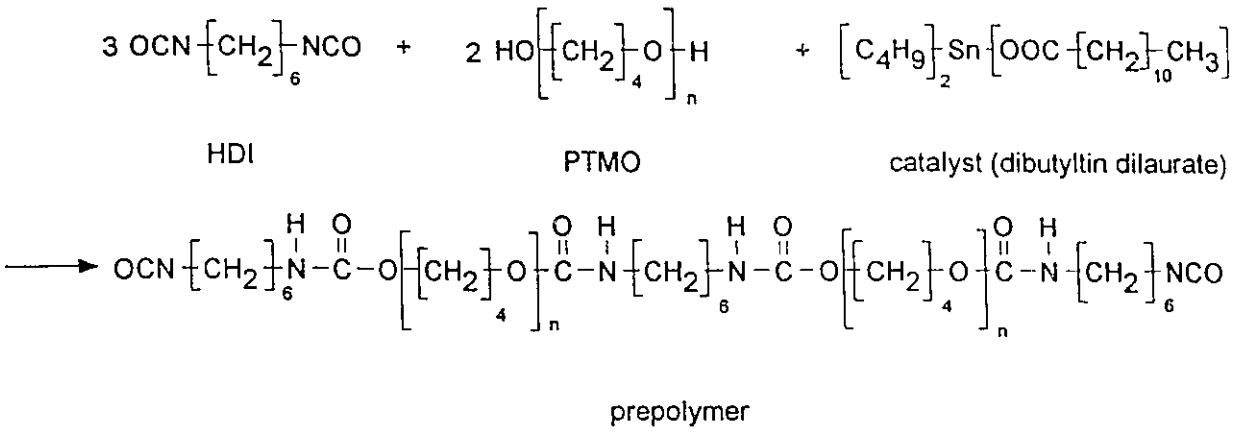

STEP 2

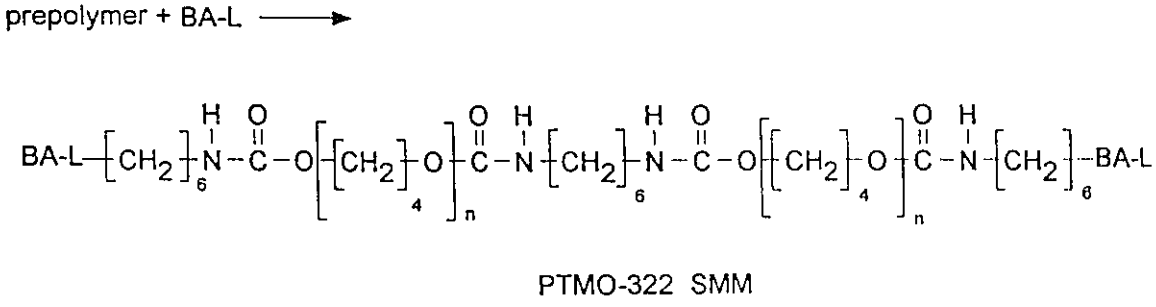

BA-L: $F_3C(CF_2)_m-CH_2-CH_2-OH$ m=odd number from 3 to 17

Figure 3.2. Synthesis procedure for PTMO-322 SMM.

Table 3.4. Materials and amounts used in the SMM synthesis.

Name of SMM	HDI (g)	PTMO /PPO (g)	BA-L (L) /BA-L (I) /BA-L (H) (g)	Catalyst (drop)	DMAC in prepolymer (mL)
PTMO-432I (SMM1)	2.24	10.0	4.0	4	70
PTMO-212L (SMM2)	3.36	10.0	9.0	3	70
PTMO-322L (SMM3)	2.52	10.0	5.0	3	70
PTMO-212H (SMM4)	1.68	5.0	4.5	2	60
PTMO-212I (SMM5)	1.68	5.0	4.5	2	60
PPO-212L (SMM6)	3.36	10.0	5.0	4	130
PPO-322I (SMM7)	2.25	10.0	9.0	3	130
PTMO-322H (SMM8)	2.52	10.0	9.0	3	130
PPO-322H (SMM9)	2.52	10.0	9.0	3	130
PTMO-322I (SMM10)	2.52	10.0	9.0	3	130
PTMO-432L (SMM11)	2.24	10.0	4.0	0.1 mL	70
PTMO-432H (SMM12)	2.24	10.0	4.0	4	100

Because of the low reactivity of HDI with polyethers, dibutyltin dilaurate was used to catalyze the polymerization. It was realised after the first stage of work that the amount of catalyst needed to be strictly controlled, since minimal changes in the amount

of catalyst introduced significant differences in the polymer product. 42.5 mg of dibutyltin dilaurate was used in each SMM synthesis. This provided just enough reactivity for the polymerization to proceed without yielding very high molecular weight SMMs. Those five SMMs selected to be synthesized in the second stage of the work were PPO-212L, PPO-322I, PTMO-322I, PPO-322H and PTMO-322H.

Because the materials in the second stage of this work is more important to this thesis, the following description of synthesis procedures will focus on those five selected SMMs. The synthesis included prepolymer and "end capping" steps. An HDI-DMAC (8.5% w/v HDI for the 3:2:2 stoichiometry, 11% w/v for the 2:1:2 stoichiometry) solution containing 42.5 mg of catalyst was poured into a polyether solution (10% w/v for the 3:2:2 stoichiometry, 15% w/v for the 2:1:2 stoichiometry). The contents of the reaction vessel were held between 60°C and 70°C and maintained in a dry nitrogen atmosphere. After reacting the mixture for two hours with stirring, the prepolymer was cooled to a temperature in the range of 45-50°C within 15 minutes and a BA-L/DMAC solution (40% w/v for the 3:2:2 stoichiometry, 50% w/v for the 2:1:2 stoichiometry) was then poured into the prepolymer in order to end cap the free diisocyanate. The capping procedure was allowed to run overnight at room temperature. The polymer was then precipitated in distilled water. Since the PTMO-SMMs were normally of higher molecular weight and elastomeric in nature, they had to be chopped in a blender after the first precipitation in order to wash out the DMAC and catalyst left inside the polymer matrix. The polymer was then washed several times in distilled water. In order to favour the capping reaction, excess BA-L was used in the synthesis and therefore there was residual BA-L in the polymer. In order to remove the excess BA-L, the SMMs were also washed with 99.9% 1,1,2-trichlorotrifluoroethane (TCTFE) overnight. (PPO-212L was washed in 50% acetone-water due to its higher solubility in TCTFE and 100% acetone.) The SMMs were then dried in a conventional forced air oven (Fisher Scientific Isoterp® Oven Model 630G) for 48 hours followed by further drying in a vacuum oven (Fisher Scientific Isotemp® Vacuum Oven Model 281A) at 50°C for 48 hours.

To test the stability of the SMMs, three SMMs were selected for synthesis with ^{14}C-HDI. These were selected on the basis of their superior biostability properties and

good reproducibility during synthesis. The polymers used in this study were synthesized with a mixture of 2.5 mCi ^{14}C-HDI (Dupont, CUS030C) added to the non-radiolabelled HDI.

3.3. Polymer Characterization

3.3.1. Bulk Elemental Analysis

Pure samples of SMMs and base polymer were sent to Guelph Chemical Laboratories Ltd. for elemental analysis. The various analytical methods used by this laboratory are summarized below.

Oxygen analysis was carried out using a Perkin-Elmer Elemental Analyzer. The sample was pyrolyzed in helium at 975°C over platinized carbon and the resulting oxygen converted to carbon monoxide at 670°C. The carbon monoxide was then converted to carbon dioxide, and the latter gas was measured using a thermal conductivity detector.

Carbon, hydrogen, and nitrogen content in the polymers were also determined using a Perkin-Elmer Elemental Analyzer. A weighed amount of sample was combusted at 1100°C in a pure oxygen environment. The gases formed, i.e. oxides of carbon, nitrogen and hydrogen, were then passed through an oxidation chamber (to ensure complete oxidation) followed by a reduction chamber. The resulting gases - CO_2, H_2O, and N_2 - were separated and analyzed by standard gas chromatographic techniques using a thermal conductivity detector. The instrument was calibrated using acetanilide and phemacetin standards. The weight percent of C, H, and N were then calculated.

Fluorine content was obtained in the following manner. A sample was combusted with sodium peroxide in an oxygen-rich atmosphere using a Schoniger oxygen flask with distilled water as the absorbing medium. An aliquot of the resulting solution (after filtration) was then titrated with thorium nitrate using alizarin red S as an indicator. The volume of required titrant was then used to determine the percentage of fluorine in the sample.

3.3.2. GPC Experiments

Gel Permeation Chromatography (GPC) is a technique for measuring molecular weight. It is based on the separation of molecules according to their relative sizes, the largest molecules being the first to leave the GPC column. The equipment used in this study included i) a reservoir containing the mobile phase which carried the sample solution through the system; ii) a Waters high pressure 501 solvent delivery system; iii) a Rhenodyne 7125 sample injector and precolumn filter; iv) a Waters thermostable oven for the columns; v) three ultrastyragel columns with three different pore sizes at 10^3 Å, 10^4 Å, and 10^5 Å; vi) a differential refractive index detector with temperature control at 80°C; vii) an IBM data acquisition system with analysis software; and viii) a solvent waste tank.

The mobile phase consisted of 0.05 M lithium bromide (LiBr) in N,N-dimethylformamide (DMF) (BDH Inc., Toronto). On the day before the analysis, the system was switched to this solvent system. A fresh batch of LiBr/DMF was prepared in a glove box (dry nitrogen atmosphere) prior to use since LiBr quickly absorbs water from the atmosphere. Polymer samples were prepared by dissolving 0.01 grams of dried polymer in 5 mL of the LiBr/DMF solvent. If the polymer was not completely dissolved, heat was applied to dissolve the sample. The solution was then filtered using a 0.5 μm PTFE filter. Prior to use, the GPC system was equilibrated for 1 hour. Polystyrene standards (Toson Corporation) were run to provide a calibration curve for the molecular weight determination. The molecular weights were therefore reported as polystyrene equivalent molecular weights.

3.3.3. Differential Scanning Calorimetry (DSC)

Differential Scanning Calorimetry (DSC) was used to characterize the thermal transitions of polyurethanes, and subsequently to assess the degree of microphase separation. The DSC equipment used in this work (model number 910, Dupont Instruments) was located at the National Research Council of Canada, Institute for Environmental Chemistry, Ottawa. Samples for the DSC experiments were prepared in

the following manner: DSC films were cast from 10% w/w solutions of base polymer or mixtures of base polymer and SMM in DMAC. Solutions were filtered through a 0.5 μm PTFE filter in order to remove particles and then poured into wells on a Teflon® sheet. The solvent was evaporated off in an oven at 50°C for 48 hours and the samples further dried in a vacuum oven for another 48 hours. The final sample sheet was approximately 1 mm thick. Each DSC sample size was approximately 6$\pm$2 mg. The specimens were pre-cooled to -160°C using liquid nitrogen. Data were recorded from -160°C to 220°C for the pure base polymer and SMM/base mixtures, to 120°C for the pure PPO-SMM, and to 150°C for the pure PTMO-SMM. Following heating, the samples were rapidly cooled to room temperature, then cooled to -160°C prior to performing a second scan. This second scan allowed for observation of the internal structure of the polyurethanes after their structural features have been relaxed by heating. Figure 3.3 shows the thermograms for two different scans. Usually, a third scan was run in order to check the peak stability of the thermograms. The DSC results present in this work will consist of those thermograms that were reproducible.

Depending on which SMM was being analyzed, a peak associated with the glass transition temperature of the soft-segment was always detected and then additional peaks

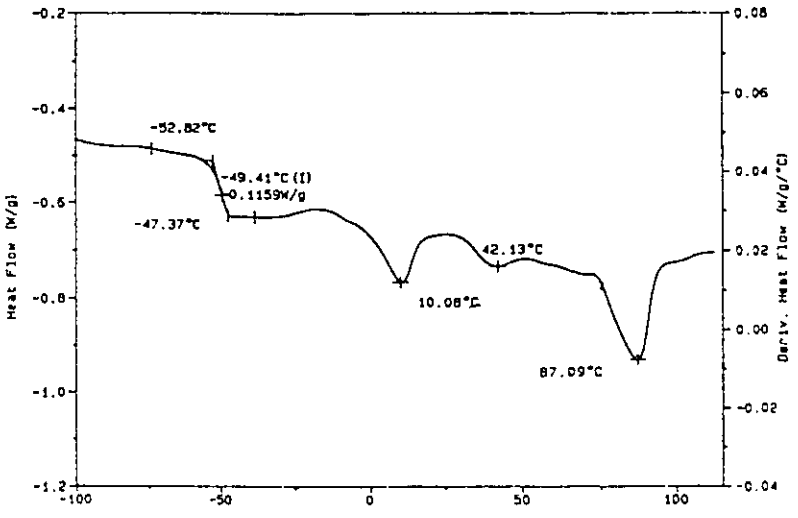

Figure 3.3 (A) Initial DSC scanning thermogram for PPO-212L.

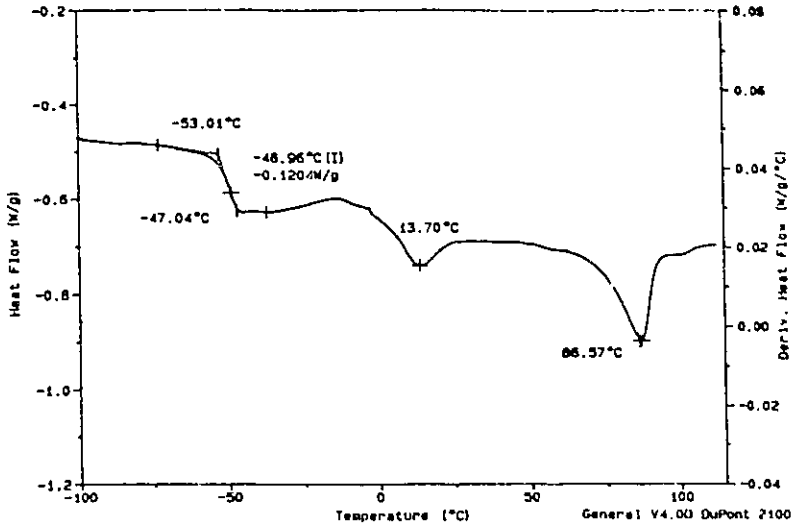

Figure 3.3 (B) Second DSC scanning thermogram for PPO-212L.

associated with various higher ordered structures (i.e. crystalline phases) were also observed for some SMMs. For example, it can be seen that the DSC thermogram for PTMO-322I (Figure 3.4) has a different profile than that of the PPO-212L (Figure 3.3). The first transition is the glass transition temperature for the soft segment matrix of the SMM. The second transition is the melting of the soft segment crystalline phase. In this study, the glass transition temperature (Tg) is reported as a temperature range, i.e. for PTMO-322I, the Tg range is -73.12 to -62.98°C.

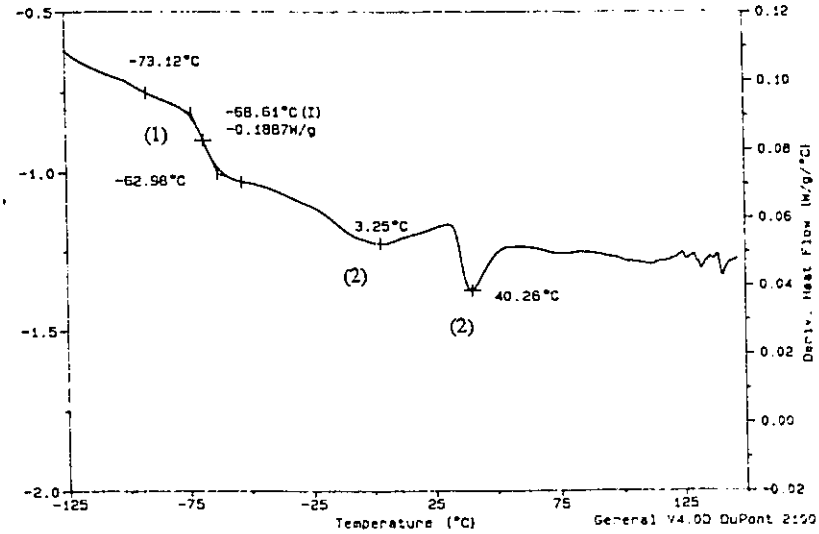

Figure 3.4. DSC curve for PTMO-322I 1) glass transition temperature; 2) melting temperature.

3.4. Material Surface Characterization

It is the surface of a biomaterial which interacts with the bio-environment. Hence, surface analysis techniques are needed to gain knowledge of the type of chemical structures present at the surface. Specifically, it was important in this study to determine whether the SMMs showed a preferential migration towards the surface of the base polymer. The following methods were employed to this end.

3.4.1. X-ray Photoelectron Spectroscopy (XPS)

XPS is useful for characterizing both elemental and chemical group composition at a material surface. In XPS, an X-ray beam is used to induce a photoelectron emission from the sample. The energy of the photoelectrons emitted identifies the chemical elements and their bonding environment, while the intensity of the emission gives the concentration of chemical species. Atomic concentrations can be determined with a relative accuracy of about 10% (44).

Material samples for XPS analysis were prepared with a 10% (w/w) solution ((total weight of SMM and base polymer)/weight of DMAC) of polymer in DMAC and then cast onto a clean aluminum dish. The SMM concentrations in the base polymer were 1.0%, 2.5%, 5.0% and 7.5% (weight of SMM/weight of total polymer). After drying in an oven at 60°C for 48 hours, the samples were further dried in a vacuum oven for another 24 hours. The surfaces were then washed with TCTFE (99.9%) and a foam applicator and rinsed with distilled water. This step was done in order to remove silicon contaminants accumulated at the surface. The samples were then wrapped with a Kimwipe® to act as a filter and dried in an oven at 50°C in order to remove the residue solvent, prior to being sent for analysis. XPS analysis was carried out at the Centre for Biomaterials, University of Toronto, Toronto, ON.

XPS measurements were performed at a series of takeoff angles to determine if a compositional gradient existed near the surface of the material. The takeoff angle was defined as the angle between the normal to sample surface and the analyzer lens; it controls the depth in the sample from which photoelectrons reach the detector (see Figure

3.5). By varying the takeoff angle, the chemical composition can be analyzed over a range of 20 Å (θ = 15°) to 100 Å (θ = 90°) in depth.

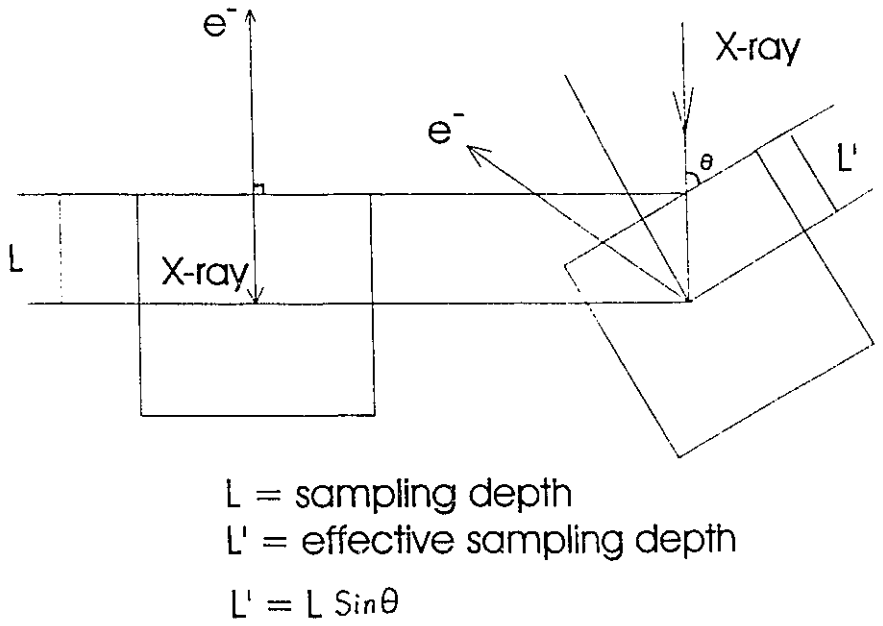

Figure 3.5. Schematic diagram of the takeoff angle in XPS analysis.

A low resolution/high sensitivity spectrum of each element present was obtained over the range of takeoff angles from 15 to 90°. Intermediate resolution spectra of carbon 1s (C_{1s}) peaks were used to detect the presence or absence of carbamate, hydroxyl/ether groups, C-C groups, $C\text{-}F_2$ groups, $C\text{-}F_3$ groups and the ester bonds. Figure 3.6 shows a typical intermediate resolution spectra.

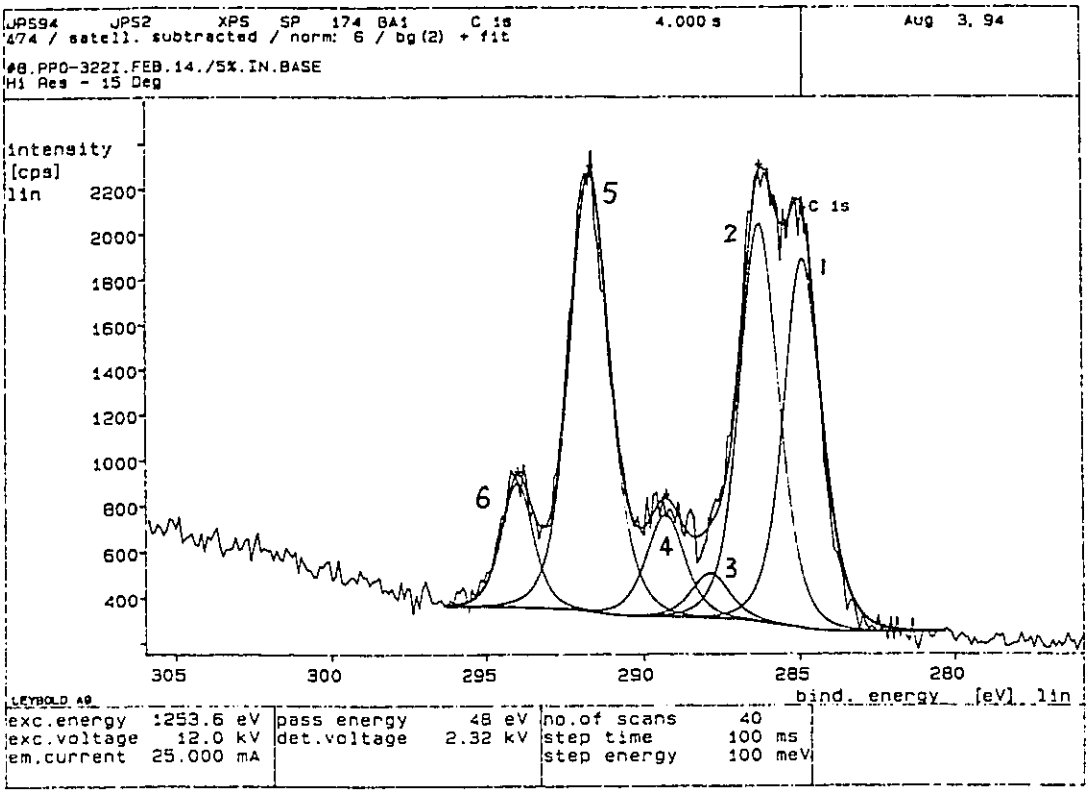

Figure 3.6. Typical XPS intermediate resolution spectra of carbon 1s peaks: 1) C-C; 2) C-O; 3) ester; 4) urethane/urea; 5) CF_2; and 6) CF_3 (provided by Dr. R. Sodhi, Centre for Biomaterial, University of Toronto).

3.4.2. Contact Angle Measurements

Water is the main constituent of all biological environments; therefore, it was appropriate to characterize the polymer surface in the aqueous phase. This was done by measuring water contact angles, which provided information on the hydrophilicity of the material surface. The polyurethane surfaces were prepared by a dip-coating technique. Glass slides were cleaned with chromic acid and were coated with a polymer solution and then dried in an oven at 50°C for 12 hours. Four coatings were needed to produce a smooth surface. Prior to taking measurements, the samples were allowed to cool to

room temperature. The coating solutions consisted of 10% polymer ((total weight of SMM and base polymer)/weight of DMAC). The SMM concentrations in base polymer solution were 1%, 2.5%, 5%, 7.5% and 10% (SMM/Base polymer).

The contact angle measurement was taken using a Contact Angle Goniometer (Rame-Hart Inc.). Five to ten μL of ultrapure water were pumped out from a micro syringe onto the surface of the film. Advancing and receding angles were measured by increasing or decreasing the volume until the three-phase boundary moved over the surface. As was discussed earlier, the advancing angle was more closely related to the hydrophobic chemistry of the material while the receding angle was more characteristic of the hydrated state of the surface. In order to obtain reproducible results, care was taken to avoid vibration and distortion of the drop during volume changes. Twenty readings were obtained for every sample and standard errors were calculated.

3.5. Biodegradation Test of Base Polyurethane and Polyurethane Containing SMM

A semi-batch system was used in this work to carry out the *in-vitro* biodegradation test for the materials. A radiolabelled base polymer ^{14}C-TDI/PCL/ED was synthesized, based on the radiolabelling technique of Santerre et al. (67). Cholesterol esterase (CE), a hydrolytic enzyme which is synthesized and released by monocyte derived macrophages, was used as a model enzyme in this study. Previous work demonstrated that this enzyme could degrade the polyester-urea-urethane (67). The details of the biodegradation test are described below.

3.5.1. Preparation of Coated Glass Tubes for Enzyme Experiments

The polyurethanes (^{14}C-TDI/PCL/ED without and with SMM) were coated onto small hollow glass tubes (3 mm O.D, 2 mm I.D) using a 10% w/w polymer-DMAC solution. This provided a standard surface area for each test sample. After the coated tubes were dried in an oven at 50°C for 24 hours, they were coated again. Altogether four coatings were required. After the final coating, the tubes were then allowed to dry

in a vacuum oven at 50°C for 48 hours under a vacuum at -100 KPa (gauge pressure). The resulting film thickness was approximately 10 μm. Following coating, the tubing was then sectioned into 10 pieces of 2.55 mm length and placed into a sterile 15 mL vacutainer® (Becton-Dickinson). A total surface area of approximately 36 cm^2 was obtained from the glass tubing. All incubation tubes were prepared and sampled in a laminar flow hood, employing sterile techniques including sterilized tips and vacutainers. The initial radioactivity of the tubes was determined by dissolving polymer from randomly picked sample tubes in DMAC and measuring the radioactivity with a liquid scintillation counter (LKB Instruments).

3.5.2. Incubation of Polymers with Cholesterol Esterase

The coated tubes were inserted into vacutainers with 0.05 M sodium phosphate buffer solution, pH 7.0, either without CE (i.e. control solution), or containing a concentration of CE at 0.1 unit/mL. The CE solution was prepared by dissolving the enzyme powder (#C 70-1081-01, Bovine pancreas, Genzyme) in 0.05 M phosphate buffer, and storing the frozen solution at -40°C until required. The units of active enzyme per mL were calculated based on the specifications of the esterase as they were obtained from Genzyme. The actual enzyme activity for this work was determined using p-nitrophenylacetate at pH 7.0 and 25°C. A unit is defined for this study as a change in absorbance of 0.1 min^{-1} (at 410 nm). All solutions were sterile filtered using a 0.22 μm filter.

During the degradation tests, aliquots were removed from the polymer incubation solutions and counted in a liquid scintillation counter for radioactivity. In a standard experiment, samples were removed once a week for three weeks. For those samples which underwent long-term biodegradation tests (more than 3 weeks), samples were removed once every two weeks after four months. The amount of activity lost between sample times was calculated. When the samples were removed for counting, fresh enzyme was added in order to maintain the enzyme activity. Each reaction condition was run in triplicate. In order to prevent bacterial contamination, antibiotics were added.

The final composition of the medium (10 mL) contained 100 units/mL of penicillin and 0.1 mg/mL of streptomycin (contained in 100 μL). Bacterial cultures were run on samples at the conclusion of the tests in order to determine if sterility was maintained throughout the experiment. No baterial contamination was found during the biodegradation test.

3.6. Stability Test of SMM Materials

To test the stability of the SMM materials, radiolabelled SMMs were synthesized using ^{14}C-HDI and then mixed with non-radiolabelled TDI/PCL/ED base polymer in different concentrations: 1%, 2.5%, and 5%. Using the same semi-batch system described above for the biodegradation tests, the coated tubes were incubated with phosphate buffer and cholesterol esterase. The results for the buffer incubation provided a measure of possible SMM leaching from the base polyurethane. On the other hand, the products released from the enzyme incubation test may be considered to be a measure of the SMMs' stability against enzymatic degradation.

4. Results and Discussion

The hypothesis of this work is based on the amphiphilic nature of the surface modifying macromolecules (SMMs). After being mixed with a base polyurethane, the SMMs are anticipated to migrate to the surface because of their low surface energy component, i.e. the "fluorine tail". At the same time, due to the chemical similarity of the SMMs' polar urethane bonds and polyol backbones with those of the soft-segment of the base polyurethane, SMMs may entrain some base polymer soft-segments to the surface as they migrate. Hence, an SMM enriched layer is formed with the main chain (prepolymer chain) of the SMMs buried in the soft segment of the base polymer, thereby providing a stable attachment force while the fluorine tail is exposed to the air/material interface. The enhanced fluorinated surface chemistry, meanwhile, is expected to yield a more chemically stable surface, resisting hydrolytic, and possibly oxidative, attack. Figure 4.1 shows a schematic diagram of this hypothesis.

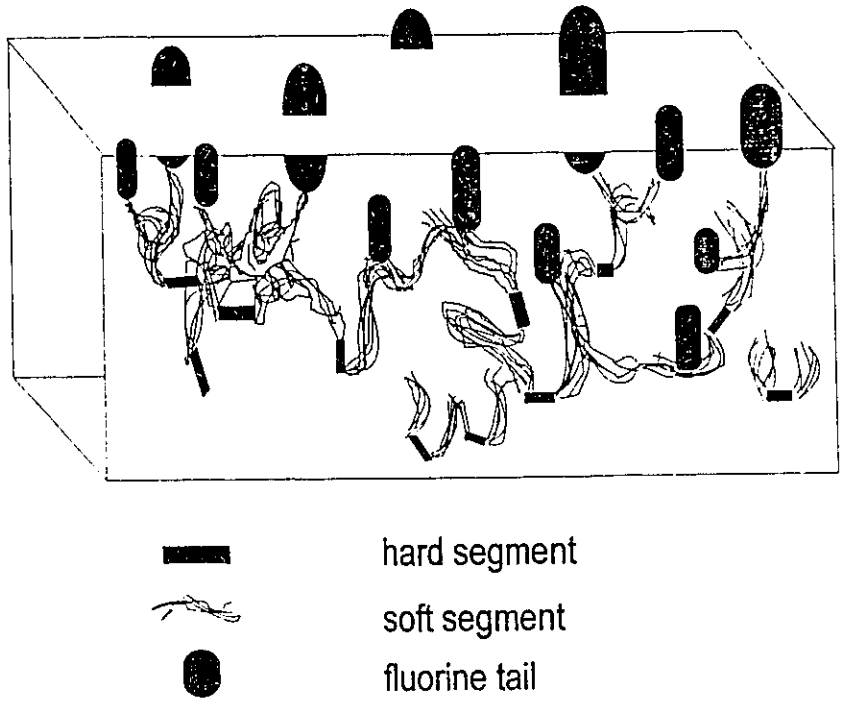

Figure 4.1. Schematic representation of SMM in base polymer mixture.

4.1. Fluorinated SMM Synthesis

The incorporation of fluorine chemistry into the polymers was achieved by using a fluorinated alcohol. Unlike the chain extenders used in the synthesis of segmented polyurethanes, this fluorinated alcohol was monofunctionalized. Accordingly, adding the fluorine alcohol into the prepolymer resulted in "end-capped" diisocyanate groups at the tails of the prepolymer and termination of the polymerization reaction. Hence, the molecular weight of the final SMM was highly dependent on the prepolymer synthesis conditions, which included the stoichiometry of the diisocyanate and polyol. However, in some polymerizations, the "capping" procedure did not occur rapidly. The possible reasons for this will be discussed below. As a result, the molecular weight of the SMM would vary according to the relative rates of the polymerization and "end-capping" reactions. Therefore, in general, the molecular weight of the SMM would be determined by the rate and ease of the end-capping process to occur with respect to the continued reaction of the prepolymer.

4.1.1. Optimization of SMM Chain Chemistry and Molecular Weight

In order to achieve optimal migration of the SMM, the reaction synthesis would have to yield an SMM with a relatively long fluorine tail (in comparison to the prepolymer) that would provide the driving force for SMM migration to the surface of a cast polymer, an SMM with a relatively low molecular weight in comparison to the bulk polymer was desired. Since the fluorine containing reactant was monofunctional and theoretically could not allow for further increases in molecular weight beyond its own addition to the prepolymer, the molecular weight of the SMM could be controlled by controlling the size of the prepolymer.

It has been shown that polymer chain mobility in a polymer matrix can be limited by chain entanglements, the presence of reinforcing agents such as carbon black, or the extent of crosslinks (125). (In this study, the SMMs could become entangled with the base polyurethane backbone.) Accordingly, the longer the SMM prepolymer chain, the greater would be the entanglement force. In addition, the mobility of SMMs could be

restricted by polar interactions of the urethane/urea bonds between the SMMs and the base polymer. The driving force towards the surface as a result of the fluorine chemistry and the resistance associated with polymer entanglement and polar interactions must be balanced. If the molecular weight is too small, the SMM would be too easily leached out. On the other hand, if the prepolymer chain length of a SMM is too large, the entanglement and polar interactions would restrain the migration of the molecule to the surface.

Excess HDI was added during prepolymer synthesis. In fact, if the mixture contained n moles of polyol, n+1 moles of HDI were also added to favour the formation of an isocyanate-endcapped polyol. However, it must be kept in mind that a distribution of products will result. Computer studies by Peeble (126,127), for example, have indicated that not all of the monomers react in the prepolymer synthesis. According to his computer simulated reactions, three different products are formed in a 2:1 (diisocyanate:polyol stoichiometry) reaction. The principal reaction products would be as follows:

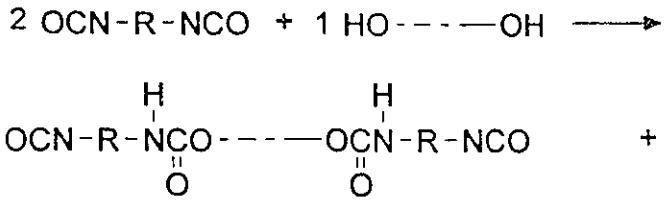

(a compound)

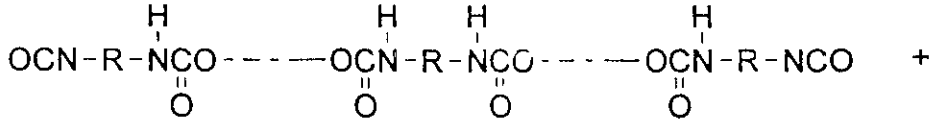

(b compound)

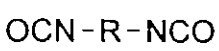

(c compound)

In the first stage of the synthesis in this work, twelve SMMs were produced. Their component stoichiometry were systematically varied, as listed in Table 3.4. The measured molecular weight and experimental fluorine content are given in Table 4.1. Several points in this regard should be noted.

i) In the GPC technique for molecular weight analysis, it is important to calibrate the column using a sample of known molecular weight under similar test conditions. The molecular weight determined by GPC in this study was based on a polystyrene equivalent molecular weight. The molecular weight of PTMO and PPO were 1000 as provided by the supplier. (It is not clear whether this is a weight-averaged molecular weight or, as is more likely because of its low value, a number average molecular weight). Meanwhile, the weight average molecular weight of these two polyols, as obtained from GPC measurements, were 6000. In addition, because of the hydrodynamic volume of the polymer chains in the mobile phase, the molecular weight results may not express their true relative size (128). Accordingly, it should be kept in mind that the molecular weight measured by GPC is a relative measure and was employed here to detect the reproducibility of the product polymers. A measurement of the intrinsic viscosity would be required to determine the absolute molecular weight of the SMMs.

ii) The amount of solvent used in the prepolymer reactions for the twelve preliminary SMMs was not varied systematically. In some instances, it was felt that the monomer concentration was too high, and this resulted in overly large prepolymer chains. Unfortunately, there is no extensive literature on polyurethane solution polymerization reaction kinetics to provide insight into this problem. However, Potts et al. (129) found that the monomer concentration affected the reaction rate during solution polymerization of hexachlorocyclotriphosphazene, specifically when a catalyst was involved in the polymerization. Similar results were obtained by Gao et al. (130) who found that the copolymerization of an amphiphilic polymer from polyethylene glycol was very sensitive to the reaction conditions. In that case, insoluble crosslinked gels were easily formed if the initiator concentration and the macromonomer concentration were too high. Since it was beyond the scope of the thesis to examine the reaction kinetics for this system, the

Table 4.1. Molecular weight and fluorine content (before and after wash) of SMMs synthesized in the first stage of the work.

SMM Code Number	Syn. Date	Before Wash		After Wash	
		M.W/P.D	F%	M.W/P.D	F%
SMM1 (PTMO-432I)	July 27 1993	1.3 x 10^5/ 2.2	10.33	1.1 x 10^5/ 2.0	N.F
SMM2 (PTMO-212L)	Aug. 3 1993	3.2 x 10^4/ 1.5	9.60	3.0 x 10^4/ 1.5	7.98
SMM3 (PTMO-322L)	Aug. 3 1993	2.4 x 10^5/ 1.8	N.F	N.D	N.D
SMM4 (PTMO-212H)	Aug. 9 1993	1.5 x 10^5/ 1.9	20.01	9.7 x 10^4/ 2.1	0.72
SMM5 (PTMO-212I)	Aug. 12 1993	1.2 x 10^5/ 1.8	0.37	1.4 x 10^5/ 3.1	0.10
SMM6 (PPO-212L)	Aug. 21 1993	2.1 x 10^4/ 1.6	13.27	2.2 x 10^4/ 1.3	12.44
SMM7 (PPO-322I)	Aug. 21 1993	5.0 x 10^4/ 1.7	4.98	4.8 x 10^4/ 1.6	3.95
SMM8 (PTMO-322H)	Aug. 24 1993	7.7 x 10^4/ 2.4	8.23	6.1 x 10^4/ 2.1	0.71
SMM9 (PPO-322H)	Aug. 24 1993	2.6 x 10^4/ 1.6	10.56	2.6 x 10^4/ 1.6	5.11
SMM10 (PTMO-322I)	Sept. 24 1993	6.7 x 10^4/ 1.8	N.D.	5.0 x 10^4/ 1.7	4.97
SMM11 (PTMO-432L)	Sept. 24 1993	3.0 x 10^5/ 2.0	N.D.	1.8 x 10^5/ 2.0	N.F
SMM12 (PTMO-432H)	Oct. 3 1993	6.8 x 10^4/ 1.8	N.D	7.1 x 10^4/ 1.7	3.28

M.W: weight average molecular weight
P.D: polydispersity
N.D: not done
N.F: not found
F%: fluorine content

solvent volume was set constant for the study of polymers in second stage of this work.
iii) The presence of catalyst will influence the rate of polymerization (129). The temperature employed during polymerization will also affect the reaction rate. Although no comprehensive study in this respect has been done for our system, Wang et al. (131) found that the temperature was important in solution polymerization of polyamide acid and polyamide imide, and, in their case, a low temperature was desired when a polar solvent (i.e. DMAC, DMF) was employed.
vi) The data presented in Table 4.1 show that some of the polymer systems yielded very high molecular weights, even though their stoichiometry should have given a low molecular weight material (e.g., SMM4). In addition to the above-mentioned influences on SMM formation, it was also possible that, in the process of BA-L "capping", hydroxyl groups from the unreacted polyols reacted with HDI end-capped polymer instead of BA-L, particularly if the polyol was more reactive than BA-L. In fact, because of the hydrophobic-hydrophilic incompatibility of BA-L with the prepolymer, BA-L may have been excluded from the reaction zone of the HDI end-capped prepolymer, resulting in the continuing reaction of polyol end-capped prepolymers and diisocyanate end-capped prepolymers. This effect would be amplified when the amount of solvent was low and the BA-L reactivity became dependent on its solubility within the prepolymer.

The hypothesis that the prepolymer polymerization continued during the end-capping step was supported in tests carried out on SMM33 synthesis (Appendix 3). In that experiment, some of the prepolymer was rapidly quenched by methanol, yielding a molecular weight of 4.4×10^4. However, the same prepolymer undergoing the BA-L end-capping process had a final molecular weight of 5.7×10^4. The increased molecular weight could not be attributable to the addition of the two fluorine tails alone, since the latter cannot account for all of the molecular weight increase.

The results of the twelve preliminary SMM syntheses suggested that a higher solvent volume (i.e. lower reactant concentration) led to a lower molecular weight SMM (see Table 3.4 and Table 4.1). For example, SMM3 (PTMO-322L) and SMM8 (PTMO-322H) were synthesized using similar reactant stoichiometries during the prepolymer

step, but the latter SMM was synthesized in a more diluted system (see Table 3.4). Meanwhile, SMM8 had one fourth of the molecular weight of that of SMM3. In addition, it was expected that the BA-L (High) in SMM8 would have had a slower reaction rate with the prepolymer than the BA-L (Low) in SMM3, because of the increased size of the hydrophobic chain in BA-L (High) leading to greater incompatibility between BA-L and the polar prepolymer. Hence, it was anticipated that SMM8 would have a larger molecular weight than that of SMM3. However, the reverse was observed (see Table 4.1). Based on this and a similar trend observed in the SMM1 and SMM12 results (see Table 4.1), it was decided to increase the solvent volume empirically and to maintain it at a constant volume in future syntheses. However, since the reaction kinetics were not the main focus of this thesis, no further investigation of optimal reaction concentrations was performed. Further work is needed in this area.

The amount of catalyst used for the polymer synthesis was based on the work of Ramesh (132). Since the catalyst was a very viscous liquid, it was difficult to control the exact amount added to the system through direct addition. During the syntheses performed before Feb. 1994 (see Appendix 4), the molecular weight and fluorine content of SMMs were inconsistent, in part because of variations in the amount of catalyst as a consequence of direct addition. In the syntheses after Feb. 1994 (see Appendix 4), the catalyst was weighed and diluted with freshly distilled DMAC. Samples were then drawn from the diluted solution in order to deliver consistent amounts of catalyst to the reaction mixtures. This led to more consistent molecular weights in the synthesized polymers.

The heat source for the reactions was a stirrer/hot plate, which made precise temperature control difficult. While in all cases the temperature was controlled within the range of 60 - 70°C, the temperature profile during the two hour reaction period for the prepolymer could not be controlled in exactly the same fashion for each batch synthesis (see Appendix 4). It is not clear to what extent this affected the prepolymer product. However, since Wang et al. (131) did indicate the importance of temperature for catalyzed systems, we may anticipate that this was also a contributing factor to the variable molecular weights and the range of fluorine content observed in the preliminary

SMMs.

Because of the above-mentioned difficulties, it was not possible to compare the effect of the three BA-L fractions on the SMM syntheses. However, it was observed that PTMO-based SMMs (SMMs synthesized with PTMO as the polyol) consistently yielded larger molecular weight materials than the PPO-based SMMs (i.e., SMMs synthesized with PPO as the polyol). During the prepolymer synthesis, some of the reaction solutions (i.e. those for SMM4 (PTMO-212H) and SMM11 (PTMO-432L)) became so viscous that more solvent had to be added. The reason for this may be associated with the higher reactivity of PTMO, compared to PPO. (The PTMO chain polyol contains a primary hydroxyl group on each end (133), and so has a higher reactivity than PPO.)

This was suggested also by Rand's work (133) in which it was observed that the primary hydroxyl groups of the polyether reacted more rapidly with the diisocyanate than secondary hydroxyl groups (as were found in PPO). The enhanced reactivity of PTMO with HDI possibly reduced the availability of HDI to react with BA-L. In contrast, PPO, a polyol with a methyl branch outside the main chain and a secondary hydroxyl end, did not show the same degree of reactivity, so that BA-L easily capped the HDI. In addition, Wang's work (134) confirmed that, in a prepolymer synthesis, PTMO led to longer prepolymer chains and more free diisocyanate than did PPO. In our case, the free diisocyanate (HDI) could react with BA-L and be removed during washing, leading to PTMO-derived SMMs with longer chains and lower than expected fluorine content. This hypothesis is supported by the change in fluorine content in the SMM1 (PTMO-432I) before and after washing (Table 4.1).

4.1.2. Fluorine Content

Elemental analysis for fluorine and tin (a catalyst residue) content was performed after the first stage of work (see Table 4.1). No tin residue was found in any of the samples. This finding is important since tin is known to be toxic to cells (135). There was also a clear trend in the twelve SMMs in which the fluorine content decreased with increasing SMM molecular weight (see Table 4.2). This indicated that the contribution

to higher molecular weights was primarily from the prepolymer chain and not from the fluorine tail. It also confirmed that the addition of a fluorinated alcohol was restricted to "end capping" stage as expected. Some of the larger SMMs, such as SMM1 (PTMO-432I), SMM3 (PTMO-322L) and SMM11 (PTMO-432L), did not show any measurable fluorine content.

Table 4.2. Summary of the molecular weight and fluorine content of SMMs.

Name of SMM	Molecular Weight	Fluorine Content (%)
SMM6 (PPO-212L)	2.2×10^4	12.44
SMM9 (PPO-322H)	2.6×10^4	5.11
SMM2 (PTMO-212L)	3.0×10^4	7.98
SMM7 (PPO-322I)	4.8×10^4	3.95
SMM10 (PTMO-322I)	5.0×10^4	4.97
SMM8 (PTMO-322H)	6.1×10^4	0.71
SMM12 (PTMO-432H)	7.1×10^4	3.28
SMM4 (PTMO-212H)	9.7×10^4	0.72
SMM1 (PTMO-432I)	1.1×10^5	N.F.
SMM5 (PTMO-212I)	1.4×10^5	0.10
SMM11 (PTMO-432L)	1.8×10^5	N.F
SMM3 (PTMO-322L)	2.4×10^5	N.F.

N.F: not found

It was hypothesized that BA-L (High) SMMs should have higher fluorine content than the BA-L (Int) and BA-L (Low) SMMs, but the experimental results showed no clear trend in this regard. For example, SMM8 (PTMO-322H) had a much lower fluorine content than that of SMM10 (PTMO-322I). The experimental results clearly suggested that the prepolymer chain determines the molecular weight of the SMM chain, confirming the importance of the competitive reactions between the polyol and the

fluorinated alcohol with diisocyanate groups during the end-capping step.

It was also expected that, if the molecular weights were similar, an SMM produced with BA-L (High) should have a higher fluorine content than that of an SMM using either BA-L (Int) or BA-L (Low). This was, in fact, observed. For example, SMM20 (PTMO-322H) (see Appendix 3) has a molecular weight similar to that of SMM36 (PTMO-322I) - approximately 4.5×10^4 - while SMM20 has a higher fluorine content (6.87%) than that of SMM36 (3.98%).

In order to drive the reaction equilibrium towards the product and increase the reactivity of BA-L with the prepolymer, excess BA-L was used in the end-cap reaction. To remove the excess BA-L, the SMMs were washed with TCTFE (1,1,2,-trichlorotrifluoroethane), since BA-L was very soluble in TCTFE. Fluorine analysis was done before and after washing and the results showed that the washing method was effective in removing residual BA-L materials (see Table 4.1). For some SMMs, such as SMM6 (PPO-212L), a 50% acetone/water mixture was used to remove the excess BA-L, since the SMM itself was soluble in 100% TCTFE.

4.1.3. Biodegradation Test Results

As introduced in section 3.5, the biodegradation tests carried out in this work were conducted using radiolabelled polymers exposed to cholesterol esterase (an *in vitro* system). The radiolabelled products released into the incubation medium during the test provided a measure of enzymatic degradation.

In each case, the SMMs listed in Table 4.1 were mixed in different concentrations with ^{14}C-TDI/PCL/ED. No tests were run on those SMMs whose elemental analysis showed no fluorine content (i.e. SMM1, SMM3, and SMM11). All of the statistical analysis associated with this work was based on the student t-test, and in all cases the p value was < 0.05. The biodegradation results indicated that five of the SMMs (SMM6, SMM7, SMM8, SMM9, and SMM10) could inhibit the hydrolytic degradation of

TDI/PCL/ED by cholesterol esterase. Three others (SMM2, SMM4, and SMM5) showed increased biodegradation. It was interesting to note that SMM12 had no significant effect on the apparent biostability of the base polymer.

The three SMMs which increased the biodegradation of TDI/PCL/ED were all from the PTMO-212 series (Figures 4.2 and 4.3). While there may be many possible explanations for the observed behaviour of these specific SMM/base polymer mixtures, it is believed that the SMMs disrupted the structure of the polymer's microdomain in a manner that enhanced the accessibility of hydrolysable groups in TDI/PCL/ED. Furthermore, the effect does not seem to be dependent on fluorine content (see Table 4.1). Neither the presence of PTMO or 2:1:2 stoichiometry alone appeared to be responsible for the increased degradation, since the PTMO-322I system did not show enhanced degradation, nor did PPO-212L system. It would appear that the problem is related to a combination of the 2:1:2 stoichiometry with the PTMO chemistry.

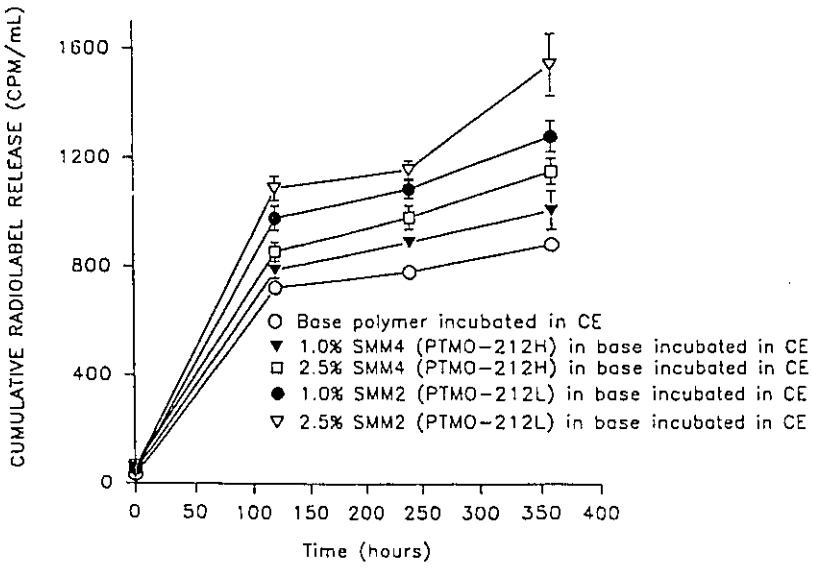

Figure 4.2. Biodegradation results of SMM2 (PTMO-212L) and SMM4 (PTMO-212H).

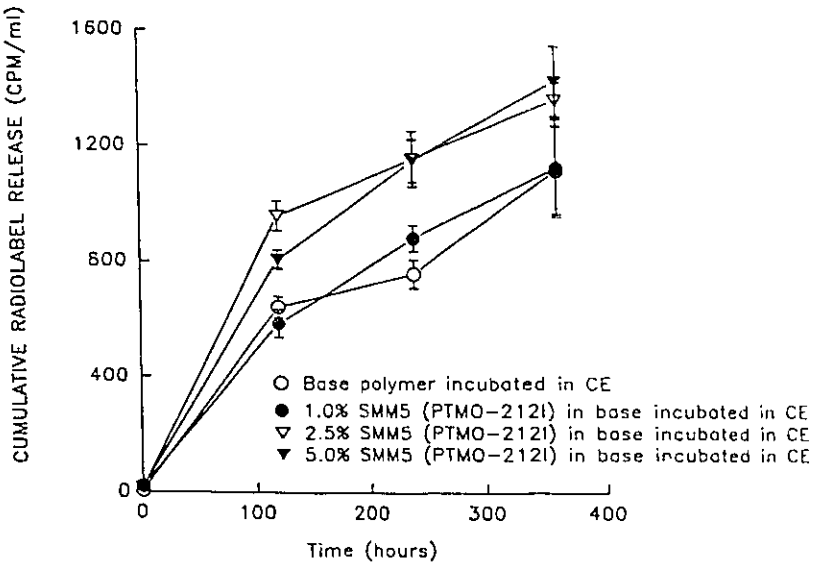

Figure 4.3. Biodegradation results of SMM5 (PTMO-212I).

It should also be kept in mind that the casting procedure for this work was a very important factor in the formation of microdomain structures, and that this might influence the degradation characteristics of the SMM-base polymer mixture. As well, other factors, such as the solvent used for the casting and the total polymer concentration (i.e., amount of SMM and base polymer/solution weight), may also influence the results of the degradation studies. Because of the limited time, no further research was done in these areas.

The biodegradation data showed that SMM12 (PTMO-432H) had no significant effect on TDI/PCL/ED degradation (Figure 4.4). The molecular weight of SMM12 (PTMO-432H) was 7.1×10^4, indicating a SMM with a relatively long prepolymer chain. It was initially thought that this SMM's large prepolymer chain would increase the entanglement and polar interactions between it and the TDI/PCL/ED base polymer, which might limit the migration of fluorine tail towards the surface. However, XPS data showed that, in fact, there was fluorine on the top 100 Å of the polymer mixture (see, for example, the

5% SMM12/base polymer mixture analysis - Appendix 5).

Another possible explanation for the ineffectiveness of this SMM to limit biodegradation was that the reorientation of the polymer microdomain when the polymer is exposed to the water. In the SMM-TDI/PCL/ED polymer mixture, the most hydrophilic component is the hard-segment which contains a high concentration of polar urea and urethane groups. When the polymer film is exposed to air, the fluorine tail of the SMM moves to the air/polymer interface to reduce the surface energy. However, when the external environment is changed to the aqueous media of the incubation solution, a reorientation of segments within the polymer matrix could occur, leading to the migration of the hard-segment to the surface in response to the polar nature of the bathing solution. Simultaneously, the soft-segment of base polymer entangled with the SMM would move into the deeper layer along with the SMM's prepolymer chain. This, in turn, could lead to the transport of the fluorine tail below surface reducing the SMM's effectiveness in inhibiting degradation. This kind of reorientation mechanism has been confirmed by Yasuda et al. (136) who found that polymer molecules have the freedom to rearrange themselves at the surface in order to accommodate a change of chemical potential in the surrounding environment. However, XPS could not be used to confirm this in our experiments, since the XPS tests were carried out in a vacuum system.

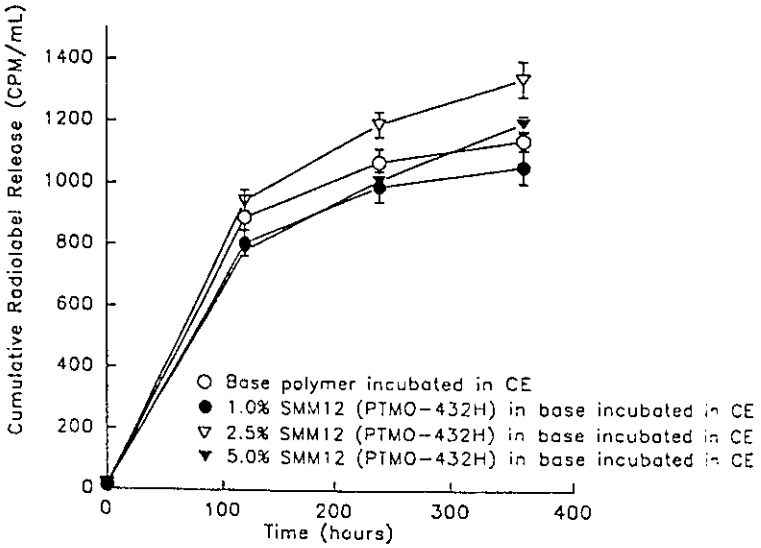

Figure 4.4. Biodegradation results of SMM12 (PTMO-432H).

While several SMMs significantly improved the biostability of the base polymer (Figures 4.5 to 4.9), their effectiveness varied with the type of additive. The level of inhibition increased with increasing SMM concentration when SMM7 (PPO-322I) and SMM10 (PTMO-322I) were used; however, SMM6 (PPO-212L), SMM8 (PTMO-322H) and SMM9 (PPO-322H) showed no significant improvement at weight fractions above 1%. By way of explanation, it was noted that SMM6 had the lowest molecular weight and highest fluorine content of the twelve SMMs synthesized (Table 4.2). These features would favour migration of the SMM's fluorine tails to the surface. It was therefore suspected that, even at the comparatively low mass fraction of 1%, enough fluorine was present to occupy the surface region and protect the hydrolysable bonds from degradation.

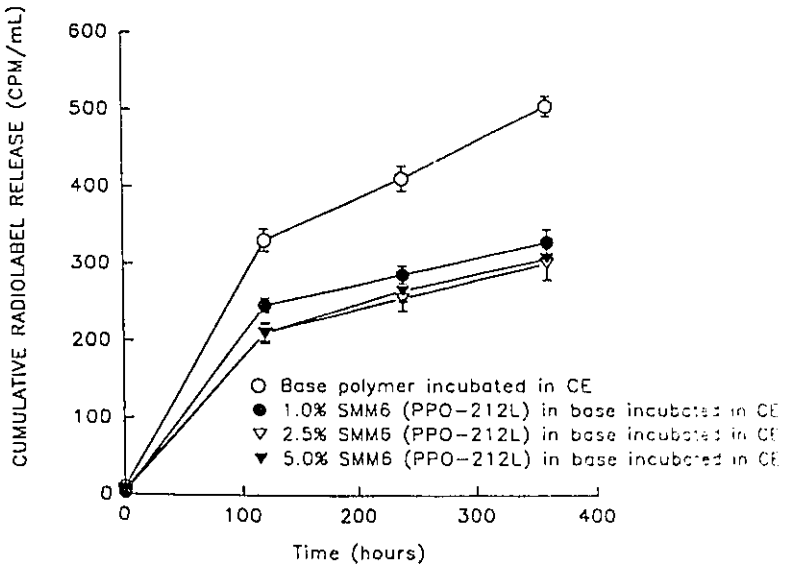

Figure 4.5. Biodegradation results for SMM6 (PPO-212L).

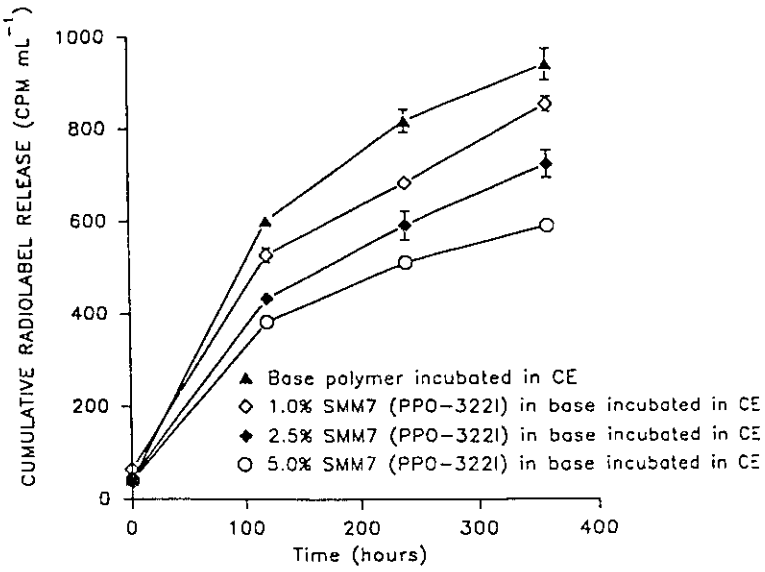

Figure 4.6. Biodegradation results for SMM7 (PPO-322I).

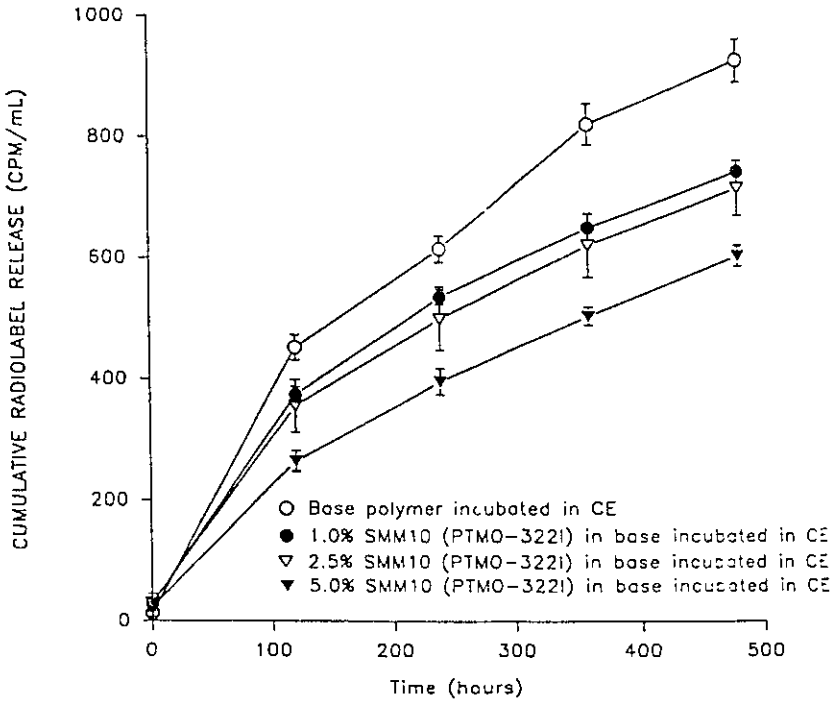

Figure 4.7. Biodegradation results for SMM10 (PTMO-322I).

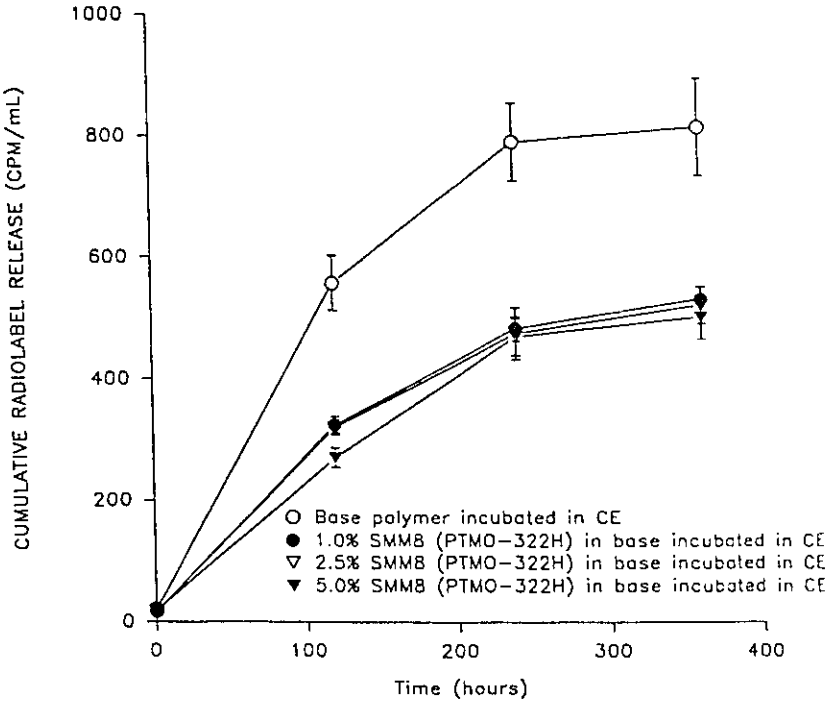

Figure 4.8. Biodegradation results for SMM8 (PTMO-322H).

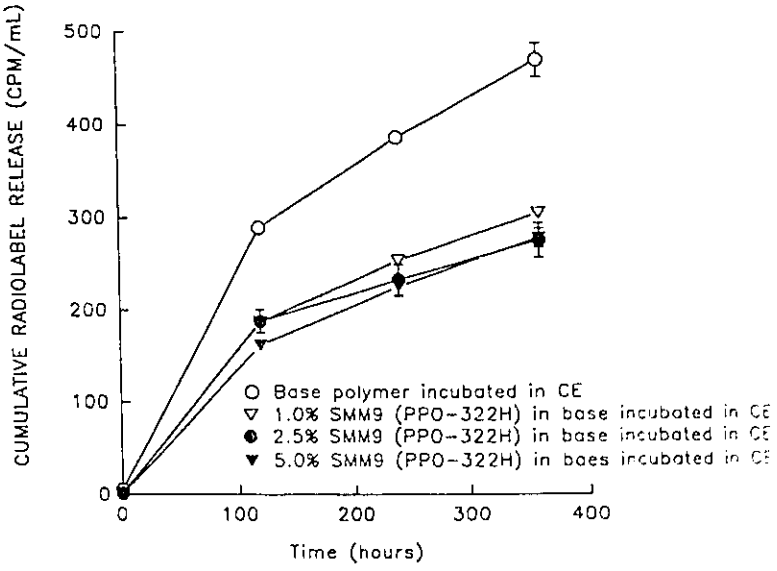

Figure 4.9. Biodegradation results for SMM9 (PPO-322H).

Based on the findings described above, the mechanism for the inhibition of enzymatic degradation might be described in the following manner. As discussed previously, when SMMs are mixed into the base polymer, a SMM-enriched layer is established. Assuming that the entanglements and polar interactions of the SMM/soft-segment are sufficiently small due to the relative size of the SMM compared to the base polymer, then the fluorine tail will remain in the upper surface layer (i.e. upper 100 Å), thus hindering the preferential migration of polar hard-segments of TDI/PCL/ED towards the surface. Because of the hydrolytic stability of the fluorine component, enzyme access to cleavable bonds such as the urea/urethane bonds and ester bonds will be inhibited.

The lack of further inhibition with increasing SMM content above 1% (i.e., a "saturation effect" with respect to biostability), as in the case of SMM6 (PPO-212L), can be attributed to the prepolymer chain length of the SMM. The shorter chain would likely lead to a thinner zone of SMM-enriched matrix but a higher concentration of SMM molecules in the layer. This is illustrated by a simplified schematic diagram in Figure 4.10. Thus less SMM material would be required to saturate the SMM-enriched zone.

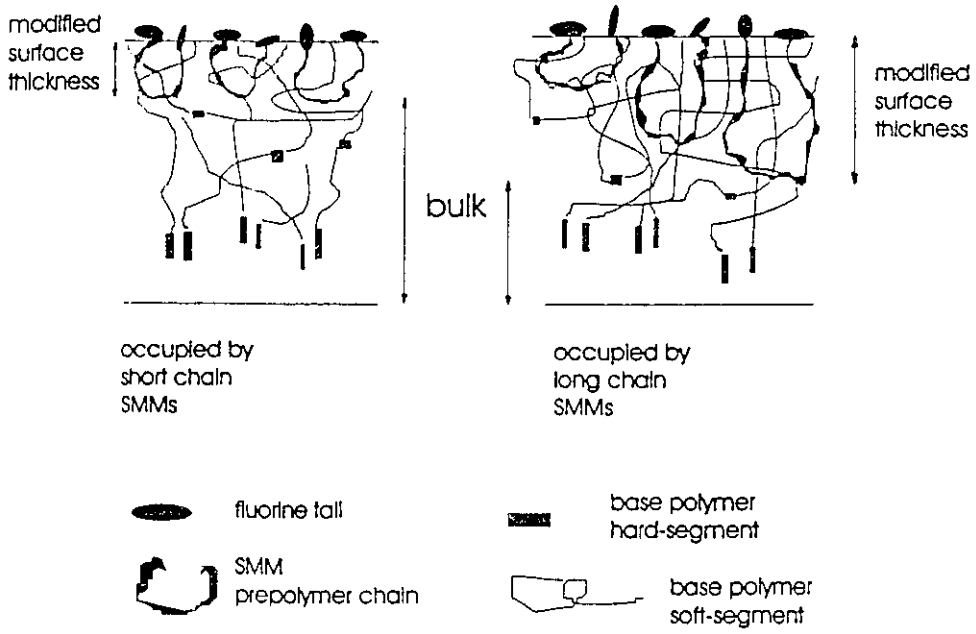

Figure 4.10. Schematic diagram of the chain length dependent thickness of SMM-enriched layer.

Assuming that, following surface saturation, no further inhibitory effects are seen, increasing the bulk concentration of SMMs in this case would not increase the enzymatic stability of the mixture. It should be noted that the icons depicting different SMM and polyurethane components in Figure 4.10 are not exactly to scale. The length of each component can be estimated based on the assumption that the polymer chains are fully extended. Using chemical bond lengths (137), the estimated length of the fluorine tail is approximately 1 to 3 nm (dependent on BA-L fraction), while the hard-segment of base polymer is about 4 nm. The saturation effect observed for SMM8 (PTMO-322H) and SMM9 (PPO-322H) can be explained in a similar manner. The fluorine content of the SMM chain will affect the composition of the SMM-enriched zone: a larger fluorine tail for similar SMM chain lengths would lead to a lower concentration of SMM molecules in the enriched layer. Therefore, fewer SMM molecules would then be required to saturate the surface zone with fluorine tails; thus no further inhibition would occur at higher SMM concentrations. This is shown schematically in Figure 4.11.

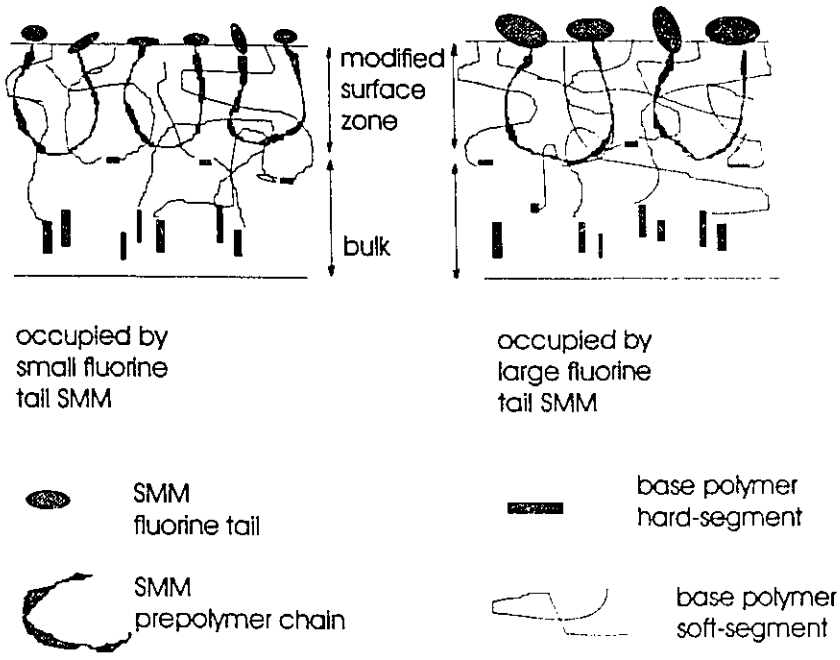

Figure 4.11. Schematic diagram of fluorine tail size dependent thickness of SMM-enriched layer.

These conceptual models also explain the biodegradation results of SMM7 (PPO-322I) and SMM10 (PTMO-322I) (see Figures 4.6 and 4.7). PPO-322I and PTMO-322I, both of which have a moderate fluorine content and a longer prepolymer chain than PPO-212L, did not exhibit a saturation effect in the biodegradation tests as the SMM content was increased from 1% to 5%.

Based on the above *in vitro* biodegradation tests, five SMMs (PTMO-322I, PTMO-322H, PPO-212L, PPO-322I, and PPO-322H) were selected for a more comprehensive study of their respective reaction syntheses and material properties. The reader is reminded that these SMMs were selected on the basis of these preliminary data. Because there was insufficient time to carry out a full analysis of the reaction kinetics for each formulation, it cannot be concluded that only these five SMMs are able to inhibit the biodegradation of TDI/PCL/ED base polymer. It is also possible that those materials which did not show promising results for inhibiting TDI/PCL/ED degradation may function well with other base polymers.

4.2 Resynthesis of SMMs

The second phase of this work focused on the reproducibility of the synthesis product for the five selected SMMs: PTMO-322I, PTMO-322H, PPO-212L, PPO-322I, and PPO-322H. The average molecular weight and fluorine content of these five SMMs are summarized in Table 4.3. As discussed in the previous sections, the reaction temperature, solvent volume and the amount of catalyst were all important in determining the size of the SMMs (see Table 4.1). It was found that PPO-322I, PTMO-322I, and PPO-212L could be reliably reproduced as long as the above parameters were kept relatively constant from batch to batch; however, PTMO-322H and PPO-322H were more difficult to reproduce. This may be related to the BA-L (High) reagent itself. As discussed previously, BA-L (High) contained the largest fluorine tail, and so may not be as reactive as the other two BA-L fractions due to the chemical incompatibility of this longer hydrophobic chain with the prepolymer chain. As discussed earlier, this lower

reactivity could lead to less effective capping and greater variability in the resulting SMM's molecular weight.

Several batches of the individual SMM chemistries were selected for further biodegradation studies with ^{14}C-TDI/PCL/ED: two of the PPO-212L SMMs (SMM19 and SMM24) and two of the PPO-322I polymers (SMM7 and SMM14). The molecular weights and fluorine content of these samples are given in Appendix 3. As the results show in Figure 4.12, the two PPO-212L SMMs did not display significantly different results, as determined by the student T-test. This was anticipated since these two different batches produced SMMs with similar molecular weights and fluorine content. In contrast, the two PPO-322I SMMs showed a noticeable difference in the biodegradation tests (see Figure 4.13), presumably due to greater variability in their molecular weights and fluorine content which led to different properties and behaviour.

Table 4.3. The molecular weight and fluorine content of the SMMs selected.

Name of SMM	Molecular weight (Mw)	Fluorine content (%)	Code of SMM for calculation
PPO-212L	(1.6 ± 0.16) x 10^4	18.87 ± 2.38	SMM6, SMM19, SMM24, SMM37, SMM39
PTMO-322I	(4.6 ± 0.53) x 10^4	5.50 ± 1.21	SMM10, SMM13, SMM15, SMM25, SMM34, SMM36
PPO-322I	(3.3 ± 0.41) x 10^4	9.37 ± 1.70	SMM7, SMM14, SMM16, SMM26, SMM29
PTMO-322H	(5.5 ± 0.81) x 10^4	3.83 ± 1.80	SMM8, SMM17, SMM20, SMM23, SMM43
PPO-322H	(2.9 ± 0.49) x 10^4	4.63 ± 2.55	SMM9, SMM18, SMM21, SMM22

Mw: weight average molecular weight

Note 1: the data are presented as mean ± standard error

Note 2: the molecular weight and fluorine content used for SMM19 were those before wash data.

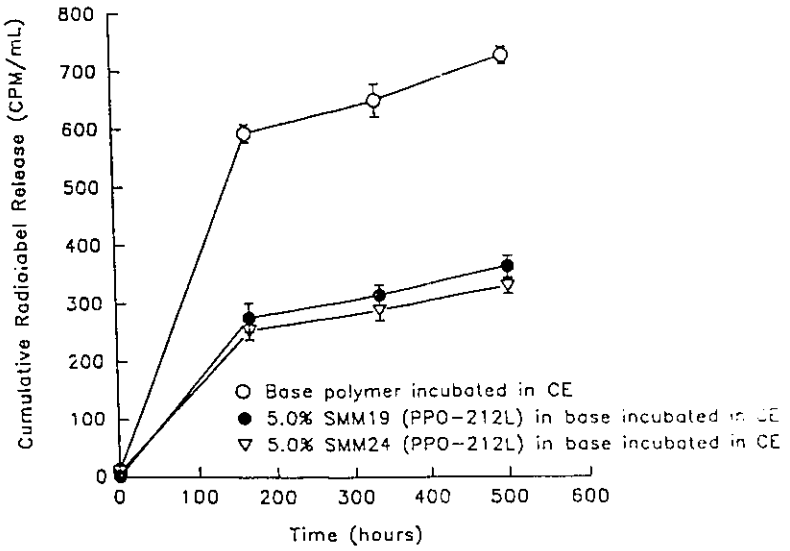

Figure 4.12. The biodegradation results of SMM19 and SMM24 (PPO-212L).

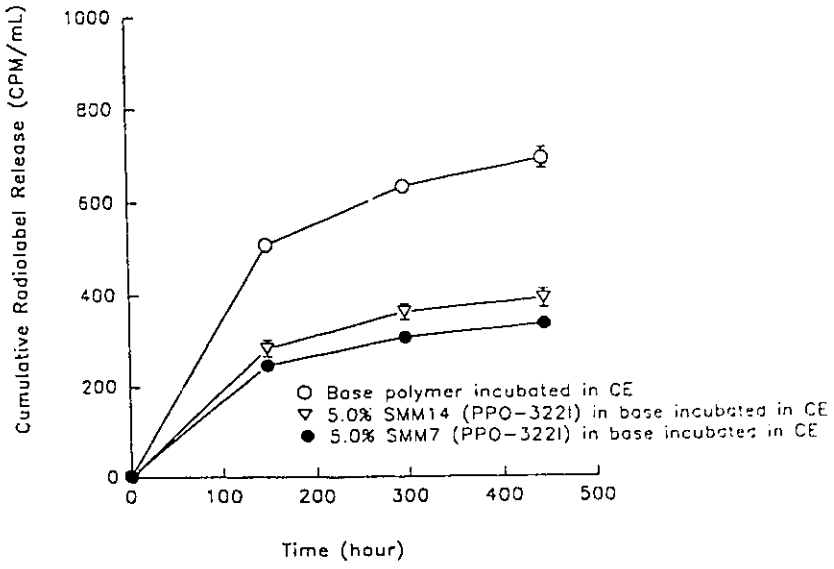

Figure 4.13. The biodegradation results of SMM7 and SMM14 (PPO-322I).

However, even in these cases the difference was marginal. This may be due to the fact that the enriched layer is nearly saturated at a 5% SMM concentration. It is possible that the same test, performed at a 1% or 2.5% SMM content, would have shown greater differences in the release of radiolabelled material.

4.3. SMM Characterization

In light of the previous discussions, the five SMMs selected for further studies (PPO-212L, PPO-322I, PTMO-322I, PPO-322H and PTMO-322H) were characterized using a number of techniques. This section reviews the results of these tests.

4.3.1. Differential Scanning Calorimetry (DSC)

The thermal transitions of the SMM and SMM-TDI/PCL/ED base polymer mixtures were assessed by Differential Scanning Calorimetry (DSC). In order to determine if the presence of SMM in TDI/PCL/ED influenced the bulk microdomain structure, mixtures containing 5% SMM were studied. (Of all of the SMM concentrations investigated in the biodegradation studies, the 5% mixture would have the highest probability of altering the microdomain structure.) In this regard it is noted that, in Theocaris's work (138), the addition of polyurethane into polystyrene at a mass fraction of 5% gave a clear shift in the polystyrene's glass transition temperature.

The DSC samples were cooled down from room temperature to -160°C using liquid nitrogen, after which the samples were scanned. The rate of temperature increase was 10°C/min in each case. After the first scan the sample was quenched to -160°C by liquid nitrogen and another thermogram was recorded. Typically, the sample was run three times to check the reproducibility of the transitions. The thermograms presented in this thesis are those samples having reproducible transitions.

Figure 4.14 shows DSC data for pure SMM34 (PTMO-322I), pure base polymer and their mixture (5% SMM in base polymer), plotted as heat flow versus temperature. The base polyurethane, TDI/PCL/ED, showed a glass transition temperature (Tg) range between -47.79°C and -36.73°C; no soft-segment melting temperature (Tm) was found.

There was also no observed transition at a higher temperature related to changes in the hard-segment domain. Previous work by Santerre and Labow explained the lack of a hard segment domain transition as due to phase mixing within this system (67). Similar effects have been observed by Yoon et al. (139).

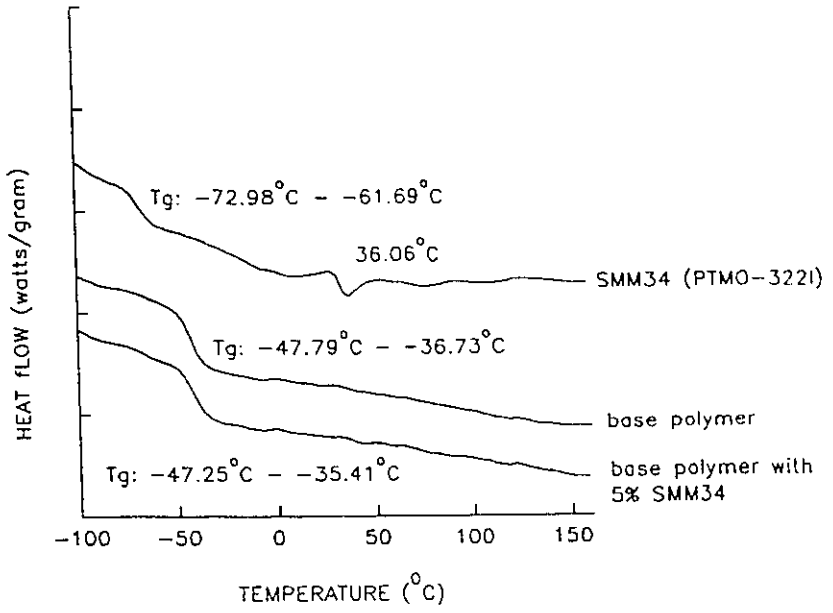

Figure 4.14. DSC thermograms of TDI/PCL/ED, SMM34 (PTMO-322I) and their mixture.

It should also be noted that, depending on processing conditions, it is possible to crystallize the soft-segment structure of the base polymer, as demonstrated by the following test. After the first DSC run, the sample was allowed to cool down from 220°C to room temperature overnight. On the second day, the sample was cooled down by liquid nitrogen to -160°C and run again. The second thermogram gave a melting peak for the soft-segment near 41.2°C, but no significant glass transition temperature was observed (see Figure 4.15). The same phenomenon was reported in Shibayama et al.'s

work (140), in which they found that the greater the cooling rates, the lower the degree of crystallization of the sample.

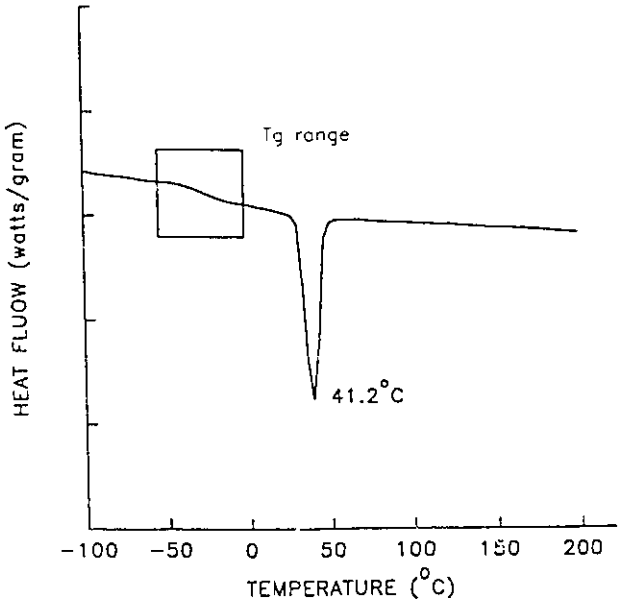

Figure 4.15. DSC thermogram of TDI/PCL/ED cooled with a slow cooling rate.

The pure SMM34 (PTMO-322I) showed a glass transition temperature in the range of -72.98°C to -61.69°C, as well as a melting temperature for the soft-segment at 36.06°C. This is lower than the glass transition temperature of the pure TDI/PCL/ED base polymer, but similar to the transition temperatures of the pure soft-segment of the base polymer, PCL. (The Tg for PTMO is -79.4°C while the Tg for PCL is -68.86°C). Despite the difference in thermal properties between the base polymer and SMM34 (PTMO-322I), the mixture of the two materials (5% SMM34 in base polymer) displayed thermal characteristics similar to the base polymer: not only was the glass transition temperature of the mixture similar to that of the TDI/PCL/ED (-47.25°C to -35.41°C for the mixture compared to -47.79°C to -36.73°C for the pure base polymer), but the

features of the thermograms were also similar.

Figure 4.16 displays the DSC thermograms of SMM29 (PPO-322I), the base polymer and their mixture (5% of SMM in base). Compared to SMM34 (PTMO-322I), SMM29 showed a higher glass transition temperature which ranged from -54.32°C to -48.15°C, indicating that PPO, the soft-segment component, influenced the thermal properties of this SMM. Unlike SMM34, SMM29 did not show a melting temperature of the soft-segment. This could be due to the presence of the side methyl chain in PPO which may hinder packing and crystallization of the polymer. It was observed that, the PPO-322I SMM was a tacky powder, while the PTMO-322I SMM was a soft fibrous material. The shape of the thermogram and the corresponding Tg for pure SMM29 (PPO-322I) was significantly different from that of the base polymer. However, the thermal properties of the SMM29 mixture and that of the base polymer remained the same, suggesting that the bulk properties were not modified by the addition of this SMM.

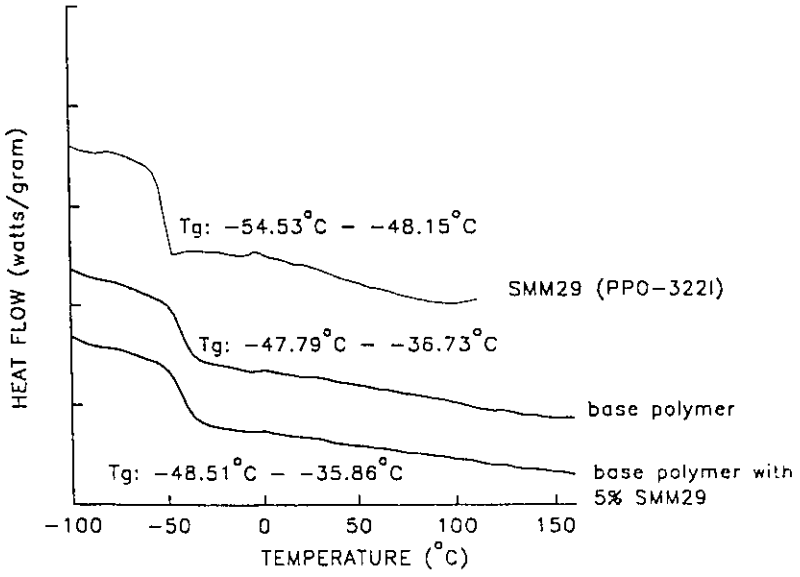

Figure 4.16. DSC thermograms of TDI/PCL/ED, SMM29 (PPO-322I) and their mixture.

SMM37 (PPO-212L), as shown in Fig 4.17, revealed the most complicated thermogram of the five SMMs, displaying one Tg as well as two sharp melting temperatures. The Tg of this polymer ranged from -53.01°C to -47.04°C. The similarity of this range to that of PPO-322I (SMM29) indicates that the polyol is the dominant factor determining the Tg of these SMMs. However, the two melting temperatures indicated that the SMM stoichiometry also influenced the thermal properties. The shorter prepolymer chain for PPO-212L could possibly favour the interactions between the two fluorine tails of the same polymer chain by bringing them into closer proximity to each other. The two melting points observed in PPO-212L may indicate a higher order in the microstructure of this SMM induced by the proximity of the two fluorine tails. Figure 4.18 shows a schematic diagram of such a hypothetical structure.

In addition, according to the discussion in section 2.2.1, a polyurethane chain extended by a backbone having an even number of carbon atoms shows superior

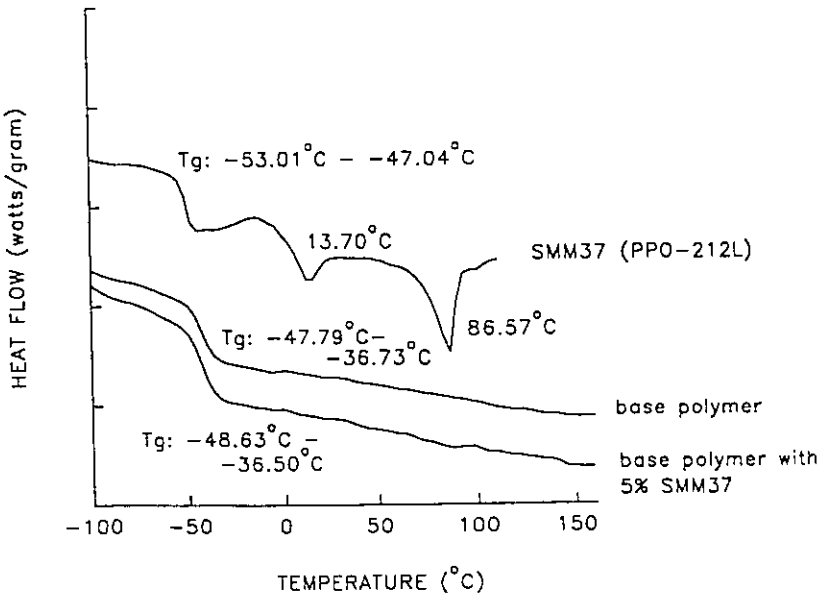

Figure 4.17. DSC thermograms of TDI/PCL/ED, SMM37 (PPO-212L) and their mixture.

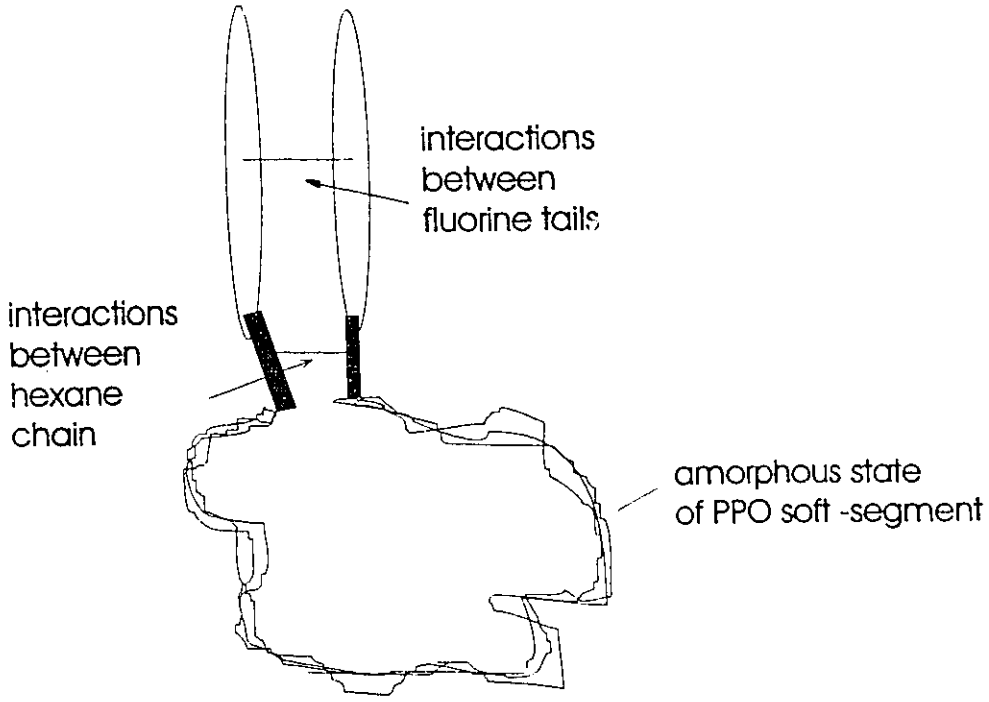

Figure 4.18 Schematic presentation of structure of PPO-212L.

mechanical properties to one produced with a backbone having an odd number of carbon atoms. As HDI is a even numbered carbon backbone diisocyanate, it might produce some effect in addition to hydrogen bonding. However, further work to characterize the crystalline structure of the material will be required in order to test this hypothesis. It is none-the-less interesting to note that the thermogram for the 5% mixture in base polymer did not show any difference from that of the pure base polymer thermogram.

Both SMM8 (PTMO-322H) and SMM21 (PPO-322H) had glass transition temperatures similar to their BA-L (Int) analogs, i.e. PTMO-322I and PPO-322I, showing again that the glass transition temperature is highly dependent on the type of polyol used (see Figure 4.18 and Figure 4.19). However, these two BA-L (High) SMMs displayed several other transitions which did not occur in the BA-L (Int) analogs. The

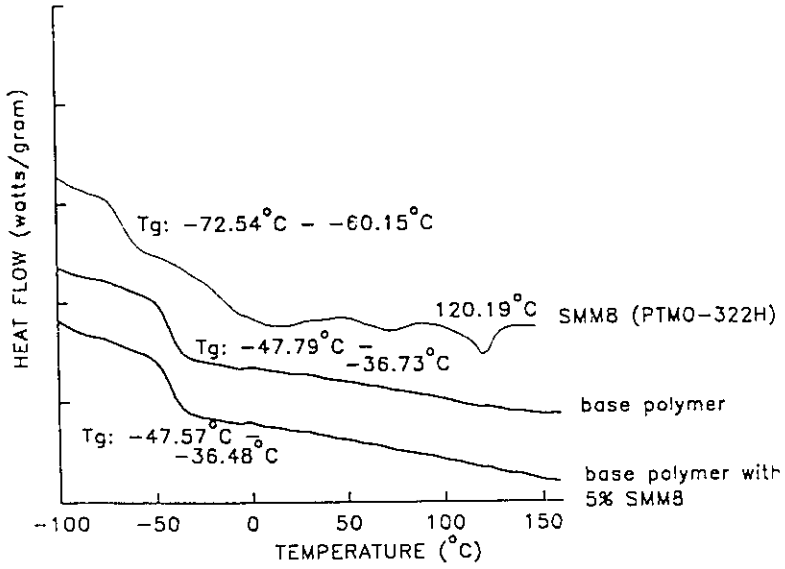

Figure 4.19. DSC thermograms of TDI/PCL/ED, SMM8 (PTMO-322I) and their mixture.

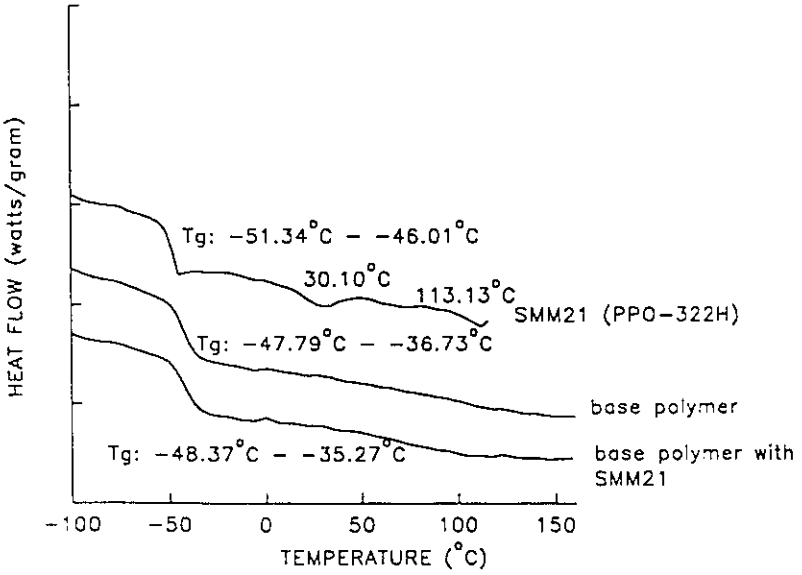

Figure 4.20. DSC thermograms of TDI/PCL/ED, SMM21 (PPO-322H) and their mixture.

increased size of the fluorine tail was likely responsible in part for these new structures. Again, neither one of the thermal properties of mixtures of SMM8 or SMM21 with base polymer were different from that of pure base polymer.

Various samples of the five SMM formulations selected for study were also characterized by DSC to verify whether the thermal properties of the materials differed from one batch synthesis to another. As shown in Appendix 6, every pair of reproduced SMMs had similar glass transition temperatures. Further, with the exception of PTMO-322H, the higher temperature transitions related to the higher ordered structures were also similar for the different batches.

In summary, incorporating SMMs into the base polyurethane at a concentration of 5% (w/w) did not alter the bulk thermal properties of the base material. However, it was noted that, since the SMM is highly concentrated near the surface, as indicated by XPS data and contact angle data to be presented below, the sensitivity DSC is likely insufficient to show any difference in structure in this limited region. Further work is planned which will investigate the mechanical stress/strain character of the polymer mixtures, in order to confirm the DSC findings with respect to the mixture's bulk properties.

4.3.2 Contact Angle Measurements

Water/air contact angle measurements on films of the base polymer and SMM-base polymer mixture films were carried out in our lab. It was observed that the SMM-TDI/PCL/ED mixtures were difficult to cast onto glass slides when the total polymer concentration (weight of SMM and base polymer/weight of solvent) was lower than 10%. However, there was no difficulty associated with the coating films of the pure base polymer, even when the polymer solution was only 2% by weight. The different behaviour observed in the mixtures may be due to the surface activity of the SMM which caused the film to be unstable when exposed to the four phases present during casting (air-SMM-base polymer-glass - see Figure 4.21). The instability is likely due in particular to the incompatibility of the hydrophobic SMM with the hydrophilic glass.

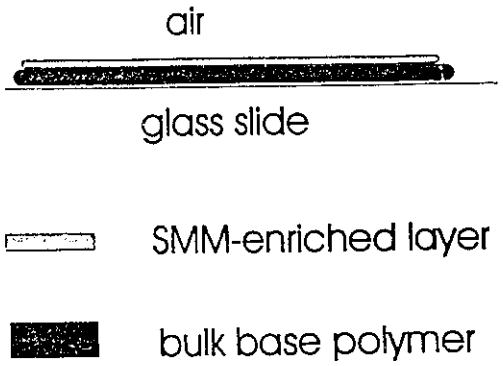

Figure 4.21. Schematic diagram of four phase equilibrium.

As shown schematically in Figure 4.21, during the evaporation of solvent the SMM migrates to the surface, forming an SMM-enriched layer and a base polymer matrix layer. Accordingly, the final slide yields a four phase equilibrium between air, an SMM-enriched layer, the base polymer matrix layer and the glass. If the total concentration of the polymer in the casting solution is too low, the base polymer matrix layer will not be thick enough to separate the SMM-enriched layer from the glass. Since the hydrophobic nature of the SMM inhibits its spreading on glass, a discontinuous film forms in that case. However, if the total polymer concentration is increased to 10%, there is enough base polymer to cover the glass, thereby providing a three phase system (air-SMM-base polymer) and making it possible to cast a continuous film. The work by another graduate student in our lab has shown that the value of the contact angle of SMM-base polymer mixtures could change when the total polymer concentration was significantly increased, indicating that the migration of SMM onto the polymer surface was also related to the total polymer content relative to the solvent. While these observations were important with respect to ultimate processing of the materials, no further optimization of solvent content or solvent type was initiated in this thesis. However, the importance of maintaining the total polymer concentration constant for each experiment was recognized.

It has been suggested that, during film formation, as the solvent evaporates the solubility of an additive within a base polymer decreases, leading to phase-separated microparticles of the additive within the base polymer matrix (141). However, Brenstedt et al. (142) found that such phase-separation would not occur until the additive content reached a certain level. He also noted that the microparticles did not inhabit the surface region. Instead, they were found in the deep layer mixed with the base polymer matrix.

As shown in Table 4.4, both the advancing and receding contact angles increased with increasing content of SMM in the TDI/PCL/ED film, until a plateau value was approached. For example, this trend is very clear in SMM26 (PPO-322I). As the concentration of SMM26 increased from 1% to 2.5%, 5%, 7.5% and 10%, the advancing contact angle increased from 98.9°, to 106.1°, and then stabilized near 116° for concentrations of 5%, 7.5% and 10%. This indicates the existence of a saturation point, implying that, beyond a certain value of SMM content in the mixture, the addition of more SMM does not influence the surface chemistry. Instead, these additional SMM molecules would likely merge in the bulk phase and possibly form what we have termed SMM sub-microdroplets within the deep layer of the base polymer (Figure 4.22). This would be analogous to the model that Brenstedt proposed for the formation of methacrylate microdroplets in polyurethanes (142). The formation of the sub-microdroplets in this work would result, in part, because of the chemical incompatibility of the fluorine tails with the base polymer. These sub-microdroplets would exist as hydrophobic fluorine tails surrounded by the prepolymer chain. Their size would be on the order of the SMM molecule itself. Based on chemical bond lengths (137) and the assumption of a fully extended molecule, the length of the sub-microdroplets would be 20 - 70 nm (actual size depends on molecular weight of a specific SMM). It should be noted that the icons depicting fluorine tails and SMM sub-microdroplets in Figure 4.22 are not to scale.

In the presence of many sub-microdroplets, it would be difficult to cast the film because of the incompatibility of the SMM with the glass slide. Indeed, it was observed that, with the addition of more SMM into the mixture, it became more difficult to get a smooth and continuous surface for contact angle measurements.

Table 4.4. Contact angle results for TDI/PCL/ED and SMM mixtures.

Name of polymer or SMM mixture	Concentration of SMM	Hysteresis (°)	Advancing contact angle (θ_{adv}) (°)	Receding contact angle (θ_{rec}) (°)
Base TDI/PCL/ED	0%	36.7 ± 0.3	77.3 ± 0.4	39.6 ± 0.6
SMM36 (PTMO-322I)	1.0%	33.6 ± 0.7	94.8 ± 0.5	60.9 ± 0.6
	2.5%	30.4 ± 0.9	99.1 ± 0.2	68.7 ± 0.8
	5.0%	25.4 ± 0.7	107.4 ± 0.5	81.4 ± 0.6
	7.5%	26.9 ± 0.8	108.9 ± 0.4	81.5 ± 0.7
	10.0%	27.7 ± 0.6	112.1 ± 0.5	84.2 ± 0.6
SMM34 (PTMO-322I)	2.5%	21.9 ± 0.7	92.4 ± 0.6	67.8 ± 0.4
	5.0%	26.1 ± 0.8	105.9 ± 0.7	79.8 ± 1.1
SMM26 (PPO-322I)	1.0%	48.2 ± 0.6	98.9 ± 0.6	51.1 ± 0.4
	2.5%	58.0 ± 0.8	106.1 ± 0.6	48.4 ± 0.6
	5.0%	62.2 ± 1.0	116.2 ± 0.6	54.3 ± 0.8
	7.5%	47.0 ± 0.8	115.3 ± 0.5	68.7 ± 0.7
	10.0%	46.6 ± 1.7	115.6 ± 0.5	67.8 ± 1.7
SMM29 (PPO-322I)	2.5%	45.9 ± 0.5	107.8 ± 0.4	52.0 ± 0.5
	5.0%	50.1 ± 0.7	114.0 ± 0.4	53.9 ± 0.5

Name of SMM	Concentration in mixture	Hysteresis (°)	Advancing contact angle (θ_{ad}) (°)	Receding contact angle (θ_{re}) (°)
SMM39 (PPO-212L)	1.0%	38.8 ± 1.0	98.9 ± 0.5	59.9 ± 0.9
	2.5%	27.2 ± 2.1	102.5 ± 1.2	75.9 ± 1.8
	5.0%	19.9 ± 1.2	109.1 ± 1.1	77.2 ± 1.3
	7.5%	36.2 ± 0.8	115.3 ± 0.5	78.6 ± 0.8
SMM37 (PPO-212L)	2.5%	22.8 ± 1.1	80.0 ± 0.8	57.2 ± 0.5
	5.0%	26.8 ± 0.8	86.6 ± 0.6	59.5 ± 0.7
SMM20 (PTMO-322H)	2.5%	21.0 ± 0.7	113.5 ± 0.5	91.5 ± 0.8
	5.0%	13.9 ± 0.6	115.8 ± 0.5	101.9 ± 0.3
SMM43 (PTMO-322H)	2.5%	14.4 ± 0.5	113.8 ± 0.4	99.4 ± 0.3
	5.0%	10.4 ± 0.5	115.6 ± 0.4	105.2 ± 0.6
SMM9 (PPO-322H)	2.5%	43.1 ± 1.0	99.9 ± 0.6	56.9 ± 0.9
	5.0%	50.4 ± 0.8	110.0 ± 0.5	61.7 ± 0.3
SMM21 (PPO-322H)	2.5%	51.1 ± 1.0	103.6 ± 0.8	52.4 ± 0.8
	5.0%	56.5 ± 0.7	113.1 ± 0.8	56.5 ± 0.8

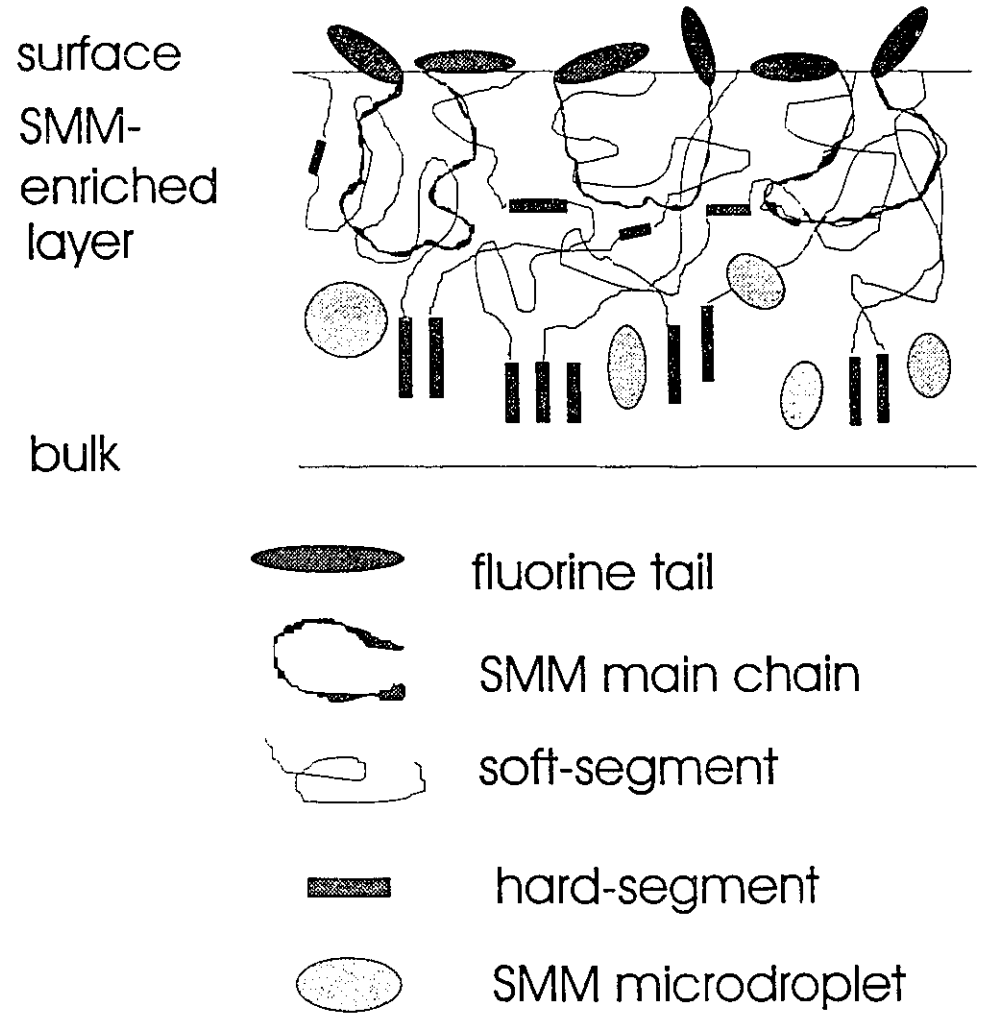

Figure 4. 22. Schematic diagram of SMM-TDI/PCL/ED base polymer mixture.

The advancing angle of the base polymer was 77.3° while its receding angle was 39.6°. By comparison, the contact angle values for the surface of the SMM-mixtures were significantly higher, indicating that the SMM was present in an enriched layer on or near the polymer-air interface. Although different SMMs may occupy an enriched layer of different thicknesses, the contact angle measurement was unable to detect such variations. The fact that receding angles of the polymer mixtures were consistently higher than that of the base polymer indicates that, after any reorientation due to the change in environment (from air to aqueous surroundings), there was still hydrophobic

segments of the SMM remaining at the interface.

It was observed that the PTMO-322I-base polymer mixture had a lower advancing contact angle than that of the PPO-322I-base polymer mixture. This may be due to the difference in chemistry between PTMO and PPO. PPO, with a methyl group outside of the main chain, is more hydrophobic than PTMO (45). It may also be explained by the fact that PTMO-322I had a longer chain than that in PPO-322I; hence, the total interchain forces (entanglement, polar interaction, and Van der Waals forces) would be larger in the former case. This force could restrict the migration of the fluorine tail to the surface, resulting in a more hydrophilic surface.

It was also observed that the contact angle of the PTMO-322I mixture did not start to level off until the concentration of the SMM increased to 10%. According to the schematic presentation of Figure 4.11, the longer molecular chain could increase the thickness of the SMM-enriched layer, although this layer would have a lower fluorine tail density. Thus, a greater quantity of SMM would be required to saturate the layer with fluorine tails. Since the advancing contact angle of the PTMO-322H mixture was higher than that of the PTMO-322I and PPO-322H mixtures, the size of the fluorine tail is also likely an important factor contributing to the SMM distribution.

It is worth noting that the receding angles of the PTMO-322I and PTMO-322H mixtures were all higher than those of the PPO-322I and PPO-322H mixtures. This has been attributed to the fact that the PTMO-SMMs had higher molecular weights and longer chains than the PPO-SMMs, allowing for more interaction with the TDI/PCL/ED soft-segment and yielding a more stable matrix of base polymer/SMM. Once established through casting, the increase in matrix stability would reduce the degree of chemical group interchange (i.e. reorganization of hydrophobic fluorine groups away from the surface and mobilization of polar groups at the aqueous interface).

This increase in matrix stability is also likely responsible for the differences in hysteresis (i.e., differences in advancing and receding contact angles) between the PTMO-containing SMM materials and PPO-containing SMM materials. As shown in Table 4.4, the PPO-SMM mixtures (both PPO-322I and PPO-322H), always displayed greater hysteresis than their PTMO-SMM analogs (PTMO-322I and PTMO-322H).

Based on the work by Freij-Larsson et al. (143), who showed that an additive with less hysteresis was less susceptible to leaching, it may be expected that these two mixtures will perform differently in the biodegradation tests.

Tests were performed to verify the reproducibility of the contact angle measurements for SMMs synthesized in different batches. The values of advancing and receding contact angles for most of the SMMs were similar. However, the results for two different batches of PPO-212L SMMs were quite different. This may be attributed to difficulties encountered in casting films for this particular SMM, due to its high fluorine content. However, it should be noted that both batches of PPO-212L showed less hysteresis than did the PPO-322I and PPO-322H mixtures, indicating that the surface structures in the former case were more stable after contact with the aqueous media. The significance of this is not entirely clear at this time, but it may be related to the secondary states that PPO-212L exhibited in the DSC thermograms.

4.3.3. X-ray Photoelectron Spectroscopy (XPS) Results

Over the past decade, XPS has become an important technique for the surface analysis of biomaterials because it is a relatively simple technique, generally nondestructive (although it was not the case in this work). It provides chemical compositions in a region closer to the surface than other available methods (144).

In the present experiments, a survey scan (0 to 1000 eV binding energy) of each sample was done at takeoff angles of 90°, 30°, and 15°. The takeoff angle was defined as the angle between the normal to sample surface and the analyzer lens (see Figure 3.4). The greatest sampling depth (approximately 100 Å, and this should be related to the sample material) occurred at a takeoff angle of 90°, and the most shallow sampling depth (about 20 Å) was found at a takeoff angle of 10°. Detailed scans for C_{1s}, O_{1s}, N_{1s}, F_{1s} and Si_{1s} were recorded. A high resolution scan of C_{1s} was acquired at all takeoff angles and the spectra were resolved into individual Gaussian peaks using a least-squares curve-

Table 4.5. C_{1s} XPS peak position for some carbon atoms (117,145).

Group	Chemistry	Peak position (eV)
hydrocarbon	—CH	285.0
amine	—CN	285.7-286.3
ether, alcohol	—C-O—	286.5
ketone	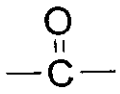	288.0
amide	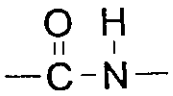	288.2
acid, ester	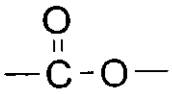	288.8
urea	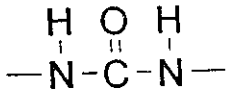	288.8
urethane	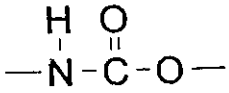	289.3 - 289.7
	$-CF_2$	291.6
	$-CF_3$	293.3

fitting program. From the C_{1s} curve-fitting and elemental composition, the amounts of each carbon species present at each takeoff angle were calculated. A listing of XPS peak position for various carbon atom types is given in Table 4.5 (117,145).

Si_{1s} was scanned in order to detect the presence of any contamination during the sample preparation, since silicon contamination has been considered to be a common problem in the laboratory environment. However, it was found that silicon contamination in all the samples was less than 1% and was considered negligible.

The Gaussian analysis of the C_{1s} spectra developed in this work produced six peaks which could be assigned to hydrocarbon (285.0 eV), ether (286.5 eV), ester (from base polymer) (287.9 eV), urea and urethane (289.1 eV), $-CF_2$ (291.2 eV), and $-CF_3$ (293.6 eV). The previous C_{1s} high resolution data for the twelve polymers discussed in section 4.1 had only five peaks in the Gaussian analysis. The newly resolved peak at 287.9 eV is most likely associated with a carbonyl carbon. The dominant chemistry at the surface of TDI/PCL/ED is associated with the soft-segment containing primarily ester groups (85). The SMM material, meanwhile, preferentially exposes its fluorine tail rather than its prepolymer chain which containing urethane groups. Hence, the most likely candidate for the 287.9 eV peaks would be the ester group. Because this shift was not observed for samples without SMMs (see Table 4.17), it is believed that the presence of the SMM may alter the ester group interaction with other polymers chains and causes the spectra shift to another level.

As introduced in section 3.4.1, several mixtures of SMM in the base polymer were sent for XPS analysis. However, due to the experimental protocol associated with the XPS analysis, the 2.5% and 7.5% SMM concentration samples were damaged. This problem was attributed to the premature surface degradation of the sample by exposure to X-ray photoelectrons. It was discovered that these samples were placed in holders that were exposed to X-rays for more than 1 hour before the analysis was done. It was later noted that X-ray induced fluorine depletion of fluorinated polymer surfaces as a result of sample over-exposure has been confirmed by Chaney et al. (146). An example of this same behaviour for our system is given in Table 4.6. Given this, the remaining data associated with the damaged samples will not presented.

The low resolution data for the five SMMs are given in Tables 4.6 to 4.10. It was observed that, for all the samples, the recorded fluorine content at the original 90° takeoff angle (100 Å) decreased after the sample had been exposed to X-rays during the analyses at the 15° and 30° takeoff angles (see 90 (I) and 90 (redo) in the Table 4.6 to 4.10). The reduction of fluorine between 90 (I) and 90 (redo) was also found in the XPS scanning performed on the SMMs synthesized in the first stage of the work (Appendix 5). This provides further confirmation that the surface of the mixture was degraded with prolonged exposure to the X-rays.

Because of the effects of surface damage, all subsequent data were analyzed by doing the deeper section analysis first (i.e. 90°), followed by the 30° data and finally the 15° data (the upper surface). This was necessary in order to prove that fluorine tails were preferentially located at the surface and that depletion based on fluorine tail migration was occurring. It has been noted that the possible error inherent in XPS analysis is 10% (43). Therefore the results obtained here can only be discussed in light of other experimental observations (i.e. DSC and contact angle data). The XPS data, in particular, will be discussed in a qualitative manner (i.e. reproducible trends) rather than from a quantitative stance.

Some attempt was made to account for the effects of surface damage during XPS analysis (see column B in Tables 4.6-4.11). The calculations were based on the assumption that the exposure time to X-rays was the same for each takeoff angle and that the degradation was linearly proportional to the exposure time. This latter assumption was based on Chaney's work (146) in which it was found that the signal ratio F_{1s}/C_{1s} decreased approximately linearly with time.

As shown in Tables 4.6 to 4.10, there was a common trend for every sample that showed an increase in the relative intensity of fluorine from a takeoff angle of 90° to a takeoff angle of 15°, indicating an enrichment in fluorine within the samples' outermost layer relative to the inner layer. A similar tendency was also observed by Han et al. (117) who grafted a perfluorodecanoic acid onto polyurethane and found that the fluorine concentration changed from 29% (atomic) at a depth of 100 Å to 44% at a depth of 20 Å.

Despite the depletion of fluorine near 100 Å in depth (90° (I)), the atomic fluorine concentration in the samples always exceeded 35%. These values are considerably higher than the overall fluorine content in mixture. For example, the mixture containing 5% PPO-212L (the highest fluorine-containing SMM) should hold approximately 0.1% (weight) fluorine. The XPS data would suggest that there was a 450% enrichment of fluorine in the top 100 Å layer. Hence, while it is commonly thought that data from a 90° takeoff angle represents the bulk material composition, samples analyzed in this study at that contact angle can hardly be representative of the bulk polymer composition, given the elevated fluorine content. Furthermore, based on the XPS analysis, the ratio of O/N for the base polymer was approximately 7 (Table 4.11). However, the O/N ratio in the SMM mixture samples was around 2-3, which was close to the O/N ratio in the SMM fluorine tails connected to the prepolymer chain by HDI. Again, this supports the notion that the fluorine tail of the SMM occupied at least the top 100 Å of the polymer mixture, and possibly would be found at even greater depths.

It was noted that the ratio of F_{1s}/C_{1s} in each sample decreased from approximately 1.6 to 0.8 when the samples were scanned from 15° to 90°. The ratio of fluorine to carbon in the upper 100 Å was much higher than the F/C ratio in the whole polymer mixture; in fact, it was much higher than the F/C ratio in the SMM itself (theoretically about 0.3). The ratio in the upper layer was similar to that in the fluorine tail (theoretically about 1.1), providing further indication that, at a depth associated with a 90° takeoff angle, the mixture was still enriched with the fluorine tails of the SMM.

It was observed that the base polymer also showed the presence of elemental fluorine on the surface, yielding a surface content of 10% for the 15° takeoff angle. There are two possible sources for this contamination. The first source may be directly from the laboratory where the polymers were synthesized. It is possible that some traces of SMM may have been inadvertently mixed with the base polymer during synthesis of the base polymer or during preparation of the XPS samples. However, such a contamination may have been expected to alter the degree of biodegradation for the polymer and this was

Table 4.6. The XPS low resolution scan for SMM26 (PPO-322I).

SMM Name	takeoff angle (°)	A				B			
		F	O	N	C	F	O	N	C
* SMM26 PPO-322I 1.0% in mixture	15	53.03	5.16	2.11	39.09	56.91	4.14	1.99	36.25
	30	40.18	8.94	2.71	47.6	47.93	6.90	2.46	41.92
	90 (I)	39.02	10.18	3.16	47.00	39.02	10.18	3.16	47.00
	90 redo	27.39	13.24	3.53	55.52				
2.5% in mixture	15	43.75	8.26	2.83	44.41				
	30	32.41	11.31	3.64	52.16				
	90 (I)	30.46	13.03	4.01	52.11				
	90 redo	23.32	14.70	3.72	57.95				
* 5.0% in mixture	15	52.54	5.28	1.56	39.76	56.66	4.21	1.44	36.82
	30	38.90	9.77	3.01	47.78	47.15	7.63	2.76	41.89
	90 (I)	39.21	10.17	3.28	46.98	39.21	10.17	3.28	46.98
	90 redo	26.84	13.38	3.65	55.81				
7.5% in mixture	15	42.66	8.47	2.28	46.06				
	30	33.19	11.59	3.11	51.74				
	90 (I)	31.65	12.42	3.69	51.84				
	90 redo	23.16	14.16	4.24	58.05				

note: the unit of data in table is atomic%

*: data used for discussing (for detail see page 94)

A column: original data

B column: calculated data based on the assumption (for detail see page 95)

Table 4.7. The XPS low resolution scan for SMM36 (PTMO-322I).

SMM Name	takeoff angle (°)	A				B			
		F	O	N	C	F	O	N	C
SMM36	15	52.63	5.06	2.69	38.85	55.80	4.40	2.48	36.53
PTMO-322I	30	38.97	7.41	3.88	48.25	47.04	7.09	3.46	43.61
1.0% in	90 (I)	37.82	9.36	3.81	48.57	37.82	9.36	3.81	48.57
mixture	90 redo	28.30	11.34	4.45	55.53				
	15	54.00	4.30	2.44	38.33	58.09	3.59	2.24	35.22
	30	38.95	8.25	3.95	48.23	47.12	6.82	3.55	41.78
5.0% in	90 (I)	41.53	7.54	4.20	46.11	41.53	7.54	4.20	46.11
mixture	90 redo	29.27	9.68	4.80	55.78				

Table 4.8. The XPS low resolution scan for SMM39 (PPO-212L).

SMM Name	takeoff angle (°)	A				B			
		F	O	N	C	F	O	N	C
SMM39	15	54.47	4.28	2.43	38.06	58.79	4.32	2.30	34.58
PPO-212L	30	43.89	6.75	3.53	45.06	52.53	5.28	3.26	38.11
1.0% in	90 (I)	47.07	6.84	3.69	41.73	47.07	6.84	3.69	41.73
mixture	90 redo	34.11	9.05	4.09	52.16				
	15	48.69	5.86	3.03	41.74	51.24	5.33	2.64	40.09
	30	41.22	7.80	4.67	45.63	46.31	6.75	3.90	42.32
5.0% in	90 (I)	40.82	8.72	4.48	45.37	40.82	8.72	4.48	45.37
mixture	90 redo	33.18	10.30	5.64	50.33				

Table 4.9. The XPS low resolution scan for SMM20 (PTMO-322H).

SMM Name	takeoff angle (°)	A				B			
		F	O	N	C	F	O	N	C
SMM20	15	55.16	4.12	1.68	38.08	59.65	3.49	1.59	34.26
PTMO-322H	30	42.09	6.62	3.35	47.35	51.08	5.36	3.17	39.70
1.0% in	90 (I)	42.17	8.34	3.70	45.21	42.17	8.36	3.70	45.21
mixture	90 redo	28.69	10.23	3.97	56.68				
	15	53.35	3.89	2.28	39.65	57.45	3.16	2.14	36.35
	30	43.31	6.30	3.46	46.33	51.52	4.85	3.81	39.73
5.0% in	90 (I)	45.60	6.64	3.78	43.33	45.60	6.64	3.78	43.33
mixture	90 redo	33.29	8.82	4.20	53.23				

Table 4.10. The XPS low resolution scan for SMM21 (PPO-322H).

SMM Name	takeoff angle (°)	A				B			
		F	O	N	C	F	O	N	C
SMM21	15	53.45	4.49	1.84	39.53	57.78	3.54	1.57	36.32
PPO-322H	30	37.62	9.04	2.86	49.96	46.28	7.13	2.33	43.53
2.5% in	90 (I)	40.97	9.40	2.84	46.12	40.97	9.40	2.84	46.12
mixture	90 redo	27.97	12.26	3.64	55.76				

Table 4.11. The XPS low resolution scan for TDI/PCL/ED base polymer

SMM Name	takeoff angle (°)	A				B			
		F	O	N	C	F	O	N	C
TDI/PCL/ED	15	10.03	18.72	3.55	67.60				
	30	4.37	21.52	2.99	71.02				
	90 (I)	5.43	21.25	3.32	69.89				
	90 redo	3.29	21.26	2.65	71.75				

not observed. Therefore, it is not expected that the source of the contamination originated with the laboratory practice.

The second explanation, and perhaps the more likely one, is the following. The pure base polymer was placed on the same holder as the other samples containing SMMs. Since it is likely that the fluorine component contained within these latter samples was degraded due to prolonged exposure to X-rays, fluorine-containing degradation by products may have been released and subsequently deposited on the surface of the pure base polymer. If the contamination was associated with SMM degradation, we would expect to see no correlation between $-CF_2$ and $-CF_3$ group content in the high resolution data. This, in fact, was the case. For example, given the elemental composition of the fluorine tail, a 10% concentration of fluorine should result in approximately 4.5% $-CF_2$ and 1% $-CF_3$. However, at a takeoff angle of 15°, the $-CF_2$ content was only 1.5% and no $-CF_3$ was observed (see Table 4.17).

Tables 4.12 to 4.17 contain the high-resolution data for the C_{1s} spectra of each sample. As was done for the low resolution data, the degraded sample results are only presented for PPO-322I in Table 4.12 to illustrate the effect of the X-rays on the samples after prolonged exposure. Most polyurethanes typically show a surface depletion of the urethane/urea groups near the surface (52,92). This was also observed for the base polyurethane in this work (Table 4.17). However, after the addition of SMM to the base polymer, this depletion was no longer consistently observed. In fact, the presence of the

urethane bond in the polymer mixtures is thought to be primarily related to the urethane bonds inside the SMM molecules. This is supported by the increase in the peak at 289 eV observed in the PPO-212 mixture (Table 4.14) compared to the PPO-322 mixture (Table 4.12 and 4.16), since the 2:1:2 stoichiometry has a higher urethane content than the 3:2:2 stoichiometry.

Another trend in chemical group changes was observed for the concentration profile of $-CF_2$ and $-CF_3$: as the takeoff angle increased, the amount of $-CF_2$ and $-CF_3$ components decreased. The result was similar to that of the fluorine in the low resolution scans, indicating that the $-CF_2$ and $-CF_3$ groups were present in higher concentrations at the surface. In addition, it was interesting to compare the ratio of $-CF_3/-CF_2$ in each sample. As introduced in section 3.2.7, BA-L was separated into three fractions by distillation, and the difference between them lay in the number of $-CF_2$ groups present, while the number of $-CF_3$ groups in the chain remained the same between fractions. The XPS data revealed that the ratio $-CF_3/-CF_2$ in PPO-212L was greater than that in PTMO-322I. Similarly, the ratio in PPO-322I was greater than those in PTMO-322H and PPO-322 for all take-off angles when the BA-L fraction changed from Low to Int or from Int to High. Further it was observed that the $-CF_3/-CF_2$ ratio was the highest at a takeoff angle of 15°, indicating that the $-CF_3$ tail was preferentially found near the surface. The enhanced exposure of the $-CF_3$ groups near the surface likely contributes to the fact that the contact angle values achieved here were greater than that of Teflon ($-(CF_2)-$). (Note that, according to the technical documents from Du Pont that accompanies the BA-L, CF_3 groups are more hydrophobic than CF_2 groups.)

As discussed earlier, the 287.9 eV peak was assigned to the ester bond in the TDI/PCL/ED soft-segment. Therefore, this peak could be used as a measure of TDI/PCL/ED soft-segment content at the surface. As shown in Table 4.12 to 4.16, the ester group has the lowest concentration of all groups at the surface. This also supports the notion that the surface was composed of SMM polymer chains, with fewer TDI/PCL/ED chains found there.

Table 4.12. C_{1s} high-resolution scan for SMM26 (PPO-322I).

SMM Name	takeoff angle (°)	bond energy (eV) 285.0	286.5	287.9	289.1	291.2	293.6
*SMM26	15	25.29	26.88	3.38/2.38	7.26/6.70	30.57/34.11	6.63/7.22
PPO-322I	30	35.62	31.57	4.77/2.76	7.69/6.57	17.31/24.38	3.04/4.21
1.0% in	90 (I)	30.03	38.60	2.48	5.54	19.86	3.50
mixture	90 redo	39.98	36.19	5.50	7.37	9.23	1.74
	15	36.90	26.90	3.56	8.72	19.38	4.55
	30	44.21	30.11	4.03	8.53	11.36	1.75
2.5 % in	90 (I)	39.93	37.49	2.58	7.54	10.89	1.57
mixture	90 redo	47.50	32.47	4.14	8.47	6.21	1.21
*	15	25.43	27.42	3.07/2.28	6.95/6.95	30.13/34.16	6.99/7.98
	30	34.16	32.71	4.23/2.65	7.76/7.79	17.09/25.15	3.58/5.55
5.0% in	90 (I)	30.13	38.94	1.78	5.26	20.43	3.45
mixture	90 redo	42.16	38.07	4.15	5.26	8.34	0.49
	15	37.27	28.24	2.68	9.29	17.74	4.79
	30	43.62	31.34	2.88	8.65	11.60	1.95
7.5% in	90 (I)	38.10	38.29	2.38	7.36	12.14	1.74
mixture	90 redo	47.90	24.91	3.22	7.66	5.92	0.39

note: the unit of data in table is atomic%

the data with underline is calculated based on assumption (for detail see page 95)

*: the data for discussing (for detail see page 94)

285.0 eV: C-C
286.5 eV: C-O
287.9 eV: ester
289.1 eV: urethane
291.2 eV: $-CF_2$
293.6 eV: $-CF_3$

Table 4.13. C_{1s} high-resolution scan for SMM36 (PTMO-322I).

SMM Name	takeoff angle (°)	bond energy (eV) 285.0	286.5	287.9	289.1	291.2	293.6
SMM36	15	32.97	21.58	3.00/2.64	6.80/6.48	28.75/31.59	6.90/7.79
PTMO-322I	30	42.01	26.56	3.32/2.60	7.61/6.97	17.26/23.54	3.24/1.79
1.0% in	90 (I)	38.18	32.08	2.30	5.69	18.31	3.43
mixture	90redo	47.90	32.44	3.38	6.64	8.89	0.75
	15	30.45	20.87	3.00/2.20	8.59/8.00	29.37/33.51	7.71/8.46
	30	39.97	24.62	4.77/3.18	8.99/7.79	17.66/25.93	3.99/5.48
5.0% in	90 (I)	34.80	28.73	2.94	6.42	23.00	4.11
mixture	90redo	45.62	28.37	5.33	8.21	10.59	1.87

Table 4.14. C_{1s} high-resolution scan for SMM39 (PPO-212L).

SMM Name	takeoff angle (°)	bond energy (eV) 285.0	286.5	287.9	289.1	291.2	293.6
SMM39	15	33.90	19.63	3.52/1.74	10.63/8.93	25.18/27.03	7.14/7.17
PPO-212L	30	34.75	18.23	7.65/4.10	14.75/11.4	19.18/22.88	5.44/5.50
1.0% in	90 (I)	38.15	21.84	4.31	11.01	20.22	4.48
mixture	90redo	35.93	19.16	9.63	16.11	14.67	4.51
	15	29.59	22.99	3.22/2.79	8.52/7.29	27.97/21.44	7.71/8.61
	30	34.07	25.50	5.17/4.31	8.75/6.29	21.26/28.21	5.25/7.05
5.0% in	90 (I)	30.14	30.14	2.87	6.17	24.95	5.73
mixture	90redo	41.14	27.28	4.16	9.86	14.53	3.03

Table 4.15. C_{1s} high-resolution scan for SMM20 (PTMO-322H).

SMM Name	takeoff angle (°)	bond energy (eV) 285.0	286.5	287.9	289.1	291.2	293.6
SMM20	15	30.95	16.88	2.14/1.22	7.71/7.16	35.93/40.18	6.40/6.80
	30	39.29	23.72	4.78/2.94	8.51/7.40	20.25/28.75	3.46/4.27
1.0% in	90 (I)	35.95	28.99	2.28	5.79	23.22	3.77
mixture	90redo	46.70	29.13	5.04	7.45	10.47	1.21
	15	30.94	19.67	2.61/1.91	7.49/6.99	33.26/37.76	6.03/7.25
	30	38.51	23.89	5.09/3.70	8.45/7.45	20.89/29.88	3.19/5.63
5.0% in	90 (I)	32.72	27.39	2.94	6.30	26.14	4.52
mixture	90redo	45.93	27.75	5.03	7.79	12.65	0.86

Table 4.16. C_{1s} high-resolution scan for SMM21 (PPO-322H).

SMM Name	takeoff angle (°)	bond energy (eV) 285.0	286.5	287.9	289.1	291.2	293.6
	15	28.98	26.95	0.98/0.0	7.67/6.70	30.08/34.28	5.33/6.05
	30	38.54	29.54	4.07/1.81	8.83/6.89	16.45/24.84	2.57/4.02
2.5% in	90 (I)	29.37	36.54	1.77	5.78	22.50	4.04
mixture	90redo	41.95	32.43	5.16	8.69	9.91	1.87

Table 4.17. C_{1s} high-resolution scan for TDI/PCL/ED base polymer.

SMM	takeoff	bond energy (eV)			
Name	angle (°)	285.0	286.5	289.1	291.2
TDI/PCL/ED	15	57.98	28.73	11.86	1.53
	30	59.06	28.80	11.88	0.26
	90 (I)	60.48	25.31	13.54	0.67
	90 redo	61.17	26.06	12.76	–

note: the unit of data in table is atomic%
the data with underline is calculated based on assumption (for detail see page 95)

285.0 eV: C-C
286.5 eV: C-O
289.1 eV: urethane/urea/ester
291.2 eV: $-CF_2$

In summary, the XPS data support the concept of surface migration of the SMM and correlate well with the advancing contact angle data presented in the previous section. However, caution should be taken with the interpretation of these data since they only reflect the state of the polymer when exposed to air and do not reflect its hydrated state.

4.4. SMM Biostability Test

As discussed in the previous two sections, both the contact angle and XPS results indicated that the surface of the base polymer-SMM mixture was enriched with fluorine. While the preliminary biodegradation tests on ^{14}C-TDI/PCL/ED showed that biodegradation was inhibited by SMMs, it was important to verify that the SMMs themselves remained stable at the polymer/aqueous interface and were not being leached out or degraded by the enzyme to any significant extent. If SMMs were being removed then any inhibition would only be temporary.

To assess the biostability of the SMM materials, three SMMs were synthesized with radiolabelled ^{14}C-HDI. The three SMMs (PPO-212L, PPO-322I and PTMO-322I) were selected based on a greater confidence in their reproducibility. The radiolabel content and the weight average molecular weight and fluorine content for the three polymers are listed in Table 4.18. The molecular weights and fluorine content were similar to the non-radiolabelled analogs presented in Table 4.3.

Table 4.18. Weight average molecular weight, fluorine content and radioactivity of radiolabelled materials.

Radiolabelled SMM	Molecular weight (Mw)	Fluorine content	Radioactivity (cpm/100 mg)
^{14}C-TDI/PCL/ED Base polymer	1.2×10^5	0%	2.8×10^5
PPO-212L	1.6×10^4	20.35%	2.4×10^6
PPO-322I	3.5×10^4	4.85%	3.5×10^6
PTMO-322I	5.0×10^4	4.58%	4.0×10^6

It is noted that the radiolabelled SMMs contained approximately ten fold more radioactivity than the base polymer in order to provide enough radiolabel in the ^{14}C SMM-TDI/PCL/ED mixtures to be counted. The biodegradation tests were carried out using the same system as that used for the SMM-^{14}C TDI/PCL/ED biodegradation tests discussed in section 4.1.

Figure 4.23 shows the cumulative radiolabel release from the ^{14}C PPO-322I - TDI/PCL/ED mixture incubated with both buffer and cholesterol esterase, the model enzyme used in this study, for seven weeks. The results show that radiolabelled products were released from both the buffer- and enzyme-incubated materials and this release increased with increasing SMM content. However, the difference in radiolabel release from these two incubations was meagre; furthermore, the rate of radiolabel release slowed down after three weeks (Appendix 7). In the case of the enzyme solution, the release of SMM may have been due to a combination of buffer interactions and the biodegradation of the base polymer (which is not fully protected from degradation, see section 4.1). It is highly unlikely that the SMM itself was enzymatically degraded since the amount of radiolabel released for the highest SMM concentration (i.e. 5%) was only 100 cpm/mL, which is significantly lower than the radiolabel content in the incubated sample (i.e., 7.0×10^4). In addition, 100 cpm/mL was also significantly lower than the amount of radiolabelled material released from TDI/PCL/ED in the biodegradation tests presented in section 4.1. When it is considered that the entire surface is highly saturated with radiolabelled SMM (based on XPS and contact angle data) it would expected that, if the SMM were hydrolytically unstable, significantly higher radiolabel counts would be detected.

A comparison was also made between the amount of radiolabelled products released from the pure radiolabelled base polymer and ^{14}C SMM-TDI/PCL/ED base polymer mixture. As shown in Figure 4.24, the total radiolabel counts available for the pure ^{14}C-TDI/PCL/ED base polymer and ^{14}C PPO-322I-TDI/PCL/ED base polymer mixture were almost identical. After incubation in cholesterol esterase and buffer for approximately two months, significantly more radiolabelled products were released from the radiolabelled base polymer than were released from the SMM mixture, indicating that

PPO-322I SMM was relatively more stable, compared to the base polymer, in cholesterol esterase.

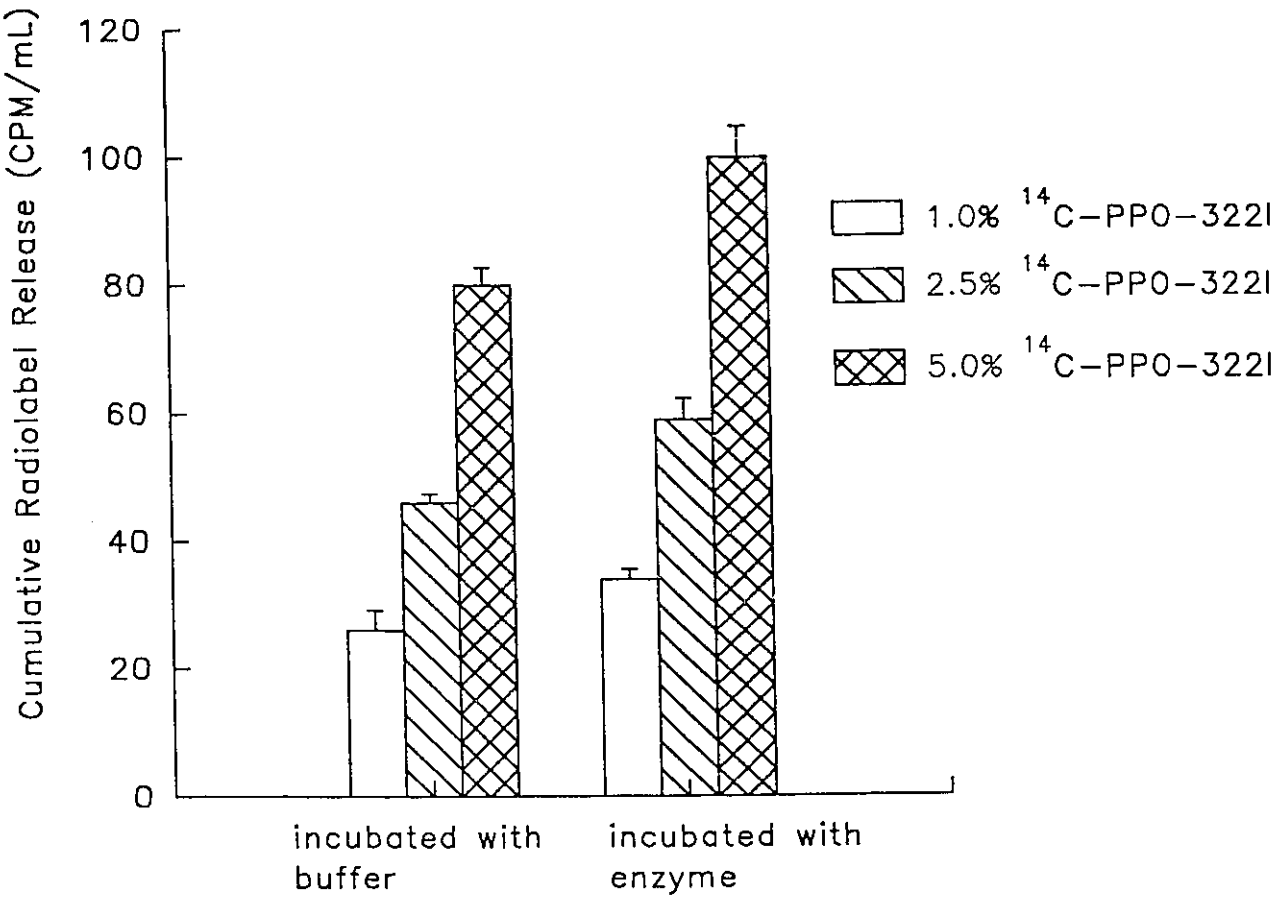

Figure 4.23. Biostability test results of ^{14}C PPO-322I after 7 weeks of incubation.

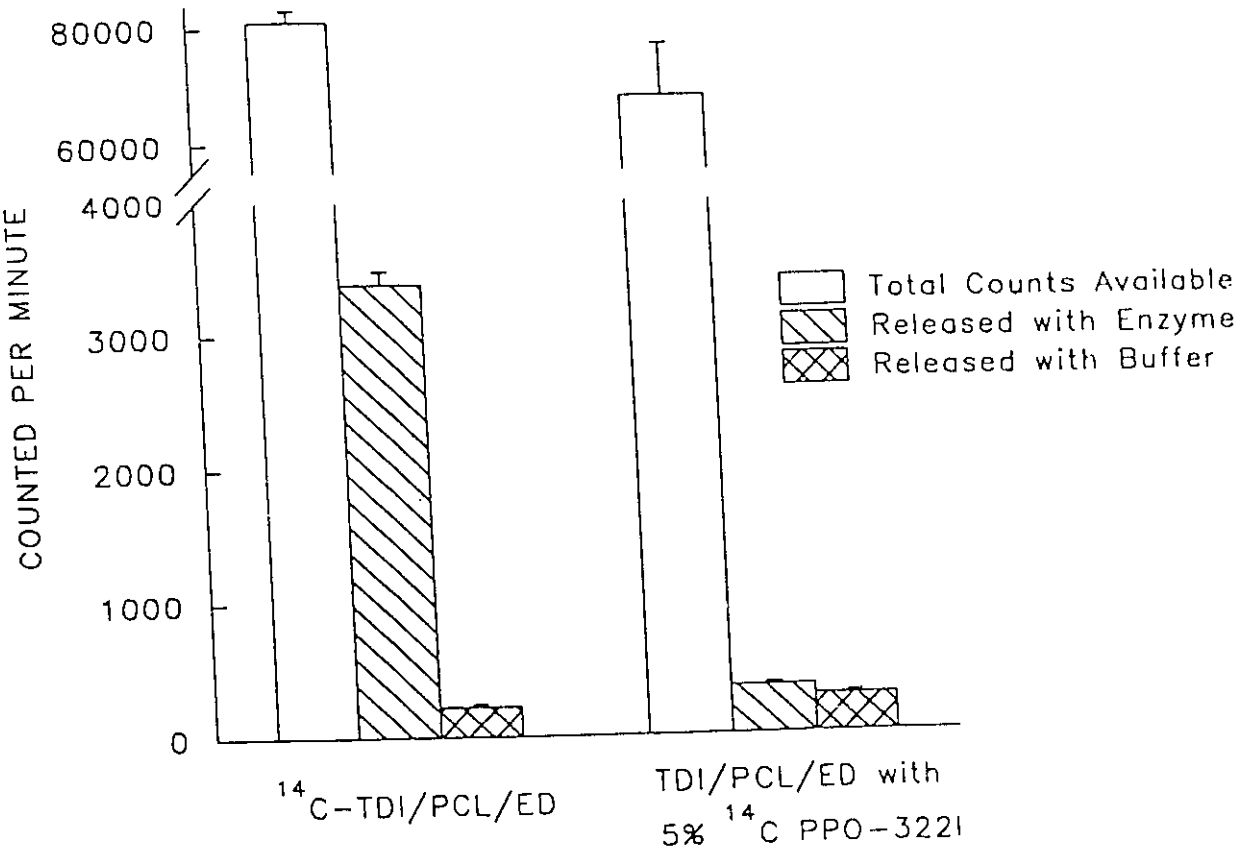

Figure 4.24. The comparison of the biostability of ^{14}C TDI/PCL/ED and ^{14} PPO-322I after 10 weeks of incubation.

It was also interesting to compare the amount of labelled products released from the various SMMs. It was apparent that the amount of radiolabelled products released from ^{14}C PTMO-322I (Figure 4.25) was lower than that from the ^{14}C PPO-322I SMM, although the two materials initially contained similar levels of radioactivity (see Table 4.18). This might be related to differences in their stability, possibly due to their different reorientation behaviour in a water environment (see the contact angle hysteresis data). As discussed in section 4.3.2, PTMO-322I yielded a more stable surface in an aqueous medium than did the PPO-322I, and it is possible that the enzymatic degradation of the former SMM could be reduced because of this stability in the upper layer of the polymer mixture. It should also be kept in mind that the polyol in PTMO-322I, i.e. PTMO, might be more compatible with the base polymer (i.e. hydrophobic versus hydrophilic), therefore stabilizing it within in the polymer matrix and providing greater protection against enzymatic attack.

Since the radioactivity of radiolabelled PPO-212L was significantly lower than the other two radiolabelled SMMs, it was difficult to directly compare the stability of PPO-212L to the other two. However, it was evident that labelled PPO-212L was being released into solution since the amount of radioactivity released was dependent on the SMM concentration in the polymer matrix (Figure 26). Bearing in mind both the biodegradation results and the stability tests (section 4.1), it is noted that there is an advantage in using the PPO-212L SMM over the other two SMMs: only 1% PPO-212L is required to achieve the same level of enzyme inhibition as do 5% mixtures of the other two SMMs. Further, at a 1% concentration this SMM showed a very low level of degradation or leaching, even after 7 weeks of incubation with enzyme or buffer.

The results suggest that the SMMs are relatively stable, and that PTMO-322I exhibits the greatest stability, although PTMO-322I is not necessarily the best candidate for inhibiting the biodegradation of the TDI/PCL/ED base polymer by cholesterol esterase (see section 4.1).

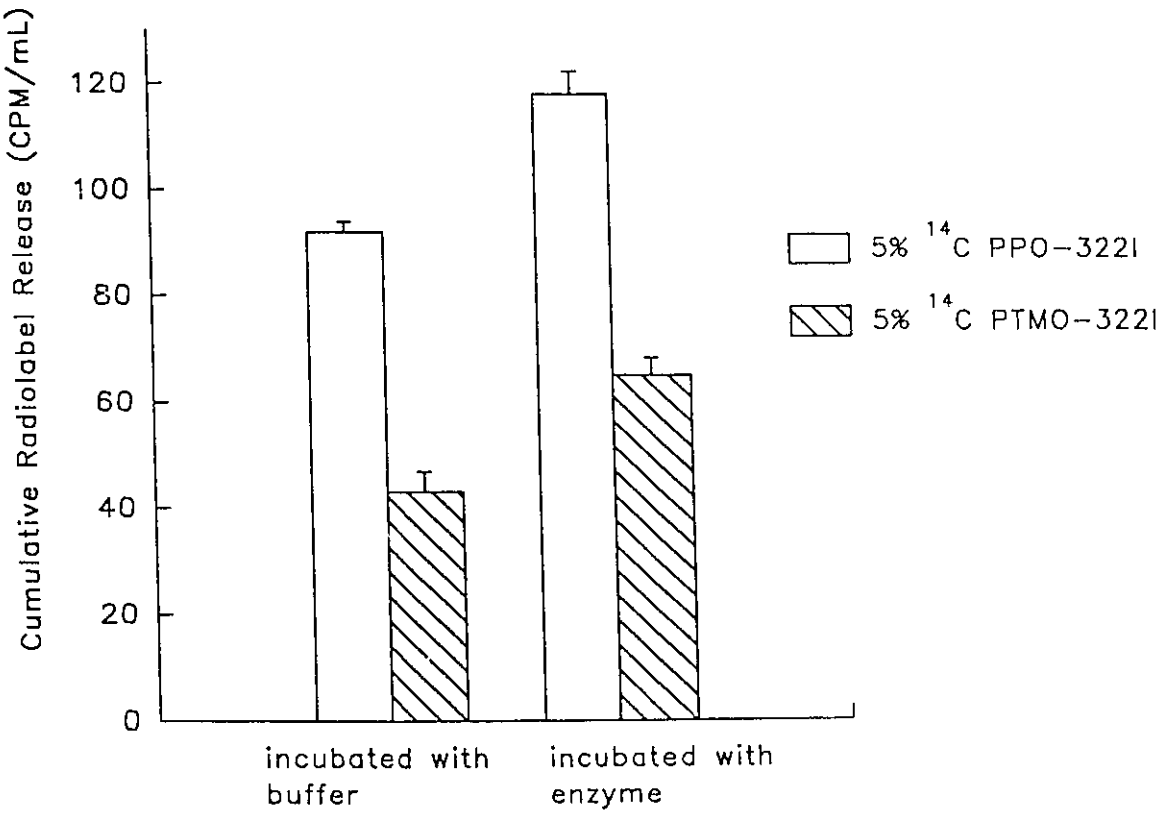

Figure 4.25. The comparison of biostability of ^{14}C PPO-322I and ^{14}C PTMO-322I after 10 weeks of incubation.

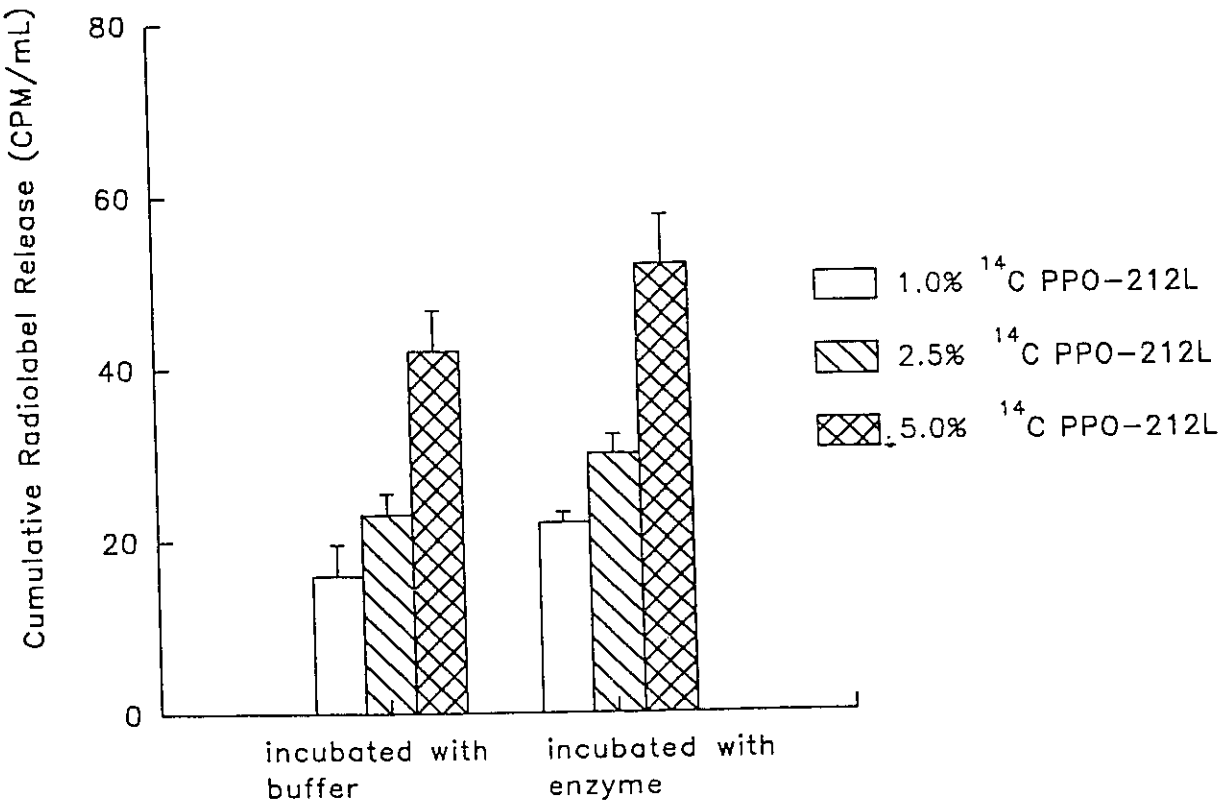

Figure 4.26. The biostability test results of ^{14}C PPO-212L after 7 weeks of incubation.

4.5. Long-term Biodegradation Test for TDI/PCL/ED Base Polymer Containing SMMs

As indicated in section 4.1.3, all five of the SMMs selected for optimization showed the ability to inhibit biodegradation of the base polymer (TDI/PCL/ED) by cholesterol esterase. However, those tests were short-term (three weeks) and did not test the stability of the SMM mixture over very long periods of time. A long-term experiment would more appropriately reflect the lifetime of a material for many cardiovascular implants.

Long-term tests for PPO-322I and PTMO-322I (2.5% and 5.0% in TDI/PCL/ED) were initiated at the end of January 1994. The data for these experiments are shown in Figure 4.27, and indicate that a significant difference in radiolabel released between the base polymer and base polymer/SMM mixtures was maintained for more than half a year. This demonstrates the relative stability of the SMM and the ability of SMMs to inhibit the biodegradation of TDI/PCL/ED for an extended period of time. Unfortunately, it is still not clear how the mechanism of TDI/PCL/ED degradation by the enzyme works and at what depth below the surface these interactions occur. Recent papers by Santerre and Labow (85) have indicated that ester groups in proximity to the hard-segment are the likely cleavage sites in the polymer. If this is correct then the reduction in number of the ester groups at the surface as indicated by the XPS data presented in section 4.3 may explain the biodegradation data for the five polymers. Since all of these mixtures had a similar number of ester groups, they would likely exhibit similar numbers of cleavage sites. In addition, from the results of XPS analysis and DSC thermograms for the pure TDI/PCL/ED and the SMM mixtures, it was clear that the surfaces of SMM mixtures contained high concentrations of SMM, while the bulk properties were not altered. It is also possible that, with such a high concentration of SMM in the surface region that a new micro-structure near the surface was established in a manner that effectively controlled the rate of the biodegradation process. This would explain why the apparent inhibition lasts for such a long time.

It should be noted that SMM15 (PTMO-322I) had almost the same inhibitory effect as that of SMM7 (PPO-322I), although their molecular weight and fluorine content were

not similar and their contact angle and hysteresis data differed. This result shows that the biodegradation mechanism is not only related to the molecular weight, fluorine content and the wettability of the additive. There must be other factors, such as the domain structure, hydrogen bonding, and distribution of SMMs within the mixture, that also affect the biodegradation process. It is also interesting to note that after thirty four weeks, PTMO-322I appeared to have become more stable than PPO-322I. While the differences in the cumulative radiolabel release for these two SMMs are still not large at thirty four weeks, it would be important in future work to monitor the degradation for longer periods. Such a trend may indicate an the enhanced stability of PTMO-322I in the polymer matrix.

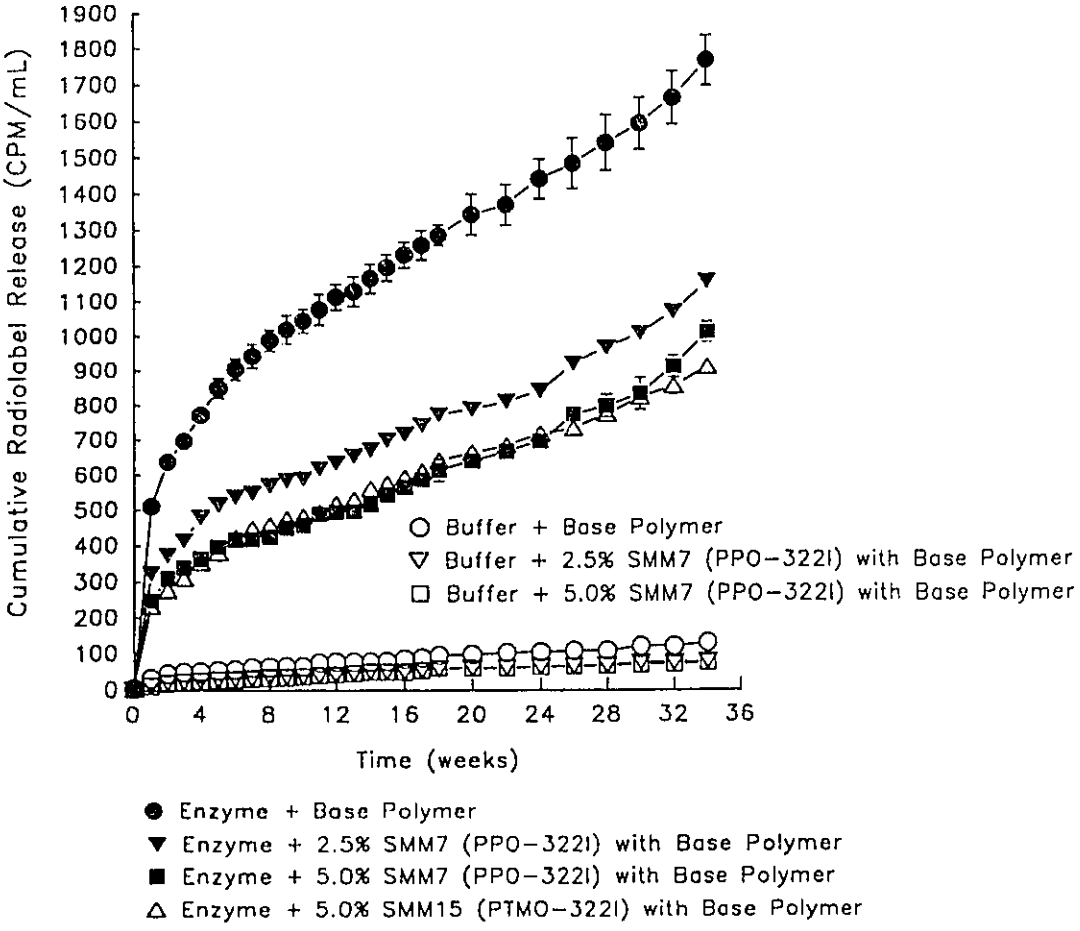

Figure 4.27. Long-term biodegradation results of SMM7 (PPO-322I), and SMM15 (PTMO-322I).

4.6. Biodegradation Test of SMM (PPO-212L) on TDI/PTMO/ED Base Polymer

The purpose of this research was to develop an additive which would improve the resistance of polyurethanes to enzymatic degradation. Assuming that the microdomain structure at the interface is critical in determining the ability of the SMM to inhibit degradation, it is of interest to compare the performance of SMMs optimized for TDI/PCL/ED in a polyurethane of a different chemistry to test the sensitivity of the SMM's inhibition characteristics to the type of base polymer.

^{14}C TDI/PTMO/ED, a polyether-urea-urethane, which differed from TDI/PCL/ED in the content of the soft-segment diol, was used in this regard. Pure TDI/PTMO/ED was found to be degraded by cholesterol esterase solutions at concentrations of 4 unit/mL (81), and its microdomain differed significantly from that of TDI/PCL/ED (85).

PPO-212L was selected to be incorporated into TDI/PTMO/ED since it was the SMM that showed the most effective inhibition of ^{14}C-TDI/PCL/ED degradation. In this test, a non-radiolabelled PPO-212L (SMM19) was added to radiolabelled ^{14}C-TDI/PTMO/ED. In addition, radiolabelled PPO-212L was added to non-radiolabelled TDI/PTMO/ED to assess the stability of the SMM in the TDI/PTMO/ED polymer mixture. The results shown in Figure 4.28 indicate that there was no inhibition of TDI/PTMO/ED biodegradation by PPO-212L. This suggests that the interaction of the SMM with a given base polymer is critical in determining the effectiveness of the SMM.

Past work in our laboratory has shown that TDI/PCL/ED is much more sensitive to degradation by CE than is TDI/PTMO/ED (81). The studies have also presented data suggesting that the cleavage sites in the polymers are different (85). If this is true, then it could be hypothesized that, although the PPO-212L could protect a number of TDI/PCL/ED cleavage sites from degradation, the SMM could not protect the CE sensitive cleavage sites in TDI/PTMO/ED. Further work with TDI/PTMO/ED will be required to find an SMM formulation suitably matched to the polyurethane's chemistry and microdomain structure. (It should be kept in mind that PTMO-322I might be a better candidate than PPO-212L, because the main chain of PTMO-322I bears greater similarity to the soft-segment of TDI/PTMO/ED.)

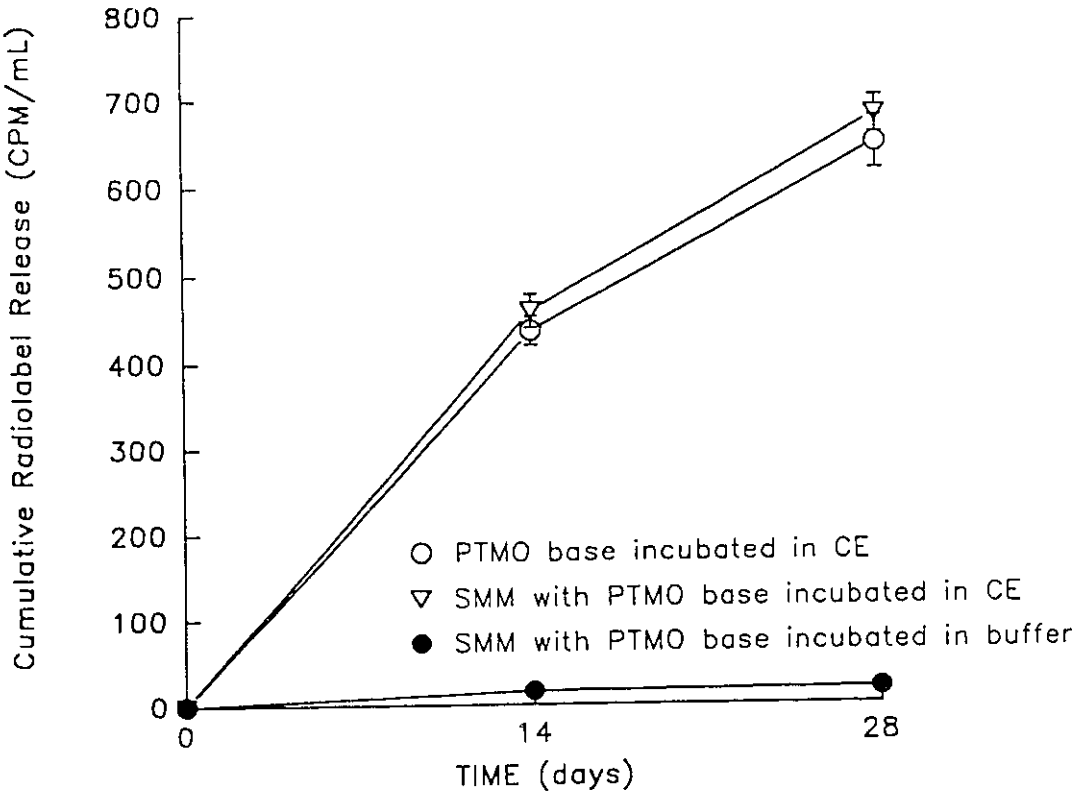

Figure 4.28. The biodegradation results of TDI/PTMO/ED with and without SMM.

In order to assess the biostability of PPO-212L in the TDI/PTMO/ED polymer, ^{14}C PPO-212L was mixed into non-radiolabelled TDI/PTMO/ED and the same experiment was done as described in section 4.4. The results of ^{14}C PPO-212L biostability tests in the TDI/PTMO/ED polymer mixture (see Figure 4.29) showed that this SMM was not as stable here as when it was contained in TDI/PCL/ED (see Figure 4.26). As shown in Figure 4.26, 5% ^{14}C PPO-212L in TDI/PCL/ED released less than 60 cpm/mL after seven weeks of incubation. However, 5% ^{14}C PPO-212L in TDI/PTMO/ED released about 80 cpm/mL after only four weeks of incubation (see Figure 4.29). These results suggest that the stability of the SMM in a matrix is not only determined by the SMM itself, but also by the matrix in which it is mixed to form the microstructure. No further study of these results were carried out at this time since a full characterization of this new substrate is beyond the scope of the current thesis. However, the fact that PPO-212L did not show any ability to inhibit the CE degradation of the poly-ether-urea-urethane indicated that a specific SMM additive could not be universally applied to all polyurethanes.

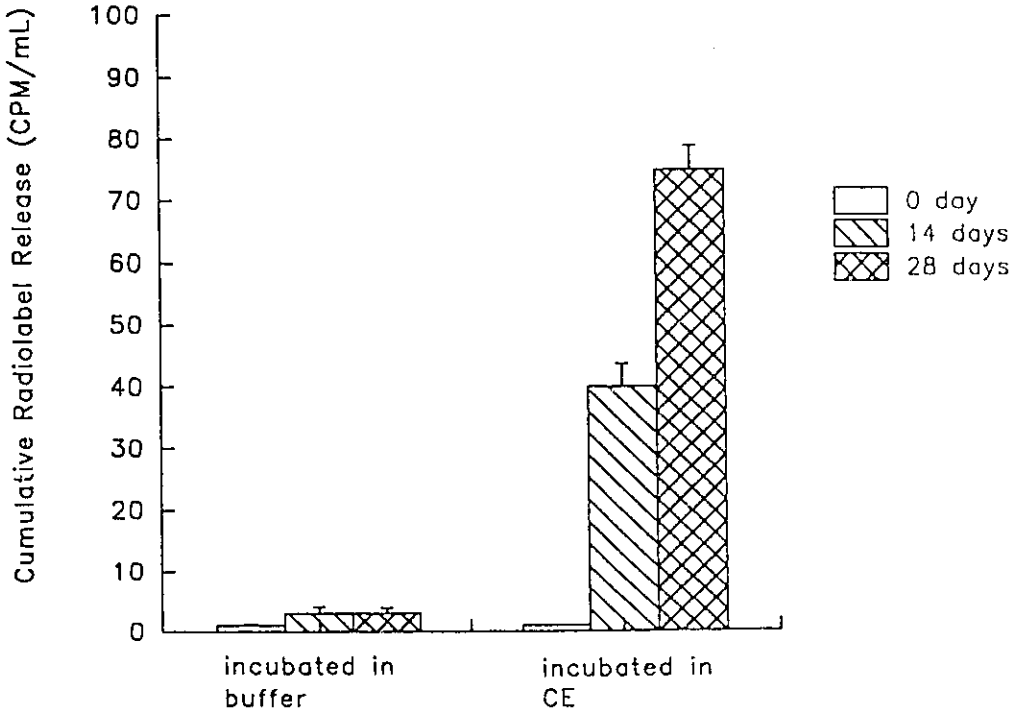

Figure 4.29. The biostability result of 5% ^{14}C PPO-212L in TDI/PTMO/ED base polymer.

4.7. Fibrinogen Adsorption Test

Since the new materials are targeted for cardiovascular applications involving contact with blood, it was of interest to carry out some preliminary blood compatibility tests. Fibrinogen adsorption has been traditionally related to the formation of blood clots and has become an important test of biocompatibility (23, 147). Fibrinogen adsorption studies were carried out, utilizing Dr. John Brash's laboratory at McMaster University, Ontario.

SMM26 (PPO-322I) was selected to be mixed with the TDI/PCL/ED base polymer. The results in Figure 4.30 showed that, for diluted fibrinogen solutions, almost 50% inhibition of fibrinogen adsorption occurred. At higher fibrinogen concentrations (0.5 mg/mL), the inhibition effect was still evident, although the degree of inhibition decreased to 20%. The reduction of fibrinogen adsorption suggests that this new surface has better blood compatibility than that of TDI/PCL/ED.

These results are somewhat suggestive of a reduced biodegradation, since Eaton et al. (148) have demonstrated that the adsorption of fibrinogen initiates the acute inflammatory response of the host by an implant polymer. As discussed in section 2.3.2, the enzymes involved in the degradation of polyurethanes are possibly released by inflammatory-related phagocytes. Thus the SMM additive can have two important roles with respect to improving the biocompatibility and biostability of polyurethanes: it can reduce fibrinogen adsorption, which is related to blood clot formation, and it can also reduce the inflammatory response and therefore inhibit the release of enzymes that can degrade polyurethanes.

It is also important to note that several studies have reported relationships between protein adsorption and surface wettability, although the data are inconclusive. Brunstedt et al. (149) mixed poly(methylene-(polyphenyl isocyanate)) based additives into a poly-ether-urea-urethane (MDI/PTMO/ED) and found that both the receding contact angle and fibrinogen adsorption decreased. Meanwhile, Han et al. (117) grafted a perfluorodecanoic acid onto the surface of Pellethane® (poly-ether-urea-urethane) and showed that a low surface tension surface was provided (i.e. poor wettability). This surface showed both lower platelet adhesion and less blood clot formation (therefore less

fibrinogen activation on the surface). These contradictory results indicate that the wettability of the surface should not be the only test for fibrinogen adsorption trends, and that other factors, such as the microdomain distribution near the surface and within the bulk, the hydrogen bonding microstructure, etc., must also be taken into account. This would be in keeping with the concluding statements on biodegradation-related phenomena presented in the previous section.

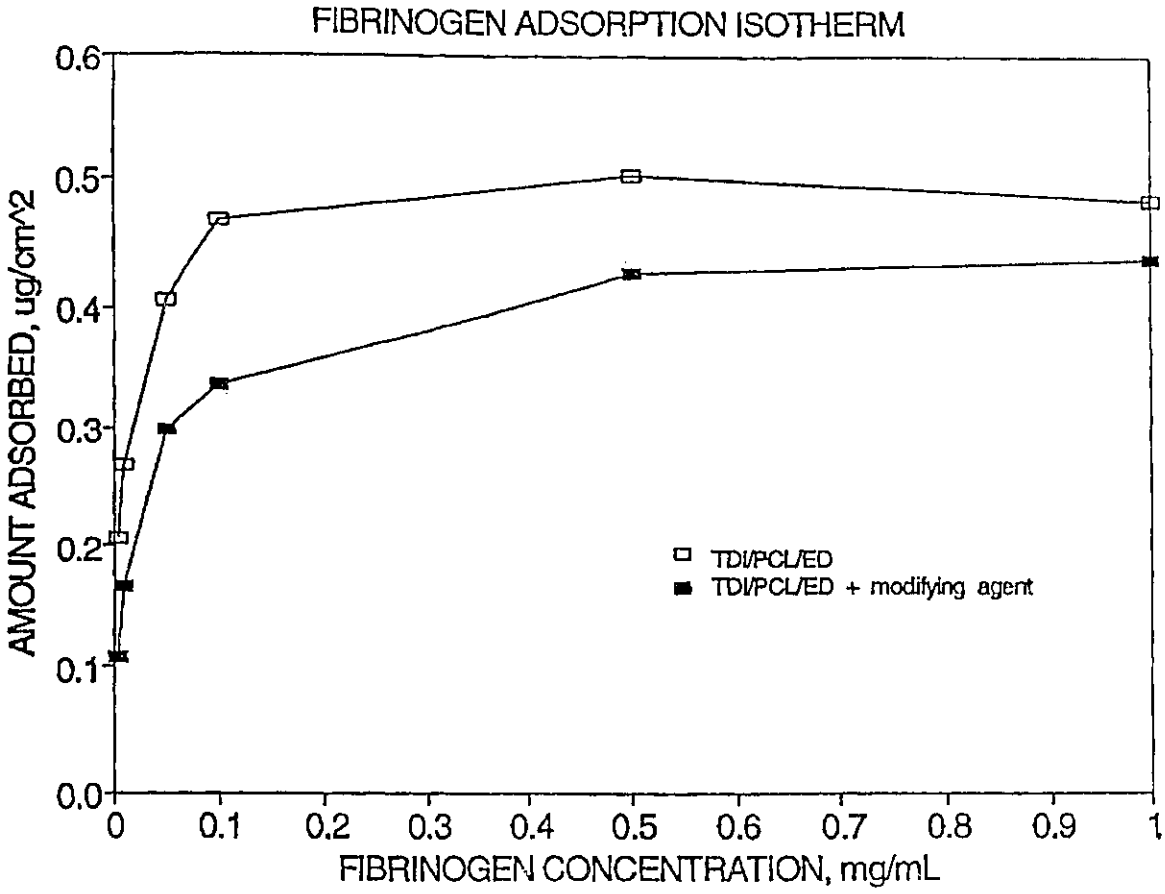

Figure 4.30. The fibrinogen adsorption isotherm for 3 hours (provided by Glen McClung, McMaster University).

5. CONCLUSIONS AND RECOMMENDATIONS

5.1 Conclusions

1. Fluorinated surface modifying macromolecules can be synthesized by reacting 1,6-hexanediisocyanate, polyether oligmers, and fluorinated alcohols in the presence of dibutyltin dilaurate as a catalyst. The properties of the synthesized polymers depend on the reactant stoichiometry, volume of solvent in the reaction, temperature applied in the reaction, as well as the amount of catalyst used. According to the observations of this work, higher solvent volume (i.e. lower reactant concentration) produces a smaller molecular weight polymer with an increased fluorine content in the polymer. However, because of the absence of kinetic studies for the polymer synthesis and the difficulties in reproducing some of the SMMs, no definitive conclusions in this regard can be made here.
2. SMMs were added into the base polymer with the purpose of changing the surface chemistry only. Differential scanning calorimetry (DSC) was used to assess the bulk thermal properties of SMM materials and the SMM blended materials (5% SMM in polyurethane/SMM mixtures). The results showed that the thermal properties of pure SMMs were significantly different from that of the pure base polymer, while the mixture of SMMs and the base polymer showed similar thermal features to that of the pure base polymer.
3. With the low surface energy component of fluorinated tails, SMM molecules showed a selective migration to the surface of the polymer mixture. Contact angle results indicated that the surface of SMM blended materials had an advancing contact angle higher than that of Teflon® which was 96° (150). It was also noted that the contact angle increased with the concentration of SMMs in the mixture until a plateau was detected. This point may indicate a saturation of SMM in the surface region. The contact angle hysteresis of these different SMMs fell into two categories, in which PTMO-SMMs always had a lower degree of hysteresis than that of PPO-SMMs.

This was attributed to the fact that PTMO was less hydrophobic than PPO, and PTMO-SMMs were more crystalline within the polymer matrix, resulting in a higher stability of PTMO-SMMs inside the polymer.

4. As supported by the contact angle results, XPS (x-ray photoelectron spectroscopy) data showed an enrichment of SMM on the top 100 Å surface. Furthermore, the XPS data suggested that the top 100 Å layer was occupied mostly by the SMM "fluorine tails". This observation supported the hypothesis that there existed an SMM-enriched layer, with the prepolymer chain of the SMM entangled within the soft-segment of the base polymer inside this layer and the "fluorine tails" residing on the outer most surface. According to the observations from the contact angle hysteresis, some reorientation of segments occurred after the polymer was placed into the aqueous environment.
5. According to the results discussed above, adding SMMs into a polyester-urea-urethane (the base polymer referred to above) could change the surface chemistry while leaving the bulk structural properties intact. In addition, the biodegradation of a polyester-urea-urethane was significantly inhibited by adding selected SMM candidates to the material cast solution. These SMMs had a molecular weight range from 1.6×10^4 to 5.5×10^4 with the fluorine content varying an average from 4.0% to 20.0%. The results of the biodegradation tests showed some differences, suggesting that the interactions of the different SMMs with the base polymer were not identical for all SMMs. Most importantly, the long-term degradation results of PPO-322I- and PTMO-322I-containing base polymer showed that enzymatic inhibition was effective for more than half a year.
6. The stability tests for SMM materials in the base polymer (polyester-urea-urethane) showed that PTMO-322I was more stable than PPO-322I, indicating that PTMO-322I interacted differently with the base polymer, in comparison to PPO-322I. This could be related to the differences observed in the other tests for these two SMMs, such as contact angle hysteresis. However, all three SMMs selected for the biostability tests (PPO-322I, PPO-212L, and PTMO-322I) were more resistant to enzyme degradation than the base polymer.

7. PPO-212L was selected to be mixed with a polyether-urea-urethane in order to study the function of SMMs in polyurethanes of other chemistries, particularly with respect to its effect on the biodegradation of this polyurethane. The results showed that there was no inhibition of biodegradation in this case. This again supports the idea that the biostability of a material is in part related to its microstructure. Furthermore, the tests show that the SMM is much more easily degraded by enzyme when in the polyether-urea-urethane. It is also more easily leached out by buffer only.
8. The fibrinogen adsorption results show that PPO-322I SMM blended polyester-urea-urethane mixture adsorbed less fibrinogen than did the pure base polymer, suggesting that the SMM may simultaneously increase the blood biocompatibility of the base material with respect to thrombus formation. As discussed before, fibrinogen adsorption is related to the inflammatory response. Thus, if less fibrinogen is adsorbed, fewer phagocytes likely adhere to the surface, resulting in less enzyme release.

In summary, this study revealed a method to improve the biocompatibility and the biostability of certain polyurethanes by blending a surface modifying macromolecule to the base polyurethane to change its surface chemistry. Although this work was based on the assertion that the bioreaction of the enzyme on the substrate would only occur at the surface of the biomaterial substrate (so that the surface chemistry of the material was the only factor in determining the biodegradation process), the final observations of this work suggested that this assertion was only partially correct. The biodegradation process is also related to the microdomain structure in depths as low as and possibly lower than 100 Å of the material's surface.

5.2. Recommendations

1. The SMM synthesis work should be done under more controlled conditions. For example, a temperature controlled heating plate should be used, and a more diluted catalyst concentration should be attempted.
2. In XPS analysis, a sample control should be done to test the error in this specific system. Furthermore, in order to analyze the bulk structure of these polymers, an attenuated total reflection infrared spectroscopy (ATR-IR) should be used. However, ATR-IR may not be able to distinguish between boundary of modified surface region and bulk component. In this case, a secondary ion mass spectrometry (SIMS) may be appropriate.
3. Dynamic mechanical testing on the materials could be done to further investigate the microdomain structure of SMM blended materials, since DSC tests may not reflect all changes in bulk properties.
4. Further biocompatibility work should be done to verify the toxicity of SMM blended materials and SMM-blood compatibility. This should include testing of the material toxicity using smooth muscle cells, as per the method of Dr. R. S. Labow at the University of Ottawa Heart Institute.
5. Enzyme adsorption tests should be done to obtain more information on the inhibition mechanism of the SMMs. These tests may reveal the role of enzyme adsorption, diffusion, and denaturation on the process of biodegradation.

The field of biomaterials is a combination of several disciplines, such as material science, biology, biotechnology, and now is joined by some other new fields, such as nanofabrication (18) and molecular assembly (18). With this combined knowledge, biomaterial scientists are attempting to engineer biomaterials or biomaterial surfaces to elicit a desired biological response. However, it is not an easy task because, in many cases, we lack an understanding of the relationship between the initial events that occur at the implant/biology interface and the final outcome. By better understanding this process, we will more likely succeed in the design of a material with the correct surface

composition and domain structure to guide the healing, integration, or function sought from the implant.

Additional fundamental studies are needed to fully define the process of biodegradation. Until this is achieved, the precise design principles for biomaterials will remain uncertain. However, the use of SMMs in the development of biostable and biocompatible materials represents one approach which shows strong promise for the future.

REFERENCES

1. Mcmillin, C. R., "Elastomers in Biomedical Applications: An Overview of Types and End-uses", Elastomerics, 22-27 Nov (1988)

2. Pangman, W. J., "Compound Prosthesis Device", U. S. Patent, No. 2,842,775 (1958) Compound Prothesis, No. 3,189,921 (1965)

3. Borestos, J. W., Pierce, W. S., "Segmented Polyurethanes: A New Elastomer for Biomedical Applications", Science, **158,** 1481-1482 (1967)

4. Stokes, K., Cobian, K., "Polyether Polyurethanes for Implantable Pacemaker Leads", Biomaterials, **3,** 225-231 (1982)

5. Szycher, M., "Biostability of Polyurethane Elastomer: A Critical Review", J. Biomat. Appl, **3(2),** 383 (1988)

6. Stokes, K., "Polyether Polyurethanes: Biostable or Not", J. Biomat. Appl, **3(2),** 248 (1988)

7. Andrade, J. D., "Surface and Interfacial Aspects of Chemistry and Physics", in "Biomedical Polymers Vol I: Surface", Plenum Press, New York, (1985), pp. 34 .

8. Philips, R., Frey, M., Martin, R. O., "Long-term Performance of Polyurethane Pacing Leads: Mechanisms of Design-related Failures", PACE, **9,** 1166-1172 (1986)

9. Bruck, S. D., "Identification of Biodegradable Products of Medical Implant in Adjacent Tissue: An Overview and Recommendations", Journal of Long-term Effects of Medical Implants, **14,** 357-364 (1992)

10. Ratner, B. D., "Characterization of Biomaterial Surfaces", Cardiovasc. Pathol, **2(3),** suppl, 87s-100s, July-Sept. (1993)

11. Hari, P. R., Sharma, C. P., "Hydrogel Grafted Surfaces: Protein Interaction and Platelet Adhesion", J. Biomat. Appl, **6,** 170-180 (1991)

12. Adamson, A. W., "Physical Chemistry of Surfaces", 4th ed., Wiley Interscience, New York, (1988)

13. Ratner, B. D., "Characterization of Biomaterial Surfaces", in "Biomaterials Science: An Introduction Test", Ratner, B. D., Schoen, F. J., Hoffman, A.,

Lemons, J., Eds., Academic Press, San Diego, CA (1993)

14. Ward, R. S. "Surface Modifying Additives for Biomaterial Polymers" IEEE Engineering in Medicine and Biology Magazine, pp. 22-25 June (1989)

15. Ratner, B. D., Weathersby, P. K., Hoffman, A., Kelly, M. A., Scharpen, L. H., "Radiation-grafted Hydrogels for Biomaterial Application as Studied by the ESCA Technique", J. Appl. Polym. Sci, **22**, 643-663 (1978)

16. Greco, R.S., "The Host Response and Biomedical Devices", in "Implantation Biology", CRC Press, Inc., (1994), pp.2

17. Williams, D. F., "Biomaterials and Biocompatibility", in "Fundamental Aspects of Biocompatibility Vol. I", CRC Press, Inc., (1986), pp.2

18. Williams, D. F., "The Cellular Response to Implanted Materials", in "Fundamental Aspects of Biocompatibility Vol. I", CRC Press, Inc., (1986) pp.95

19. Ratner, B, D., "New Ideas in Biomaterials Science - A Path to Engineered Biomaterials", J. Biomed. Mater. Res, **27**, 837-850 (1993)

20. Klinkmann, H., Ivanovich, P., "Biocompatibility: the Need for a System Approach", J. Lab. Clin. Med, **121(2)**, 203-204 Feb. (1993)

21. Lelah, M. D., Cooper, S. L., "Polyurethanes in Medicine", CRC Press, Inc., (1986), pp. 257

22. Barier, R. E., Dutton, R.D., "Initial Events in Interactions of Blood with a Foreign Surface", J. Biomed. Mater. Res, **3**, 191 (1969)

23. Bantjes, A., "Clotting Phenomena at the Blood-polymer Interface and the Development of Blood Compatible Polymeric Surfaces", Brit. Polym. J, **10**, 267 (1978)

24. Williams, D. F., "The Response of the Macrophage to Foreign Material", in "Fundamental Aspects of Biocompatibility Vol. I", CRC Press, Inc., (1986), pp. 145

25. Williams, D. F., "Cell Biochemistry in Relation to the Inflammatory Response to Foreign Materials", in "Fundamental Aspects of Biocompatibility Vol. I", CRC Press, Inc., (1986), pp. 159

26. Williams, D. F., "Toxicological Aspects of Implantable Plastics and Plastics

Used in Medical and Paramedical Applications", in "Fundamental Aspects of Biocompatibility Vol. II", CRC Press, Inc., (1986), pp. 63

27. Kutay, S., Tincer, T., Hasirci, N., "Polyurethanes as Biomaterials", Brit. Polym. J, **23**, 267-272 (1990)

28. Mirlovitch, V., Akutsu, T., Kolff, W. J., "Polyurethane Aortas in Dogs. Three-year Results" Trans. Am. Soc. Artif. Intern. Organs, **8**, 79-84 (1962)

29. Lyman, D.J., Loo, B. H., "New Synthetic Membranes for Dialysis: A Copolyether-urethane Membrane System", J. Biomed. Mater. Res, **1**, 17 (1967)

30. Boretos, J. W., "Concise Guide to Biomedical Polymers, Their Design, Fabrication and Moulding", Charles, C., Eds., Thomas Publ., Springfield, (1973), pp. 10

31. Jayabalan, M., "Biological Interaction: Cause for Risk and Failers of Biomaterials and Devices", J. Biomat. Appl, **8**, 65-71 July (1993)

32. Saunders, J. H., Frisch, K. C., " Polyurethane: Chemistry and Technology, Part I and II", Interscience, New York, (1962), pp. 36

33. Szycher, M., "Biostability of Polyurethane Elastomer: A Critical Review", in "Blood Compatible Materials and Devices ", C. P. Sharma, M. Szycher, Eds., Technomic Publishing Co., Inc. (1990), pp.33

34. Mennicken, G., "New Developments in the Field of Polyurethane Lacquers", J. Oil. Colour Chem. Ass, **49**, 639-647 (1966)

35. Lyman, D. J., "Polyurethanes", Review in Macromolecular Chemistry, **1(1)**, 191-237 (1966)

36. Gogolewshi, S., "Selected Topics in Biomedical Polyurethanes: A Review", Coll. Polym. Sci, **267**, 757-785 (1989)

37. Bonart, R., Morbitzer, L., Muller, E. H., "X-ray Investigations Concerning the Physical Structure of Crosslinking in Urethane Elastomers III. Common Structure Principle for Extensions with Aliphatic Diamines and Diols", Journal of Molecular Science, Part B: Physics, **B9(3)**, 447-461 (1974)

38. Lelah, M. D., Cooper, S. L., "Polyurethanes in Medicine", CRC Press, Inc., (1986), pp. 62

39. Sung, C. S. P., Schneider, N. S., "Structure-property Relationships of

Polyurethanes Based on Toluene Diisocyanate", J. Mater. Sci, **13**, 1689-1699 (1978)

40. Szycher, M., "Biostability of Polyurethane Elastomer: A Critical Review", in "Blood Compatible Materials and Devices", C. P. Sharma, M. Szycher, Eds., Technomic Publishing Co., Inc. (1990), pp.33

41. Wang, C. B., Cooper, S. L., "Morphology and Properties of Segmented Polyether Polyurethane", Macromolecules, **16**, 775-586 (1983)

42. Steven, M. P., Chapter 5 in "Polymer Chemistry: An Introduction", 2rd ed., Oxford University Press, (1989), pp. 169

43. Ratner, B. D., "Characterization of Biomaterial Surface", Cadiovasc. Pathol, **2(3)**, suppl, 87s-100s, July-Sept. (1993)

44. Ratner, B. D., Tyler, B. J., Chilkoti, A., "Analysis of Biomedical Polymer Surfaces: Polyurethanes and Plasma-Deposited Thin Films", Clinical Materials, **13**, 71-84 (1993)

45. Matijevic, E., "Surface and Colloid Science", Wiley-Interscience, New York, (1969) pp.109

46. Holly, F. J., Refojo, M. F., "Wettability of Hydrogels. 1. Poly(2-hydroxyethyl methacrylate)", J. Biomed. Mater. Res, **9(3)**, 315-326 (1975)

47. Changing Medical Markets, **Issue 65**, May (1984)

48. Pande, G. S. "Polyurethane Insulation for Cordia Permanent Pacing Leads", Technical Memorandum, **35**, April (1982)

49. "Clinical Application of Biomaterials", in "Consensus Development Conference, National Institutes of Health", Bethesda, Maryland, Nov. 1-3, (1984)

50. Darby, T. D., Johnson, H. D., Northrup, S. J. "An Evaluation of a Polyurethane for Use as a Medical Grade Plastic", Toxicol. Appl. Pharmacol, **46 (2)**, 4453 (1978)

51. Gueffant, K. "Biostability of a Polyurethane", Intermedics, Inc., Freeport, Texas (1981)

52. MD & DI Reports **10(12)**, Chevey Chase, Maryland, March (1984)

53. Tyler, B. J., Ratner, B. D., "Variations Between Biomer lots 2. The Effect of

Differences Between Lots in vitro Enzymatic and Oxidative Degradation of a Commercial Polyurethane", J. Biomed. Mater. Res, **27**, 327-334 (1993)

54. Fishbein, M., Levy, R. J., Ferrans, N. A., "Calcification of Cardiac Valve Bioprostheses; Ultrastructural and Biochemical Studies in a Subcutaneous Implantation Model System", J. Thorac Cardiovasc Surg, **83**, 602 (1982)

55. Coleman, D. L., Meuzelaar, H. L. L., "Retrieval and Analysis of a Clinical Total Artificial Heart", J. Biomed. Mater. Res, **20**, 417 (1986)

56. Meijs, G. F., McCarthy, S. J., Rizzardo, E., Chen, Y. C., Chatelier, R. C., Brandwood, A., Scindheim, K., "Degradation of Medical-grade Polyurethane Elastomers: The Effect of Hydrogen Peroxide in vitro", J. Biomed. Mater. Res, **27**, 345-356 (1993)

57. Takahara, A., Coury, A. J., Herenrother, R. W., Cooper, S. L., "Effect of Soft Segment Chemistry on the Biostability of Segmented Polyurethane I. In vitro Oxidation", J. Biomed. Mater. Res, **25**, 341-356 (1991)

58. Weissman, G., Smolen, J. E., "Release of Inflammatory Mediators from Stimulated Neutrophils", N. Engl. J. Med, **303**, 27-34 (1980)

59. Salthouse, T. N., "Cellular Enzyme Activity at the Polymer-Tissue Interface: A Review", J. Biomed. Mater. Res, **10**, 197-229 (1976)

60. Anderson, J. M., "Inflammatory Response to Implants", Am. Soc. Artif. Intern. Organs, **34**, 101-107 (1988)

61. Cotran, R. Z., Kumar, V., "Inflammation and Repair in Pathologic Basis of Disease", 4th ed., Philadeophia, W.B. Saunders Co., (1989), pp.33-86

62. Henson, P. M., "The Immunologic Release of Constituents from Neutrophil Leukocytes: II. Mechanisms of Release During Phagocytosis, and Adherence to Nonphagocytosable Surfaces", J. Immunol, **107**, 1547-1557 (1971)

63. Henson, P. M., "Mechanisms of Exocytosis in Phagocytic Inflammatory Cells", Am. J. Pathol, **101**, 494-511 (1980)

64. Cotran, R. Z., Kumar, V., "Inflammation and Repair in Pathologic Basis of Disease", 4th ed., Philadeophia, W.B. Saunders Co., (1989), pp. 33-86

65. Gallin, J. I., Goldstein, I. M., "Inflammation: Basic Principles and Clinical Correlates", Raven Ress, New York, (1988)

66. Johnston, R. B., "Monocytes and Macrophages", N. Engl. J. Med, **318**, 723-733 (1988)

67. Santerre, J. P., Labow, R. S., Adams, G. A., "Enzyme-Biomaterial Interactions: Effect of Biosystems on Degradation of Polyurethanes", J. Biomed. Mat. Res, **27**, 97-109 (1993)

68. Norman, S. J., Sorkin, E. (Eds), "Macrophages and Natural Killer Cells", Plenum Press, New York, (1982)

69. Cromack, D. T., Sporn, M.B., Roberts, A.B., "Transforming Growth Factor Levels in Rat Wound Chambers", J. Surg. Res, **42**, 622-628 (1987)

70. Moelleken, B.R., Mathes, S.J., "An Adverse Wound Environment Activates Leukocytes Prematurely", Arch. Surg, **126**, 225-230 (1991)

71. Marchant R. E., Anderson, J. M., Phua, K., Hiltner, A., "In-vivo Biocompatibility Studies. II. Biomer: Preliminary Cell Adhesion and Surface Characterization Studies", J. Biomed. Mater. Res, **18**, 309-315 (1984)

72. Brunsted. M. R., Anderson, J. M., "In-vivo Leukocyte Interactions on Pellethane Surfaces", Biomaterials, **11**, 370-378 (1990)

73. Spilizewski, K. L., Marchant, R. E. "In-vivo Leukocyte Interactions with the NHLBI-DTB Primary Reference Materials: Polyethylene and Silica-free Polydimethysiloxane", Biomaterials, **8**, 12-17 (1987)

74. Ratner, B. D., Gladhill, K. W., "Analysis of in-vitro Enzymatic and Oxidative Degradation of Polyurethanes", J. Biomed. Mater. Res, **22**, 509-527 (1988)

75. Bouvier, M., Chawla, A. S., Hinberg, I., "In-vitro Degradation of a Poly(ether-urethane) by Trypsin", J. Biomed. Mater. Res, **25**, 773-789 (1991)

76. Marchant, R. E., Zhao, Q., Anderson, J. M., "Degradation of a Poly(ether-urethane urea) Elastomer: Infrared and XSP Studies", Polymer, **28**, 2032-2039 (1987)

77. Zhao, Q., Marchant, R. E., "Longterm Biodegradation in-vitro of Poly(ether-urethane urea): A Mechanical Property Study", Polymer, **28**, 2040-2046 (1987)

78. Phua, S. K., Castillo, E., Anderson, J. M., Hiltmer, A., "Biodegradation of a Polyurethane in vitro", J. Biomed. Mater. Res, **21**, 231-246 (1987)

79. D. F. Williams, R. Smith, Oliver, C., "The Degradation of ^{14}C Labelled Polymers by Enzymes", in "Biological and Biomechanical Performance of Biomaterials", Christel, P., Meunier, A., Lee, A. J. C., Eds., Elsevier Science Publishers B. V., Amsterdam (1986) pp. 239-244

80. Smith, R., Williams, D. F., Oliver, C., "The Biodegradation of Poly(ether urethanes)", J. Biomed. Mater. Res, **27**, 1149-1166 (1987)

81. Santerre, J. P., Labow, R. S., Mahmoudian, M., Bryce, D., "Enzymatic Degradation of Polyether-urethane: Possible Correlation with Hard/soft Segment Domain Size", 14th Canadian Biomaterial Society Conference, Quebec City, QC, July 10-12 (1994) pp. 87

82. Labow, R. S., Santerre, J. P., Erfle, D., "Neutrophil-mediated Degradation of Segmented Polyurethanes", Biomaterials, (1994 in Press)

83. Labow, R. S., Duguay, D. G., Santerre, J. P., "The Enzymatic Hydrolysis of a Synthetic Biomembrane: A New Substrate for Cholesterol and Carboxyl Esterases", J. Biomater. Sci. Polym. Edn, **6**, 169-179 (1994)

84. Duguay, D. G, Labow, R. S., Santerre, J. P., Mclean, D., "Development of Mathematical Model Describing the Enzymatic Degradation of Biomedical Polyurethanes. 1. Background, Rationale and Model Formulation" Polymer Degradation and Stability, (1994 in Press)

85. Santerre, J. P., Labow, R. S., Duhuay, D. G., Erfle, D., Adams, G. A., "Biodegradation Evaluation of Polyether and Polyester-urethane with Oxidative and Hydrolytic Enzymes", J. Biomed. Mater. Res, **28**, 1187-1199 (1994)

86. Anderson, J. M., Hiltner, A., Zhao, Q. H., Wu, Y., Renier, M., Schubert, M. Brunstedt, M., Lodoen, G. A., Payet, C. R., "Cell/polymer Interactions in the Biodegradation of Polyurethanes", in "Biodegradable Polymer and Plastics", Vert, M., Feijen, J., Albertson, A., Scott, G., Chiellini, E., Eds., The Royal Society of Chemistry, Thomas Graham House, Science Park, Cambridge, (1992), pp. 122-148

87. Capone, C. D., "Biostability of a Non-ether Polyurethane", J. Biomat. Appl, **7**, Oct. (1992)

88. Gunatillake P. A., Meijs, G. F., Rizzardo, E., Charelier, R. L., McCarthy, S. J., Brandwood, A., "Polyurethane Elastomers Based on Novel Polyether Macrodiols and MDI: Synthesis, Mechanical Properties, and Resistance to Hydrolysis and Oxidation", J. Appl. Polym. Sci, **46**, 319-328 (1992)

89. Hergenrother, R. W., Wabers, H. D., Cooper, S. L. "Effect of Hard Segment Chemistry and Strain on the Stability of Polyurethanes: in vivo Biostability", Biomaterials, **3**, 225-231 (1993)

90. Hergenrother, R. W., Wabers, H. D., Copper, S. L. "The Effect of Chain Extenders and Stabilizers on the in vivo Stability of Polyurethanes", J. Appl. Biomat, **3**, 17-22 (1992)

91. Takahara, A., Coury, A., Hergenrother, R. W., Copper, S. L., "Effect of Soft Segment Chemistry on the Biostability of Segmented Polyurethanes I. In vitro Oxidation", J. Biomed. Mat. Res, **25**, 342-356 (1991)

92. Wabers, H. D., McCoy, T. J., Okema, A. T., Hergenrother, R. W., Wolf, M. F., Copper, S. L., "Biostability and Blood-contacting Properties of Sulfonate Grafted Polyurethane and Biomer", J. Biomater. Sci. Polym. Edn, **4(2)**, 107-133 (1992)

93. Han, K. D. P., Jeong, S. Y., Kim, Y. H., Kim, U. Y., Min, B. G., "In vivo Biostability and Calcification-resistance of Surface Modified PU-PEO-SO_3", J. Biomed. Mat. Res, **27**, 1063-1073 (1993)

94. Ward, R.S., White, K. A., Wolcott, C. A., "Use of Oligomeric End-groups to Modify Surface Properties of Biomedical Polymers", Trans. of 20th Annual Meeting of the Soc. for Biomat., Boston, MA, April 4-10 (1994), pp. 13

95. Stokes, K., Urbanski, P., Cobian, K., "New Test Methods in the Evaluation of Stress Cracking and Metal Catalyzed Oxidation in Implanted Polymers", in "Polyurethanes in Biomedical Engineering II.", Planck, H. Eds., Elsevier Science Publishers B. V., Amsterdam, (1987), pp. 109

96. Szycher, M., McArthur., W. A., "Surface Fissuring of Polyurethanes Following in vivo Exposure", in "Corrosion and Degradation of Implant Materials: Second Symposium", ASTM STP 859, Fraker, A. C., Griffin, C. D., Eds., American Society for Testing and Materials, Philadephia, (1985) pp. 308-321

97. Pande, G. S., "Thermoplastic Polyurethanes as Insulating Materials for Long-life Cardiac Pacing Leads", PACE, **6**, 858-867 (1983)

98. Pinchuk, L., Martin, J. B., Esqsuivel, M. C., MacGregor, D. C., "The Use of Silicone/polyurethane Graft Polymers as a Means of Eliminating Surface Cracking of Polyurethane Prostheses", J. Biomat. Appl, **3(2)**, 260-296 (1988)

99. MacGregor, D. C., Pinchuk, L., Esquivel, M. C., Martin, J. B., Wilson, G. J., "Corethane™ as A Substitute for Pellethane for Pacemaker Lead Insulators",

PACE, **14**, 694 (1991)

100. Pinchuk, L., Esquivel, M. C., Martin, J. B., Wilson, G. J., "Corethane™: A New Replacement of Polyetherurethanes for Long-term Implant Applications", Tans. of 17th Annual Meeting of the Soc. for Biomat., Scottsdale, AZ, (1991) pp. 98

101. Pinchuk, L., Kato, Y. P., Eckstein, M. L., Wilson, G. J., MacGregor, D. C., "Polycarbonate Urethanes as Elastomeric Materials for Long-term Implant Applications", Tans. of the 19th Annual Meeting of the Soc. for Biomat., Birmingham, AL, (1993) pp. 22

102. Pinchuk, L., "A Review of the Biostability and Carcinogenicity of Polyurethanes in Medicine and the New Generation of "Biostable" Polyurethanes", J. of Biomat. Sci. Polym. Edn, (Revised September 10, 1993)

103. Ward, R.S., "Polymer Systems Suitable for Blood-contacting Surface of a Biomedical Devices", U.S. Patent, 4, 675, 361, June 23, (1987)

104. Wilson, J. E., "Hemocompatible Polymers: Preparation and Properties", Polym. Plast. Technol. Eng, **25**, 233, (1981)

105. Park, K. D., Kim, W. G., Mohammad, S. F., Kim, S. W., "Blood Compatibility of SPUU-PEO-heparin Graft Copolymers", J. Biomed. Mater. Res, **26**, 739-756 (1992)

106. Piskin, E., "Biologically Modified Polymeric Biomaterial Surfaces: Introduction", Clinical Materials, **11**, 3-7 (1992)

107. Lyman, D. J., Kim, S. W., "Interactions at the Blood-polymer Interface", Fed. Proc., **30(5)**, 1658-1662 (1971)

108. Hari, P. R., and Sharma, C. P., "Hydrogel Grafted Surfaces: Protein Interaction and Platelet Adhesion", J. Biomat. Appl, **6**, 170-180 (Oct. 1991)

109. Brash, J. L., Lyman, D. J., "Adsorption of Plasma Protein in Solution to Uncharged, Hydrophobic Polymer Surface", J. Biomed. Mater. Res, **3(1)**, 175-189 (1969)

110. Hergenrother, R. W., Cooper, S. L., "Improved Materials for Blood-contacting Applications: Blends of Sulphonate and Non-sulphonate Polyurethanes", Biomaterials, **12**, 3 (1991)

111. Yasuda, H. K., Cho, D. L., "Plasma-surface Interactions in the Plasma

Modification of Polymer Surfaces", in "Polymer Surface and Interfaces", John Wiley & Sons Ltd., New York, (1987), pp. 149

112. Yasuda, H. H., Gazicki, M., "Biomedical Applications of Plasma Polymerization and Plasma Treatment of Polymer Surfaces", Biomaterials, **3**, 68-77 (1982)

113. Auman, B. C., "Synthesis and Properties of Novel Polyimides Based on New Rigid Fluorinated Monomers", Proceedings/Abstracts- 4th International Conference on Polyimides, (1991), pp. 5

114. Sperati, C. A., "Fluorine-containing Polymers. II. Polytetrafluoroethylene", Forschr. Hochpolym.-Forsch, **2**, 465 (1961)

115. Jennings, R. B., "Use of a Microsporous Expanded Polytetrafluoroethylene Grafts for a Aorta-pulmonary Shunts in Infants with Complex Cranotic Heart Disease. A Report of Seven Cases", J. Thorac. Cardiovasc, **76**, 489 (1978)

116. Cooley, D. A., "The Quest for the Perfect Prosthetic Heart Valve", Med. Instrum., Baltimore, 82, (1977)

117. Han, D. K., Jeong, S. Y., Kim, Y. H., Min, B. G., "Surface Structure and Inert Surface Characteristics of Perfluorodecanioc Acid Grafted Polyurethane", J. Appl. Polym. Sci, **47**, 761-769 (1993)

118. Hayer, M., "Encyclopedia of Chemical Technology" M. Grayson, Eds, Wiley, New York, Vol. 24, (1984), pp. 442

119. Han, D. K., Jeong, S. Y., Kim, Y. H., Min, B. G., "Surface Characteristics and Blood Compatibility of Polyurethanes Grafted by Perfouoroalcyl Chains", J. Biomater. Sci. Polym. Eds, **3(3)**, 229-241 (1992)

120. Ward, R. S., White, K. A., Hu, C. B., "Use of Surface-modifying Additives in the Development of a New Biomedical Polyurethaneurea", Polyurethanes in Biomedical Engineering, 181-200 (1984)

121. Brunstedt, M. R., "Protein Adsorption to Poly(ether-urethane-ureas) Modified with Acrylate and Methacrylate Polymer and Copolymer Additives", J. Biomed. Mater. Res, **27**, 367-377 (1993)

122. Ratner, B. D., Yoon, S. C., "Control of Polyurethane Surface by Synthesis and Additives Implication for Blood Interactions", Polyurethanes in Engineering, 213-229 (1987)

123. Szycher, M., Siciliano, A. A., "An Assessment of 2,4 TDA Formation from Surgitek Polyurethane Foam Under Simulated Physiological Conditions", J. Biomat. Appl, **5**, 323-336 April (1991)

124. "The Merck Index: An Encyclopedia of Chemicals, Drugs, and Biological", 11th ed., Budavari, S., O'Neil, M. J., Smith, A., Heckelman, P. E., Eds., Merck & Co., Inc., Rahway, N. J., U.S.A., (1989)

125. Seymour, R. B., "Polymer Structure", in "Introduction to Polymer Chemistry", McGraw-Hill, Inc., (1971) pp. 16

126. Peebles, Jr. L. H., "Sequence Length Distribution in Segmented Block Copolymers", Macromolecules, **7(6)**, 872-882 (1974)

127. Peebles, Jr. L. H., "Hardblock Length Distribution in Segmented Block Copolymers", Macromolecules, **9(1)**, 58-61 (1976)

128. Kuo, C. Y., Provder, T., "Application of Size Exclusion Chromatography to Polymers and Coatings", ASTM Special Technical Publication, ASTM Philadelphia, PA, USA, No. 119, pp. 57-81

129. Potts, M. K., Hagauer, G. L., Sennett, M. S., Davis, G., "Monomer Concentration Effects on the Kinetics and Mechanism of the Boron Trichloride Catalyzed Solution Polymerization of Hexachlorocyclotriphosphazene", Macromolecules, **22(11)**, 4235-4239 (1989)

130. Gao, B., Wesslen, B., Wesslen, K., B., "Amphiphilic Comb-shaped Polymers from Poly(ethylene glycol) Macromonomers", J. Polymer Sci. Part A: Polym. Chem, **30(9)**, 1799-1808 (1992)

131. Wang, H. Q., Li, J., Shang, Y. L., "Synthesis and Characteristics of Polyamide Acid (PAA) and Polyamide Imide (PAI)", Journal of Beijing Institute of Technology, English Language Issue, **18(4)**, 36-43 (1991)

132. Remech, S., Rajalingam, P., Radhakrihnan, G., "Chain-extended Polyurethane Synthesis and Characterization", Polymer International, **25**, 253-256 (1991)

133. Rand, L., Thir, B., Reegen, S. J., Fisch, K. C., "Kinetic of Alcohol-isocyanate Reaction with Metal Catalyst", J. Appl. Polym. Sci, **9**, 1781-1789 (1965)

134. Wang, T. L., Lyman, D. J., "The Effect of Reaction Conditions on the Urethane Prepolymer Formation", Polymer Bulletin, **27**, 549-555 (1992)

135. Tanzi, M. C., "Some Aspects of Thermoplastic Segmented Polyurethanes

Biocompatibility", 14th Canadian Biomaterials Society Conference, Quebec City, QC, July 10-12 (1994), pp. 3

136. Yasuda, H., Chatlson, E. J., Charlson, E. M., "Dynamics of Surface Property Change in Response to Changes in Environmental Conditions", Langmuir, **7(10)**, 2394-2400 (1991)

137. Fessenden, R. J., Fessenden, J. S., "Atoms and Molecules - A Review", in "Organic Chemistry", Willard Grant Press, Boston, MA, (1979), pp. 15-16

138. Theocaris, P. S., Kefala, V., "Dynamic Mechanical Properties of Polystyrene-Polyurethane Blends", J. Appl. Polym. Sci, **42**, 3059-3063 (1991)

139. Yoon, S. C., Sung, Y. K., Ratner, B. D., "Surface and Bulk Structure of Segmented Poly(ether urethanes) with Perfluoro Chain Extenders. 4. Role of Hydrogen Bonding on Thermal Transition", Macromolecules, **23**, 4351-4356 (1990)

140. Shibayama, M., Suetsugu, M., Sadurai, S., Yamanoto, T., Nomura, S., "Structure Characterization of Polyurethane Containing Poly(dimethylsiloxane)", Macromolecules, **24**, 6254-6262 (1991)

141. Koberstein, B. H., "Interfacial Properties", in "Encyclopedia of Polymer Science and Technology", Vol. 8, Wiley, New York, (1985), pp. 237-279

142. Brunstedt, M. R., Ziats, N. P., Roberston, S. P., Hiltner, A., Anderson, J. M., "Protein Adsorption to Poly(ether urethane ureas) Modified with Acrylate and Methacrylate Polymer and Copolymer Additives", J. Biomed. Mater. Res, **27**, 367-377 (1993)

143. Freij-Larsson, C., Kober, M., Wesslen, B., Willquist, E., Tengvall. P., "Effects of a Polymeric Additive in a Biomedical Poly(ether urethaneurea)", J. Appl. Polym. Sci, **49**, 815-821 (1993)

144. Ratner, B. D., Yoon, S.C., Nates, N. B., "Polymer Surface and Interfaces", Feast, W. J., Munro, H. S., Eds., John Wiley & Sons, Toronto, (1987), pp. 3

145. Hudson, C. B., "Studies of Segmented Polyurethanes for Blood Contacting Applications", Master's Thesis, McMaster University, Hamilton, Ont. Canada 1986

146. Chaney, R., Barth, G., "An ESCA Study on the X-ray Induced Changes in Polymeric Materials", Fresenius. Z. Anal. Chem, **329**, 143-146 (1987)

147. Baier, R. E., Dutton, R. C., "Initial Events in Interactions of Blood with a Foreign Surface", J. Biomed. Mater. Res, **3**, 191-196 (1969)

148. Tang, L. P., Eaton, J. W., "Fibrinogen Mediates Acute Inflammatory Responses to Biomaterials", J. Exp. Med, **178**, 2147-2156 (1993)

149. Brunstedt, M. R., Ziatsm N. P., Schuber, M., Hiltner, A., Anderson, J. M., "Protein Adsorption onto Poly(ether urethane ureas) Containing Methacrol 2138F: A surface-active Amphiphilic Additive", J. Biomed. Mater. Res, **27**, 255-267 (1993)

150. Dekker, A., Keitsma, K., Beugeling, T., Bantjes, A., Feijen, J., van Aken, WG., "Adhesion of Endothelial Cells and Adsorption of Serum Proteins on Gas Plasma-treated Polytetrafluoroethylene", Biomaterials, **12(2)**, 130-138 (Mar. 1991)

Appendix 1 Apparatus for Distillation

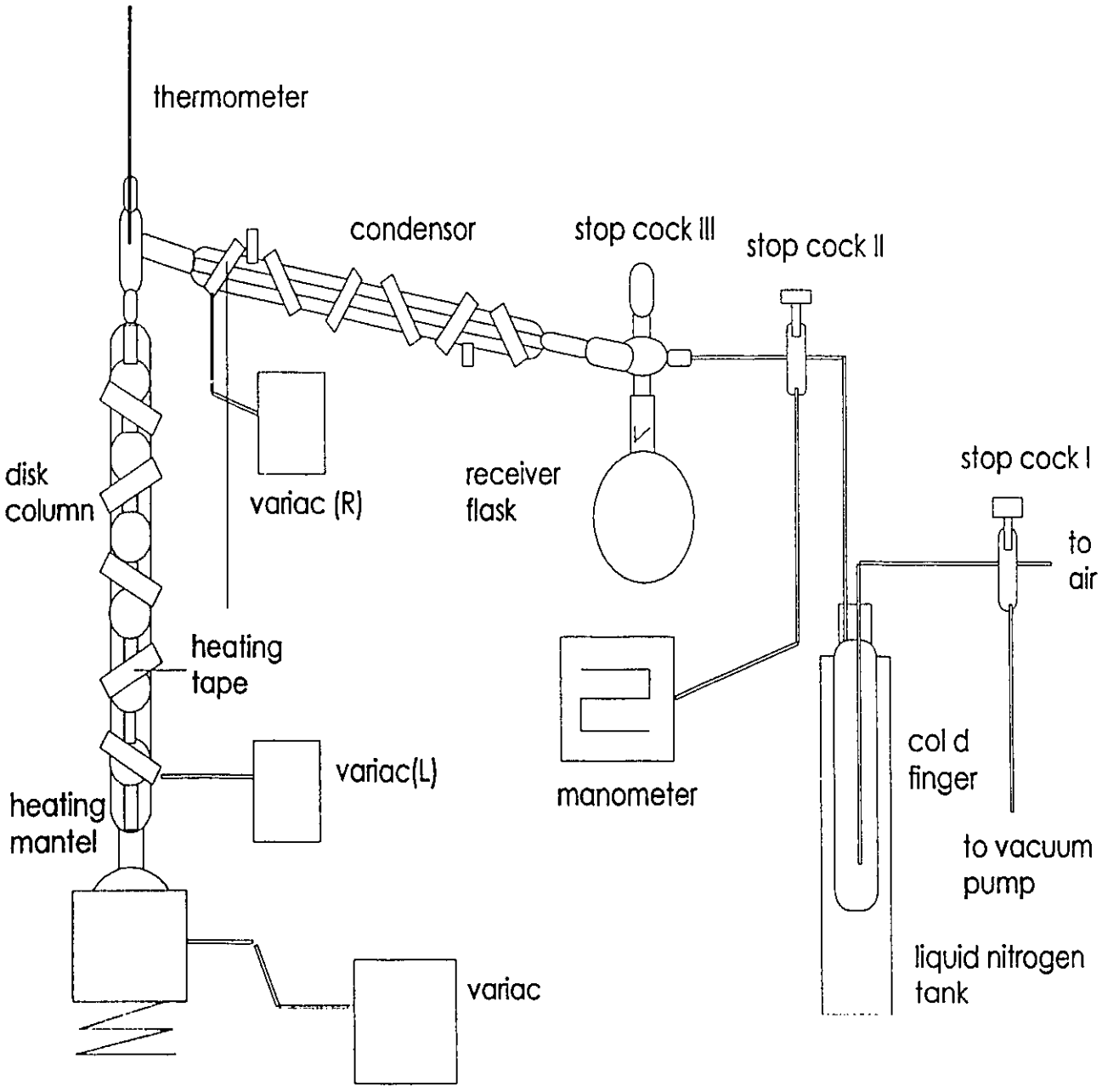

Figure A1. Distillation apparatus for synthesis reagents described in Chapter 3. Note: the heating tape is only used in the BA-L distillation.

Appendix 2 BA-L Distillation Procedure

1. Set up the standard vacuum distillation according to Appendix 1 and check the vacuum reading. Wrap the condenser with heating tape and glass wool.
2. Leave the system open to air and set the variac for the heating mantel at 60 (no units).
3. Collect the first fraction after the temperature stabilizes near 102°C. This distillate should be a clear liquid.
4. The distillation is continued until the distillate turns to a precipitated form in the condenser/collecting flask. At this time, collecting is stopped by closing the third stop cock (as shown in Figure A1).
5. The first distillate is collected as BA-L (Low) and transferred into an amber bottle which has been dried in an oven overnight at 100°C. The bottle is then sealed with teflon tape and stored in a desiccator until needed.
6. The material left in the round bottom flask following the collection of the first fraction is dark brown. Connect the vacuum distillation apparatus to the collecting stem, set the variac for the heating mantel at 40 and the condenser's heating tape at 35 (variac (R) in Appendix 1).
7. Collect the BA-L (Int) under these conditions. Monitor the temperature and ensure that the condenser remains clear of distillate. If blockage occurs, the distillation column heating tape should be turned on for a while (not too long since it will allow for higher temperature distillates to go up the column). The temperature for this fraction is 70-80°C. High temperatures should be avoided, otherwise the materials in the distillation flask will be degraded.
8. When a trace of yellow material comes out, or the temperature increases suddenly, stop the distillation by closing the 3rd stop cock. Transfer BA-L (Int) into a dry bottle. This fraction should be a semi-solid white material.
9. Turn off the pump and melt the material left in distillation flask. When it is melted, turn the pump on and distil again. The variac for the heating mantel should be set to 50 and the condenser heating tape variac should be set at 40.

10. Monitor the distillation column heating tape to keep the condenser column clear. Collect the third distillate BA-L (High). The material is a yellowish solid. The temperature range for this distillate is 80-100°C at approximately 8 mPa. After finishing the distillation, melt the High fraction and transfer it into a dry bottle.

11. Distil some 1,1,2-trichlorotrifluoroethane through the apparatus to remove all traces of the fluorinated compounds from the distillation glassware. This is very important so as not to contaminate all other materials with BA-L. It is recommended that glassware be dedicated solely to the purpose of this distillation.

Appendix 3 SMMs Synthesized and their Molecular Weight and Fluorine Content

SMM Code Number	Syn. Date	Before Wash		After Wash	
		M.W / P.D	F%	M.W / P.D	F%
SMM1 (PTMO-432I)	July 27 1993	1.3×10^5 / 2.2	10.33	1.1×10^5 / 2.0	N.F
SMM2 (PTMO-212L)	Aug. 3 1993	3.2×10^4 / 1.5	9.60	3.0×10^4 / 1.5	7.98
SMM3 (PTMO-322L)	Aug. 3 1993	2.4×10^5 / 1.8	N.F	N.D	N.D
SMM4 (PTMO-212H)	Aug. 9 1993	1.5×10^5 / 1.9	20.01	9.7×10^4 / 2.1	0.72
SMM5 (PTMO-212I)	Aug. 12 1993	1.2×10^5 / 1.8	0.37	1.4×10^5 / 3.1	0.10
SMM6 (PPO-212L)	Aug. 21 1993	2.1×10^4 / 1.6	13.27	2.2×10^4 / 1.3	12.44
SMM7 (PPO-322I)	Aug. 21 1993	5.0×10^4 / 1.7	4.98	4.8×10^4 / 1.6	3.95
SMM8 (PTMO-322H)	Aug. 24 1993	7.7×10^4 / 2.4	8.23	6.1×10^4 / 2.0	0.71
SMM9 (PPO-322H)	Aug. 24 1993	2.6×10^4 / 1.6	10.56	2.6×10^4 / 1.6	5.11
SMM10 (PTMO-322I)	Sept. 24 1993	6.7×10^4 / 1.8	N.D	5.0×10^4 / 1.7	4.97
SMM11 (PTMO-432L)	Sept. 24 1993	3.0×10^5 / 2.0	N.D	1.8×10^5 / 2.0	N.F
SMM12 (PTMO-432H)	Oct. 3 1993	6.8×10^4 / 1.8	N.D	7.1×10^4 / 1.7	3.28

SMM Code Number	Syn. Date	Before Wash		After Wash	
		M.W / P.D	F%	M.W / P.D	F%
SMM13 (PTMO-322I)	Dec. 23 1993	N.D	N.D	3.1 X 10^4/ 1.5	10.79
SMM14 (PPO-322I)	Dec. 23 1993	N.D	N.D	2.6 X 10^4/ 1.4	12.48
SMM15 (PTMO-322I)	Jan. 6 1994	N.D	N.D	3.8 x 10^4 / 1.5	7.02
SMM16 (PPO-322I)	Jan. 6 1994	N.D	N.D	2.5 x 10^4 / 1.4	13.40
SMM17 (PTMO-322H)	Feb. 4 1994	5.1 x 10^4 / 1.74	2.11	5.3 x 10^4 / 1.9	1.74
SMM18 (PPO-322H)	Feb. 4 1994	2.6 x 10^4 / 2.55	4.34	2.0 x 10^4 / 1.6	0.10
SMM19 (PPO-212L)	Feb. 5 1994	1.3 x 10^4 / 1.15	26.62	N.D	N.D
SMM20 (PTMO-322H)	Feb. 6 1994	4.5 x 10^4 / 1.61	3.60	4.6 x 10^4 / 1.6	6.87
SMM21 (PPO-322H)	Feb. 6 1994	2.7 x 10^4 / 1.36	13.30	2.7 x 10^4 / 1.3	11.60
SMM22 (PPO-322H)	Feb. 10 1994	4.0 x 10^4 / 1.57	3.32	4.3 x 10^4 / 1.6	1.70
SMM23 (PTMO-322H)	Feb. 10 1994	7.8 x 10^4 / 2.24	4.51	8.1 x 10^4 / 2.1	0.52
SMM24 (PPO-212L)	Feb. 11 1994	1.4 x 10^4 / 1.18	18.47	1.4 x 10^4 / 1.2	35.00
SMM25 (PTMO-322I)	Feb. 14 1994	6.0 x 10^4 / 1.76	3.51	6.9 x 10^4 / 1.8	3.25
SMM26 (PPO-322I)	Feb. 14 1994	3.1 x 10^4 / 1.46	7.62	3.2 x 10^4 / 1.5	9.35

SMM Code Number	Syn. Date	Before Wash		After Wash	
		M.W / P.D	F%	M.W / P.D	F%
SMM27 (PPO-322I)	April 19 1994	N.D	N.D	2.9×10^4 / 2.9	N.D
SMM28 (PPO-322I)	April 20 1994	N.D	N.D	1.8×10^4 / 1.4	N.D
SMM29 (PPO-322I)	April 21 1994	N.D	N.D	3.5×10^4 / 1.7	7.71
SMM30 (PTMO-322L)	April 22 1994	N.D	N.D	2.3×10^4 / 1.4	N.D
SMM31 (PTMO-322L)	April 25 1994	N.D	N.D	4.4×10^4 / 1.9	N.D
SMM32 (PTMO-322L)	April 26 1994	N.D	N.D	3.6×10^4 / 1.5	N.D
SMM33 (PTMO-322L)	April 27 1994	prepolymer:	4.4×10^4 / 1.8	5.7×10^4 / 1.8	N.D
SMM34 (PTMO-322I)	April 28 1994	N.D	N.D	4.4×10^4 / 1.8	3.00
SMM35 (PPO-212L)	April 29 1994	N.D	N.D	N.D	N.D
SMM36 (PTMO-322I)	April 30 1994	N.D	N.D	4.4×10^4 / 1.7	3.98
SMM37 (PPO-212L)	May 1 1994	N.D	22.02	1.6×10^4 / 1.2	20.83
SMM38 (PTMO-322I)	May 2 1994	N.D	N.D	8.3×10^4 / 1.8	N.D
SMM39 (PPO-212L)	May 3 1994	N.D	17.64	1.7×10^4 / 1.2	16.01
SMM40 (PPO-322L)	May 4 1994	N.D	N.D	N.D	N.D

SMM Code Number	Syn. Date	Before Wash		After Wash	
		M.W /P.D	F%	M.W /P.D	F%
SMM41 (PTMO-322H)	May 5 1994	N.D	N.D	6.8×10^4 / 2.1	N.D
SMM42 (PTMO-322I)	May 6 1994	N.D	N.D	N.D	N.D
SMM43 (PTMO-322H)	May 7 1994	N.D	N.D	3.2×10^4 / 1.5	9.35
SMM44 (PPO-322L)	May 8 1994	N.D	N.D	2.1×10^4 / 1.5	N.D
SMM45 (PPO-322H)	May 9 1994	1.4×10^4 / 1.4	N.D	N.D	N.D
SMM46 (PPO-322H)	May 10 1994	N.D	N.D	N.D	N.D

M.W : Weight average molecular weight
P.D : Polydispersity
N.D : Not done
N.F : Not found
F% : Fluorine content

Appendix 4 Temperature Profiles for SMMs Synthesized in Different Batches

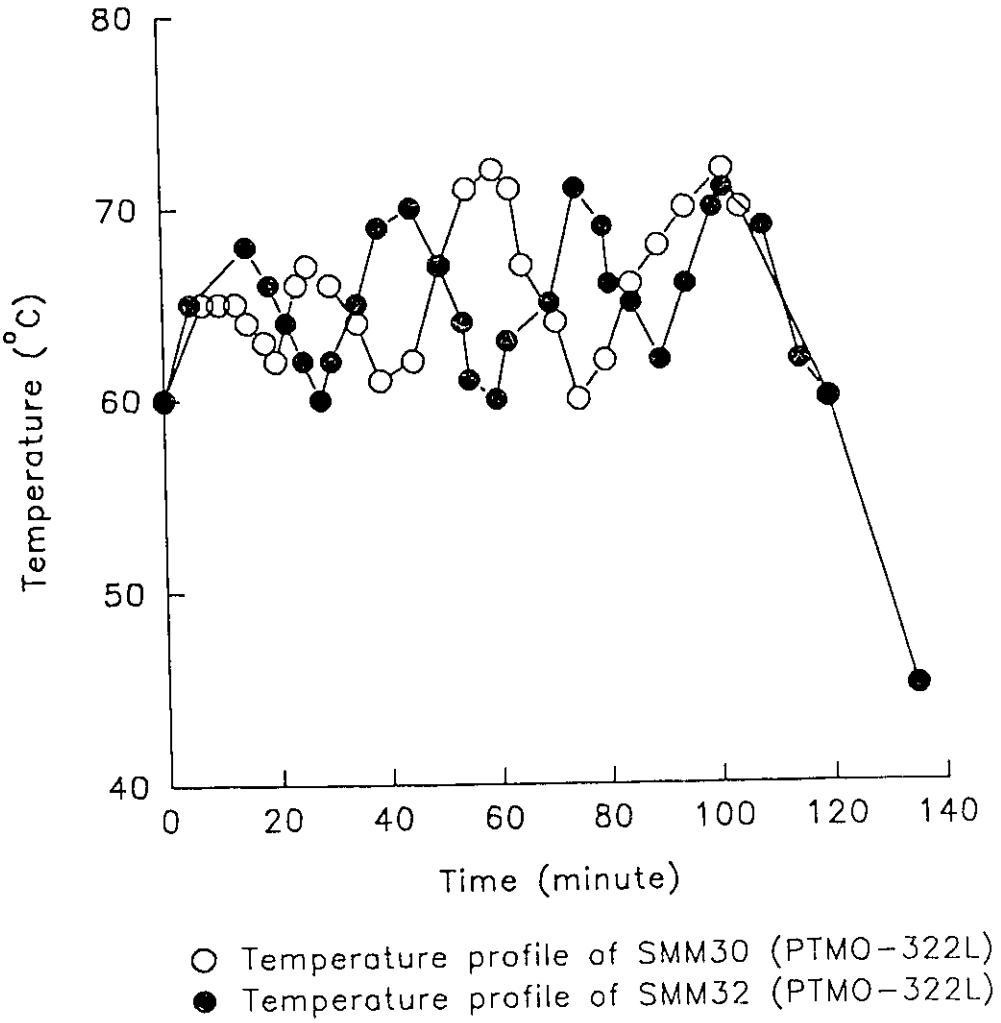

Figure A4. Temperature profiles for SMM30 and SMM32 (PTMO-322L).

Appendix 5 XPS Data of the SMM Synthesized in the First Stage of the Work

Name of polymer	Takeoff Angle (°)	Elemental Analysis (%)					C_{1s} (%)				
		F	O	N	C	Si	C-C	C-O	C=O	$C-F_2$	$C-F_3$
SMM8 (PPO-322H)	90	21.6	17.4	2.9	57.9	0.03	33.7	57.0	3.3	6.0	/
	10	40.4	10.7	1.3	47.4	0.25	30.7	45.7	3.4	17.3	2.8
	20	30.4	13.5	2.1	53.7	0.31	32.8	51.6	3.3	11.1	1.2
	30	24.3	15.7	2.5	57.1	0.40	35.2	55.7	2.9	6.2	/
	45	19.7	16.9	2.9	60.2	0.25	36.4	54.5	4.7	4.4	/
	60	16.4	18.1	2.7	62.4	0.30	37.8	53.1	5.6	3.5	/
	90red	14.9	18.9	2.8	63.3	0.07	38.6	51.9	6.7	2.8	/
BASE	90	2.7	22.9	3.1	71.2	0.0	51.9	35.6	12.4	/	/
	10	9.7	20.2	1.9	67.5	0.68	47.7	45.1	6.0	1.2	/
	20	5.5	19.9	2.8	71.7	0.0	47.3	43.0	9.0	0.7	/
	30	3.9	21.2	3.0	71.6	0.17	51.3	38.7	9.8	0.2	/
	45	3.6	21.4	3.1	71.8	0.07	52.9	35.4	11.5	0.2	/
	60	2.1	21.9	3.7	71.9	0.34	53.0	34.5	12.4	0.1	/
	90red	2.5	22.3	3.2	71.8	0.18	53.9	33.5	12.4	0.2	/

Name of polymer	Takeoff Angle (°)	Elemental Analysis (%)					C_{1s} (%)				
		F	O	N	C	Si	C-C	C-O	C=O	$C-F_2$	$C-F_3$
SMM10 (PTMO-322I)	90	41.9	8.4	3.4	45.9	0.15	29.3	39.1	6.3	22.9	2.5
	10	56.5	4.4	1.6	36.7	0.76	22.1	18.8	4.9	42.5	11.7
	20	54.4	4.2	2.1	38.9	0.45	16.5	34.7	5.1	37.9	5.7
	30	48.7	6.1	2.7	42.3	0.37	24.0	30.8	7.8	37.1	6.2
	45	43.7	7.6	3.5	44.9	0.20	30.5	32.9	8.7	23.8	4.1
	60	39.8	8.4	4.0	47.6	0.28	33.8	35.2	8.3	19.8	2.8
	90red	38.7	9.4	3.9	49.9	0.09	32.2	41.2	7.6	17.1	1.9
SMM8 (PTMO-322H)	90	35.9	10.	3.1	50.8	0.01	35.5	40.8	5.3	16.8	1.6
	10	52.2	5.4	1.4	40.6	0.42	25.4	23.9	4.8	37.8	7.9
	20	49.3	6.5	1.8	42.4	0.04	30.2	27.3	6.5	30.1	5.9
	30	42.9	7.7	2.7	46.7	0.04	32.8	32.1	7.0	24.4	3.7
	45	38.0	9.3	3.3	49.1	0.29	35.6	35.9	7.7	18.1	2.6
	60	34.1	10.	3.4	52.0	0.23	37.6	38.6	7.2	14.8	1.8
	90red	31.6	10.	3.8	53.5	0.43	39.2	40.8	7.1	12.1	0.9
SMM6 (PPO-212L)	90	40.9	9.5	3.3	46.1	0.27	27.6	37.9	8.3	21.6	4.6
	10	54.9	4.9	2.1	37.9	0.0	13.9	26.9	7.7	38.8	12.6
	20	52.3	5.3	2.1	40.3	0.0	19.7	28.6	10.2	33.2	8.3
	30	45.5	7.6	2.8	43.9	0.26	22.6	32.9	10.7	27.1	6.7
	45	41.3	9.0	3.5	45.8	0.34	25.6	37.2	10.7	21.1	5.3
	60	37.4	10.	3.7	48.7	0.0	28.1	39.6	10.7	17.8	3.8
	90red	34.8	10.	3.6	50.5	0.26	29.5	42.4	10.7	14.3	3.1
SMM7 (PPO-322I)	90	/	/	/	/	/	26.0	51.7	5.3	14.6	2.3
	10	53.6	5.9	1.8	38.7	0.0	18.3	35.2	4.5	33.9	8.1
	20	44.1	8.1	1.8	45.9	0.0	23.8	40.8	5.1	24.7	5.5
	30	39.1	10	2.9	47.3	0.0	26.7	44.5	6.9	18.3	3.4
	45	32.9	11	3.1	52.2	0.0	29.8	48.8	6.5	12.8	2.1
	60	29.3	13	3.6	53.4	0.16	30.7	51.1	6.9	9.8	1.4
	90red	26.3	14	3.4	55.9	0.08	31.0	52.8	7.0	8.4	0.8

Name of polymer	Takeoff Angle (°)	Elemental Analysis (%)					C_{1s} (%)				
		F	O	N	C	Si	C-C	C-O	C=O	$C-F_2$	$C-F_3$
SMM11 (PTMO-432L)	90	3.38	0.0	0.0	96.6	0.0	42.1	50.3	6.8	/	0.9
	10	19.9	17.8	1.5	59.5	1.25	44.3	49.6	1.7	/	4.4
	20	12.2	19.0	2.1	66.6	0.15	40.2	49.9	6.2	/	3.8
	30	8.2	21.1	2.8	67.8	0.16	41.9	50.9	6.3	/	0.9
	45	6.5	21.6	3.4	68.4	0.07	43.1	48.9	7.1	/	0.9
	60	4.8	21.4	3.3	70.2	0.32	42.9	48.8	7.3	/	0.9
	90red	4.8	21.9	3.2	69.9	0.17	45.3	46.4	8.2	/	/
SMM1 (PTMO-432I)	90	4.0	22.4	2.9	70.7	0.0	45.5	45.7	8.8	/	0.05
	10	11.4	20.5	2.0	65.0	1.18	37.7	56.6	4.7	/	1.04
	20	6.9	21.4	3.3	68.5	0.0	42.4	50.7	6.1	/	0.80
	30	5.2	22.0	2.8	69.8	0.21	43.5	48.6	7.5	/	0.46
	45	3.4	22.4	3.0	71.0	0.28	45.7	45.9	8.1	/	0.12
	60	3.6	22.6	3.7	69.9	0.19	47.8	42.9	8.9	/	0.37
	90red	3.1	21.8	3.3	71.7	0.0	46.6	43.1	9.8	/	0.45
SMM12 (PTMO-432H)	90	44.2	7.6	2.3	45.5	0.32	27.6	39.6	5.3	24.3	3.1
	10	62.4	2.7	1.1	33.7	0.09	14.9	19.9	5.0	49.7	10.5
	20	56.7	4.2	1.8	37.3	0.0	19.1	25.5	5.6	41.3	8.4
	30	51.8	5.2	2.0	41.0	0.0	23.4	27.8	6.7	35.9	6.1
	45	46.9	6.7	2.1	44.2	0.0	28.8	32.6	6.4	28.1	4.1
	60	42.6	8.3	2.3	46.4	0.41	31.3	36.8	6.3	22.5	3.0
	90red	39.9	9.5	2.4	47.9	0.25	33.7	38.6	6.0	18.9	2.8

Appendix 6 DSC Results for SMMs Synthesized in Different Batches

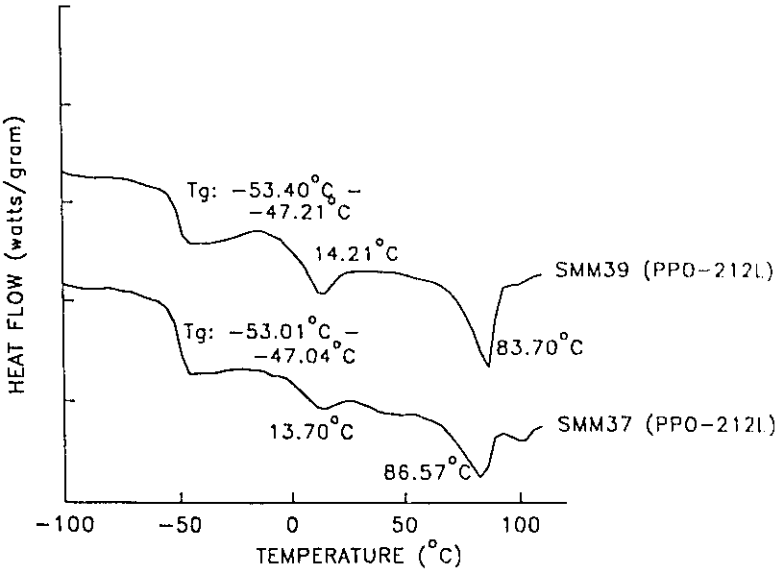

Figure A6.1 DSC thermograms for SMM37 and SMM39 (PPO-212L).

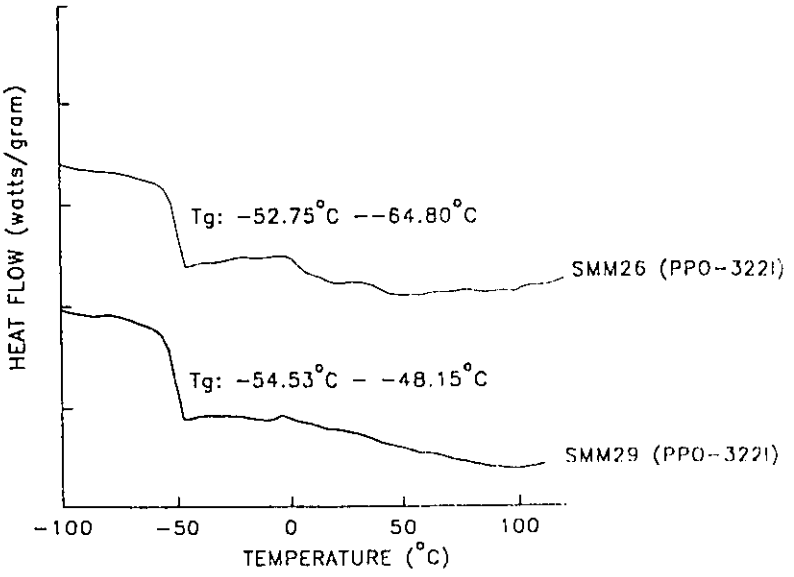

Figure A6.2 DSC thermograms for SMM26 and SMM29 (PPO-322I).

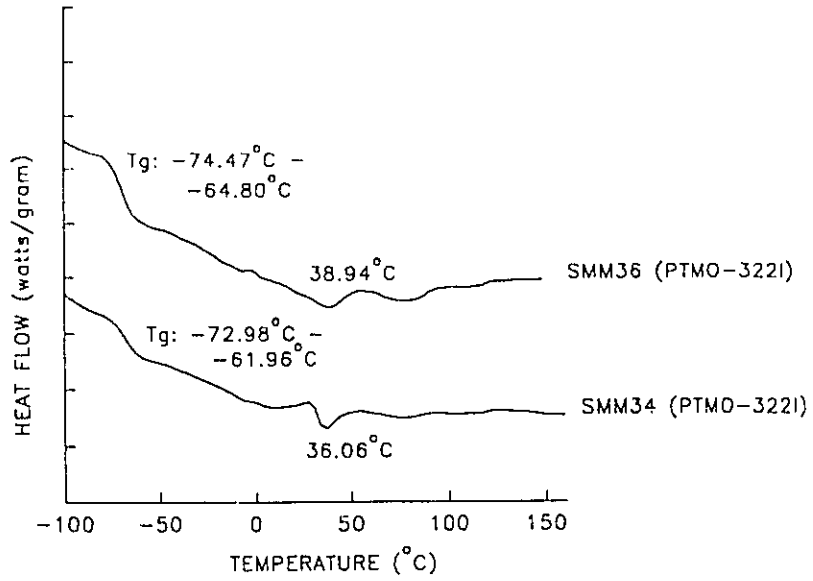

Figure A6.3 DSC thermograms for SMM34 and SMM36 (PTMO-322I).

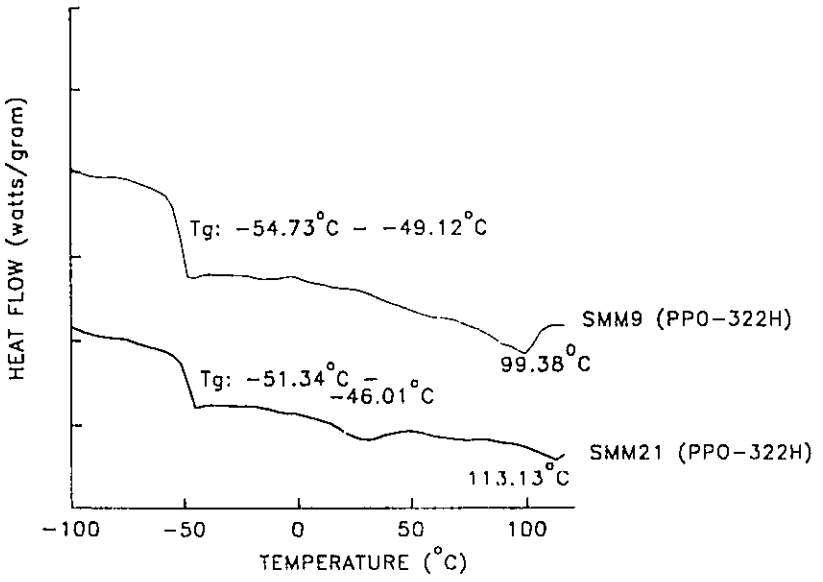

Figure A6.4 DSC thermograms for SMM9 and SMM21 (PPO-322H).

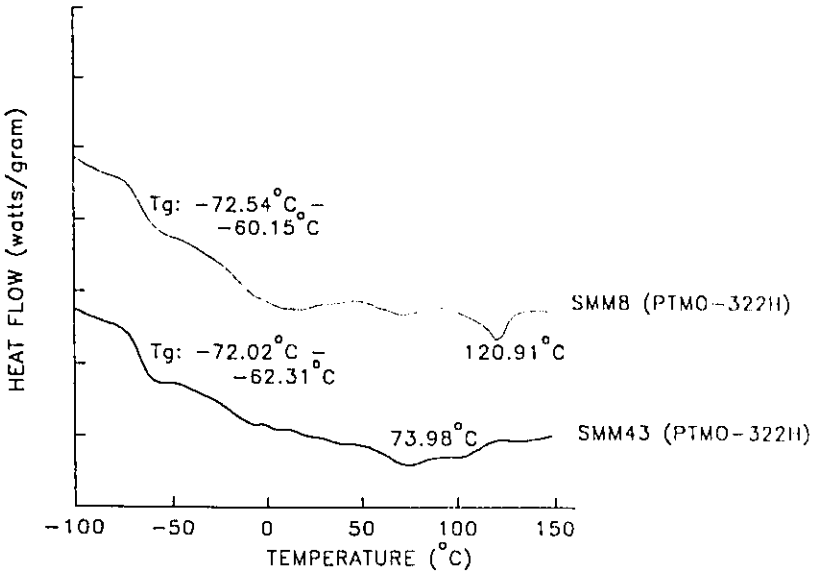

Figure A6.5 DSC thermograms for SMM8 and SMM43 (PTMO-322H).

Appendix 7 Biostability of Radiolabelled SMMs

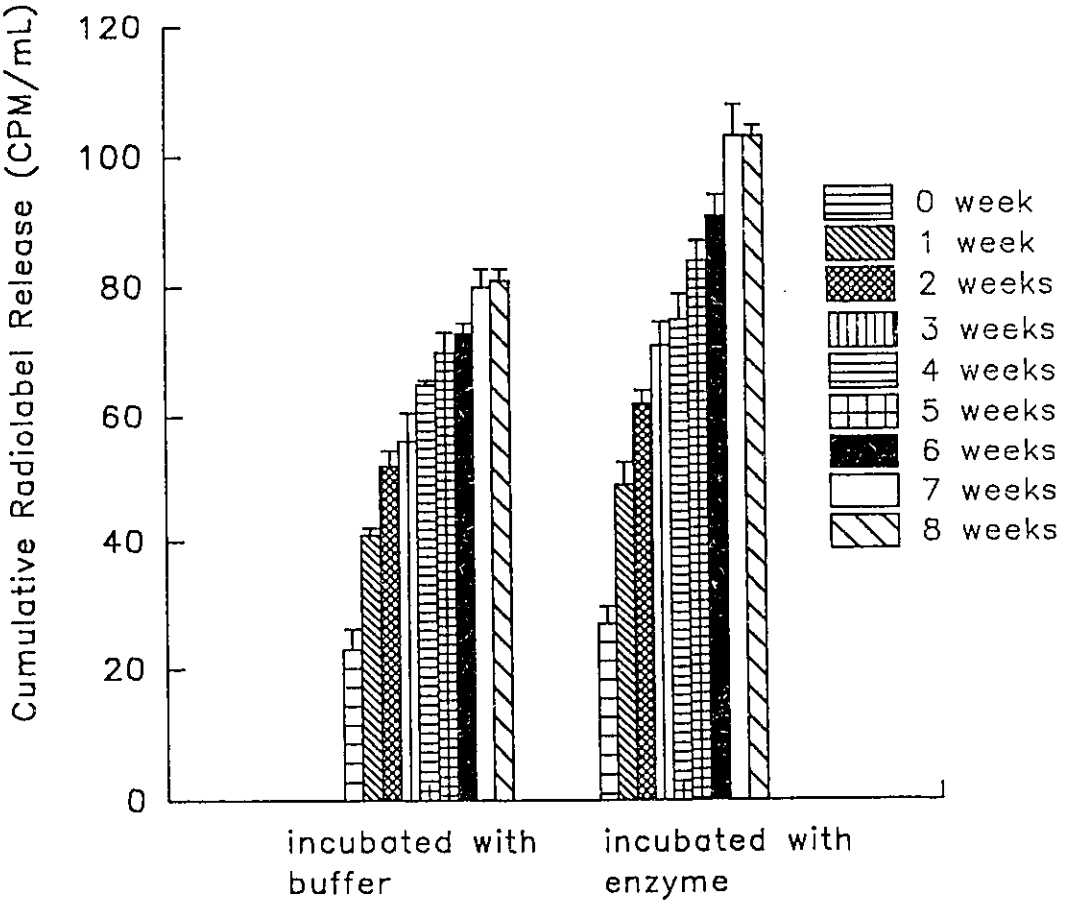

Figure A7 Biostability test results of 5% ^{14}C PPO-322I.